NASA-CR-199085

FINAL

OCIL.
61028
P-89

DESIGN OF ETO PROPULSION TURBINE USING CFD ANALYSES

F.J. de Jong, Y-T. Chan, and H.J. Gibeling

Scientific Research Associates, Inc.
Glastonbury, CT 06033

ORIGINAL CONTAINS
COLOR ILLUSTRATIONS

5

April 1995

Final Report R95-9084-F

Prepared Under

Contract NAS8-38865

for

National Aeronautics and Space Administration
George C. Marshall Space Flight Center

(NASA-CR-199085) DESIGN OF ETO PROPULSION TURBINE USING CFD ANALYSES Final Report (Scientific Research Associates) 89 p

N95-32915

Unclas

G3/37 0061028

TABLE OF CONTENTS

LIST OF FIGURES

1. INTRODUCTION

State-of-the-art in pump design for space shuttle, space transport, or general ETO propulsion systems currently is a combination of experience, simple analyses with empiricism to estimate overall performance, and input from a database generated by experiments. This aspect of the design process will remain largely unchanged in the near future, due to the fact that current CFD viscous flow codes are "analysis" codes, rather than "inverse design" codes; i.e., they analyze the flow for a specified geometry and inflow conditions, rather than determine the geometry required to provide a desired flow field. With this limitation, CFD can be best utilized in modern pump design by first producing a "baseline" design produced by current design practice and utilizing state-of-the-art CFD codes to change design details so as to evolve the base design to an improved, advanced, and hopefully near-optimum design with improved performance. This process would utilize the insight which the computations provide into the flow field structure, to refine the baseline design or suggest new geometric configurations to achieve desired performance.

In the work discussed here, a three-dimensional Navier-Stokes code was used for analysis of the STME fuel turbine, one of the tasks of the NASA/MSFC Turbine Technology Team (Refs. 1-3). The STME baseline oxidizer turbine flow field was simulated and, based upon the simulation described here and simulations performed by other members of the NASA/MSFC Turbine Technology Team, an "advanced concept" design was developed by Pratt & Whitney, which, in turn, was analyzed. In addition, simulations were performed at different turbine blade tip clearances.

The present report describes the CFD code used for these simulations, as well as results obtained. A report that details the design of the turbine by Pratt & Whitney has been included as an Appendix.

2. ANALYSIS

2.1 Navier-Stokes Equations

Solution of the flow field was obtained from a solution of the Reynolds-averaged, compressible Navier-Stokes equations. The governing equations were expressed in a rotating cylindrical coordinate system fixed to the turbine axis. In this coordinate system the mass, momentum, and energy conservation equations are:

$$\frac{\partial \rho}{\partial t} + \nabla \bullet (\rho \mathbf{U}) = 0 \tag{1}$$

$$\frac{\partial (\rho \mathbf{U})}{\partial t} + \nabla \bullet (\rho \mathbf{U}\mathbf{U}) + 2\rho \omega x \mathbf{U} + \rho \omega x \omega x \mathbf{r} = -\nabla p + \nabla \bullet \vec{\tau} \tag{2}$$

$$\frac{\partial (\rho h)}{\partial t} + \nabla \bullet (\rho \mathbf{U} h) = \frac{Dp}{Dt} - \nabla \bullet \mathbf{q} + \Phi \tag{3}$$

where **U** is the velocity vector in the rotating frame of reference, ω is the rotation vector, and **r** is a vector from the axis of rotation to the point under consideration.

The stress tensor (molecular and turbulent) $\vec{\tau}$ is given by

$$\tau_{ij} = 2\mu_{eff} e_{ij} - 2/3 \mu_{eff} \nabla \bullet \mathbf{U} \delta_{ij} \tag{4}$$

where the rate of the strain e_{ij} is given by

$$e_{ij} = 1/2 \left[\frac{\partial u_i}{\partial x_j} + \frac{\partial u_j}{\partial x_i} \right] \tag{5}$$

and where the effective viscosity μ_{eff} is the sum of the molecular and turbulent viscosities

$$\mu_{eff} = \mu + \mu_T \tag{6}$$

Here the turbulent viscosity μ_T is obtained from the turbulence model. Φ is the viscous dissipation per unit volume, which can be expressed as

$$\Phi = \mu_{eff}\left[2e_{ij}e_{ij} - 2/3(\nabla \bullet \mathbf{U})^2\right] \tag{7}$$

while the heat flux vector **q** is given by

$$\mathbf{q} = -(\kappa + \kappa_T)\nabla T \tag{8}$$

Here κ and κ_T are molecular and turbulent thermal conductivities, respectively. In the present analysis, κ and κ_T are obtained assuming constant molecular and turbulent Prandtl number Pr and Pr_T, i.e.,

$$\kappa = \frac{\mu c_p}{\mathrm{Pr}} \tag{9a}$$

$$\kappa_T = \frac{\mu_T c_p}{\mathrm{Pr}_T} \tag{9b}$$

A simple mixing-length type eddy viscosity model was used in the turbine computations, in which a mixing length distribution is specified normalized by a local freestream mixing length and modified to account for near-wall damping. The local freestream mixing length is proportional to a local shear layer thickness, which can be computed from the solution, or, as was done in the present calculations, can be specified. All boundary layers were assumed to be turbulent.

2.2 Numerical Solution Procedure

A general non-orthogonal coordinate transformation to a body-fitted grid is used to handle complex geometries in the solution procedure. The governing equations are solved by a Linearized Block Implicit (LBI) scheme (Refs. 4-5).

The method can be outlined as follows: the governing equations are replaced by an implicit time difference approximation, optionally a backward difference or Crank-Nicholson scheme (a backward time-difference scheme was used in the present application). Terms involving nonlinearities at the implicit time level are linearized by Taylor series expansion about the solution at the known time level, and spatial difference approximations are introduced. The result is a system of multidimensional coupled (but linear) difference equations for the dependent variables at the unknown or implicit time level. To solve these difference equations, the Douglas-Gunn procedure for generating alternating-direction implicit (ADI) splitting schemes is introduced in its natural extension to systems of partial differential equations. This ADI splitting technique leads to

systems of coupled linear difference equations having narrow block-banded matrix structures which can be solved efficiently by standard block-elimination methods. Details are given in Refs. 4-5.

In the present application, three-point central differences are used in the transformed coordinate system, and artificial dissipation terms of the form

$$\frac{\partial}{\partial x_j}\left[(\mu_{art})_j \frac{\partial \phi}{\partial x_j}\right] \tag{10}$$

are added to the governing equations for each coordinate direction j. The variable ϕ corresponds to the velocity component U_i for the x_i-direction momentum equation, the density ρ for the continuity equation, and the enthalpy h for the energy equation. The coefficient $(\mu_{art})_j$ is obtained from the relation

$$\rho U_j \Delta x_j \leq (1/\sigma_d)\left[\bar{\mu}+(\mu_{art})_j\right] \tag{11}$$

where Δx_j is the grid spacing at the point in question, while $\bar{\mu}$ corresponds to the effective viscosity μ_{eff} for the momentm equation, μ_{eff}/Pr for the energy equation, and is zero for the continuity equation. The artificial dissipation coefficient σ_d lies between 0 (no dissipation) and 0.5 (full artificial dissipation).

Use of artificial dissipation tends to enhance the stability and convergence properties of the numerical solution procedure, but it also tends to reduce the accuracy of the solution, in particular on coarse grids. Therefore, the turbine calculations were performed with an initial value of the artificial dissipation coefficient $\sigma_d = 0.5$ (corresponding to full artificial dissipation). After the flow field had been established, this coefficient was reduced to $\sigma_d = 0.2$. This reduction of artificial dissipation did not affect the flow field qualitatively, but it did decrease the pressure loss and increase the efficiency.

2.3 Grid Generation

An important component in a three-dimensional Navier-Stokes simulation is grid generation. Grid generation for the present study was accomplished as follows. First, the EAGLE code (Ref. 6) was used to generate a two-dimensional grid for a number of blade sections. Next, these grids were "stacked" to form a three-dimensional grid. The grid points on hub-to-casing grid lines were redistributed to cluster points near the hub and near the tip by using Oh's method (Ref.

7), and the diffusing section downstream of the blade was constructed by rescaling the local radii. In the tip clearance region, EAGLE was used to generate a two-dimensional grid "inside" the blade section at he tip (and matching the "exterior" grid). This grid was then used at all radial locations from the blade tip to the end wall. The resulting grid generation procedure is efficient, because it uses EAGLE only to generate two-dimensional grids, and uses an algebraic procedure to construct the three-dimensional grid from these two-dimensional grids.

2.4 Boundary Conditions

The computational domain chosen for the turbine calculations consisted of one passage between two blades, appropriately extended upstream and downstream of these blades. On this domain, the physical boundary conditions used were as follows:

(i) No-slip and adiabatic wall conditions were specified on all solid surfaces.
(ii) Total pressure, total temperature, and flow angles were specified at the inflow boundary.
(iii) Static pressure was specified at the outflow boundary.
(iv) Periodicity conditions were applied in the circumferential direction in the sections upstream and downstream of the blades.

These boundary conditions were augmented by the appropriate numerical boundary conditions, viz. zero pressure gradient on stationary solid surfaces, zero reduced pressure gradient on rotating solid surfaces, extrapolation of pressure at the inflow boundary, and extrapolation of velocities and temperature at the outflow boundary.

2.5 Initial Conditions

In the turbine calculations, a steady-state solution was sought in the rotating frame of reference. Therefore, the initial conditions applied to these calculations serve as an initial guess, and do not affect the converged steady-state solution (although they will, in general, affect the convergence history). In the present calculations, an initial guess was obtained by calculating a two-dimensional solution for the mid-span geometry, and by using this solution for all blade sections. No attempt was made to include the tip clearance regions and hub or casing boundary layer profiles in the initial guess.

3. RESULTS

The work presented here was generated as part of SRA's effort under the NASA/MSFC Turbine Technology Team. Results of previous work, the analysis of Pratt & Whitney's Generic Gas Generator Turbine (GGGT), can be found in Refs. 8-9. The design of the present Gas Generator Oxidizer Turbine (GGOT), Pratt & Whitney's effort under a subcontract from SRA, has been detailed in the Appendix (see also Ref. 10.). Most of the results of the present work, the analysis of the GGOT, have been presented at NASA MSFC meetings (see also Refs. 11 and 12.) Details have not been repeated here. Instead, a description is given of the different cases run, with a selection of representative results.

3.1 Baseline GGOT

The oxidizer turbine flow path and the turbine blade geometry are shown in Figs. 1-2. Additional information can be found in the Appendix. The present calculations simulate the rotor blade row in a rotating reference frame with the appropriate coriolis and centrifugal acceleration terms included in the momentum equations (cf. Section 2.1). The upstream computational boundary is located about one axial chord from the leading edge. The boundary conditions at this location have been determined by Pratt & Whitney, using an Euler analysis without the vanes to obtain approximately the same flow profiles at the rotor as were obtained with the Euler stage analysis including the vanes. Inflow boundary layer profiles were then constructed assuming the skin friction coefficient at both the hub and the casing. The downstream computational boundary is located about one axial chord from the blade trailing edge, and the circumferentially-averaged static pressure at this location was also obtained from the Pratt & Whitney Euler analysis.

The simulation was run with a grid containing about 216,000 grid points: 90 grid points in the streamwise direction, 60 grid points in the circumferential direction, and 40 grid points in the hub-to-casing direction (with 14 grid points in the tip clearance region). Figures 3 and 4 show the grid at the hub section and the tip section, respectively. The tip section grid contains 37 x 31 grid points in the "interior" of the blade section. Figure 5 shows the calculated pressure contours on the blade and particle traces in the tip clearance region. The vortical flow behavior of the fluid that passes through the clearance region and exits at the downstream edge of the gap is clearly visible.

3.2 GGOT with Mini-Shroud

Results obtained for the 3-D baseline GGOT geometry and the full-scale design Reynolds number show a region of high loss near the casing, attributed to the formation of the tip vortex (cf. Fig. 5). In an effort to reduce the clearance flow losses, the mini-shroud concept was proposed by the Pratt & Whitney design team: a "lip" or "mini-shroud" is added to the blade tip by replacing the blade pressure side at the tip by a straight line. The "thickness" of the mini-shroud (in the radial direction) has been kept fairly small (0.1"). The airfoil shape below the mini-shroud is unchanged. Figures 6 and 7 show the geometry of the blade with the mini-shroud and the corresponding tip section grid used in the present calculations. To allow use of the grid generation procedure described in Section 2.3, the mini-shroud has been faired smoothly into the part of the blade below the mini-shroud. Results of the calculations indicate that, at the design tip clearance, the mini-shroud does not significantly affect the flow in the passage region. Although the tip region flow is affected, the results are qualitatively the same as those obtained without the mini-shroud, as can be seen by comparing Fig. 8 with Fig. 5.

3.3 Effect of Tip Clearance

To further investigate the effect of the mini-shroud on the tip clearance flow, calculations were carried out for both geometries (i.e., with and without the mini-shroud) at two additional tip clearances: 0.03" (1.5% span) and 0.06" (3% span), corresponding to 2x and 4x the design tip clearance, respectively. All calculations show flow patterns like those in Figs. 5 and 8 (see also Ref. 12). The results of the calculations have been summarized in Fig. 9, which shows the distribution of the blade lift coefficient as a function of radius for all six cases. For the baseline geometry, the unloading of the blade tip with increasing tip clearance is clearly visible. For the mini-shroud geometry, this effect is less pronounced. At the largest clearance, however, the hub loading decreases significantly for the mini-shroud geometry. But, since the calculations were performed with less grid resolution in the hub region than in the tip region, the prediction of the hub flow may not be quantitatively correct.

To quantify the differences between the six cases, efficiencies were calculated. The "ideal work" was computed from the exit-to-inlet total pressure ratio (using isentropic relations); the "actual work" was computed from the decrease of tangential momentum from inlet to exit. In these efficiency calculations, the "exit" was taken about one chord downstream of the blade. Its precise location did not significantly affect the results. The "actual work" was also computed from the torque on the blade (without taking into account the effect of shear stress); the difference with

the work calculated from the tangential momentum was less than 1% in all cases. Table 1 lists the efficiencies as differences from the efficiency of the baseline case (the baseline geometry with the design tip clearance of 0.015"). Clearly, the efficiency decreases as the tip clearance increases. The mini-shroud seems to improve the efficiency a little bit at the design clearance and twice the design clearance, but this "improvement" is well within the accuracy of the calculations. At the largest tip clearance, the efficiency of the mini-shroud geometry has dropped off significantly, possibly due to hub-effects (cf. Figure 9).

The conclusion that can be drawn from the calculations is that the effect of the mini-shroud on the tip clearance flow and the associated losses is not as large as was originally anticipated.

Tip Clearance	Baseline Geometry	Geometry with Mini-shroud
0.015"	0	+0.1%
0.03"	-1.2%	-0.9%
0.06"	-2.4%	-3.3%

Table 1. Efficiencies Relative to the Baseline Efficiency

4. CONCLUSIONS

Under the present effort, a three-dimensional Navier-Stokes code was used for various turbine flow field calculations. The emphasis was on the flow in the tip clearance region and the associated losses. Both a baseline turbine blade geometry and an "advanced-concept" blade geometry (with a "mini-shroud") were analyzed at different tip clearances. The results show that a current state-of-the-art CFD code can be used as an analysis tool in turbine design and the development of advanced hardware concepts.

REFERENCES

1. McConnaughey, P.K. and Schutzenhofer, L.A.: "Overview of the NASA/MSFC CFD Consortium for Applications in Propulsion Technology," AIAA Paper 92-3219, AIAA/SAE/ASME/ASEE 28th Joint Propulsion Conference and Exhibit, July 1992.

2. Griffin, L.W. and Huber, F.W.: "Turbine Technology Team: An Overview of Current and Planned Activities Relevant to the National Launch System," AIAA Paper 92-3220, AIAA/ SAE/ASME/ASEE 28th Joint Propulsion Conference and Exhibit, July 1992.

3. Griffin, L.W.: "A Status of the Turbine Technology Team Activities," Tenth Workshop for Computational Fluid Dynamic Applications in Rocket Propulsion, NASA CP-3163, Part 2, 1992, pp. 1205-1226.

4. Briley, W.R. and McDonald, H.: 'Solution of the Multidimensional Compressible Navier-Stokes Equations by a Generalized Implicit Method," *J. Computational Physics*, Vol. 24, 1977, pp. 372-397.

5. Briley, W.R. and McDonald, H.: "On the Structure and Use of Linearized Block Implicit Schemes," *J. Computational Physics*, Vol. 34, 1980, pp. 54-72.

6. Thompson, J.F. and Gatlin, B.: "Program EAGLE User's Manual," Air Force Armament Laboratory Contract F08635-84-C-0228, 1988.

7. Oh, Y.H.: "An Analytical Transformation Technique for Generating Uniformly Spaced Computational Mesh," Numerical Grid Generation Techniques, NASA CP 2166, 1980, pp. 385-398.

8. Gibeling, H.J., Roscoe, D.V., Buggeln, R.C., Briley, W.R., Sabnis, J.S., and McDonald, H.: "Computation of Flow Past a Turbine Blade with and without Tip Clearance," SRA Final Report 90-380001-F, Subcontract No. 2000-017-514, NASA Ames Prime Contract NAS2-11555, March 1990.

9. Briley, W.R., Roscoe, D.V., Gibeling, H.J., Buggeln, R.C., Sabnis, J.S., Johnson, P.D., and Huber, F.W.: "Computation of Flow Past a Turbine Blade with and without Tip Clearance," ASME Paper 91-GT-56, June 1991.

10. Huber, F.W., Johnson, P.D., Montesdeoca, X.A., Rowey, R.J., and Griffin, L.W.: "Design of Advanced Turbopump Drive Turbines for National Launch System Application" AIAA Paper 92-3221, AIAA/SAE/ASME/ASEE 28th Joint Propulsion Conference and Exhibit, July 1992.

11. Gibeling, H.J., and Sabnis, J.S.: "Navier-Stokes Analysis of an Oxidizer Turbine Blade with Tip Clearance," Tenth Workshop for Computational Fluid Dynamic Applications in Rocket Propulsion, NASA CP-3163, Part 2, 1992, pp. 1243-1274.

12. Chan, Y-T. and de Jong, F.J.: "Navier-Stokes Analysis of an Oxidizer Turbine Blade with Tip Clearance with and without a Mini-Shroud," Eleventh Workshop for Computational Fluid Dynamic Applications in Rocket Propulsion, NASA CP-3221, Part 2, 1993, pp. 1397-1422.

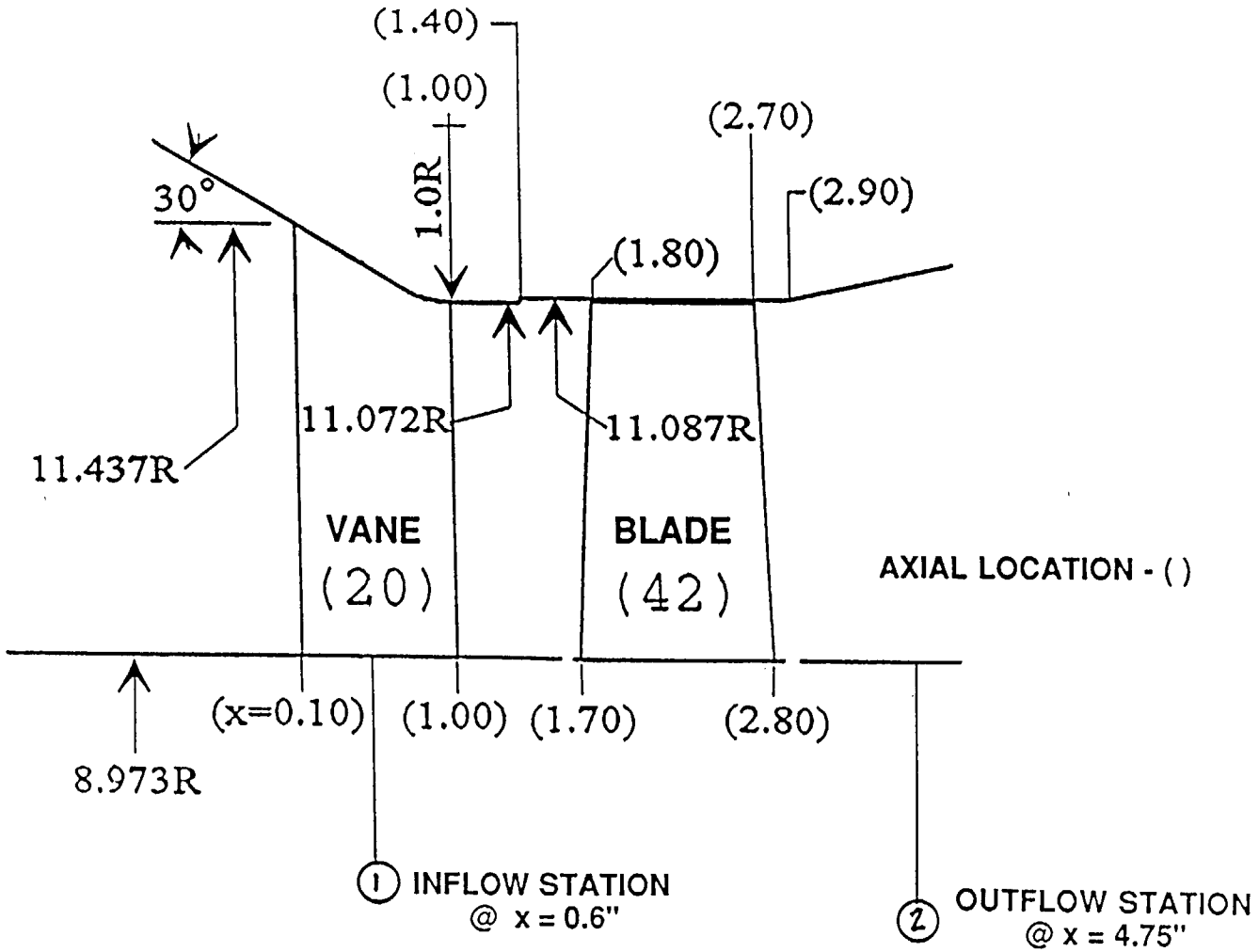

FIGURE 1 - OXIDIZER TURBINE FLOW PATH

FIGURE 2 - BASELINE TURBINE BLADE GEOMETRY

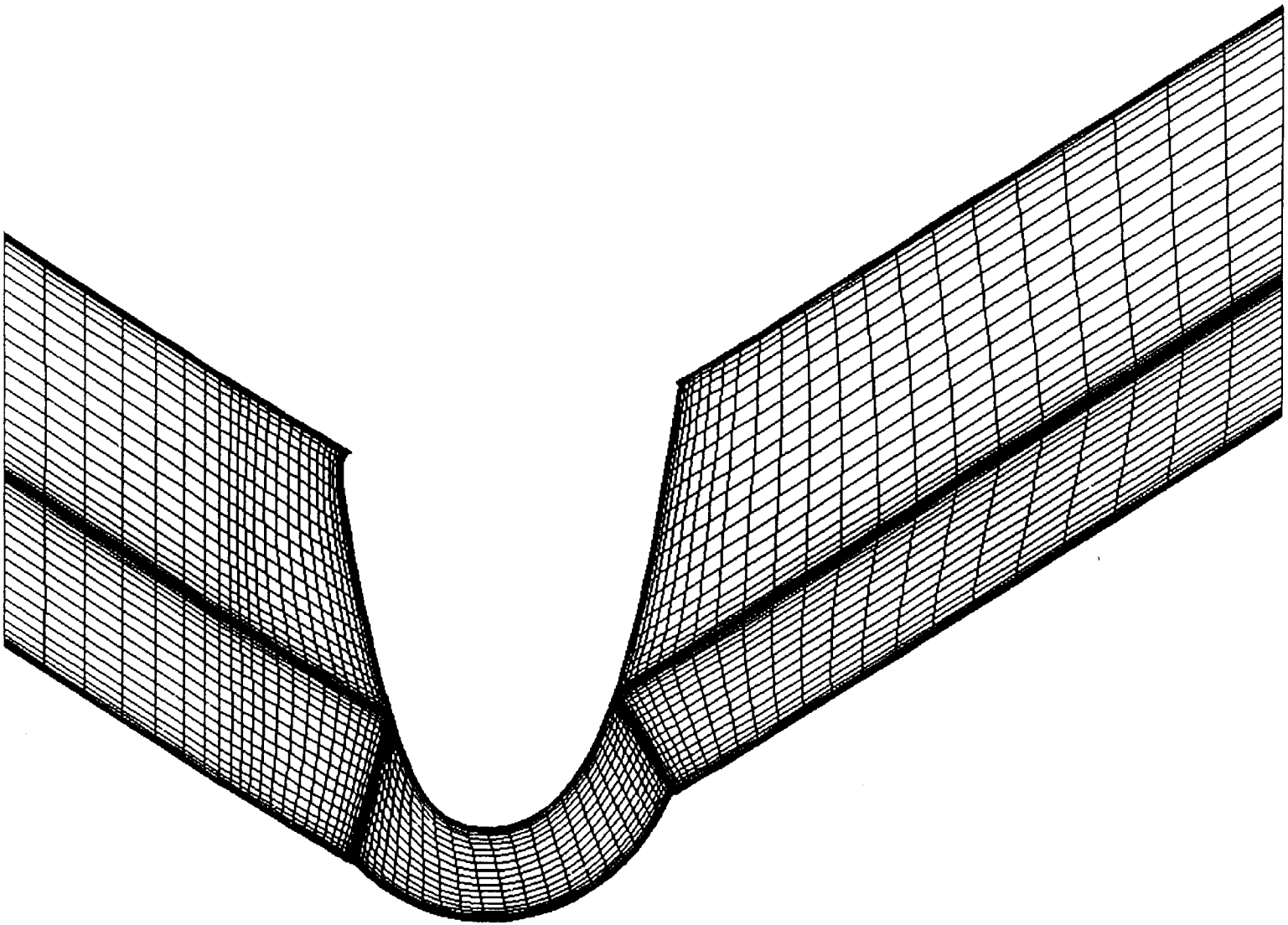

FIGURE 3 - HUB SECTION GRID

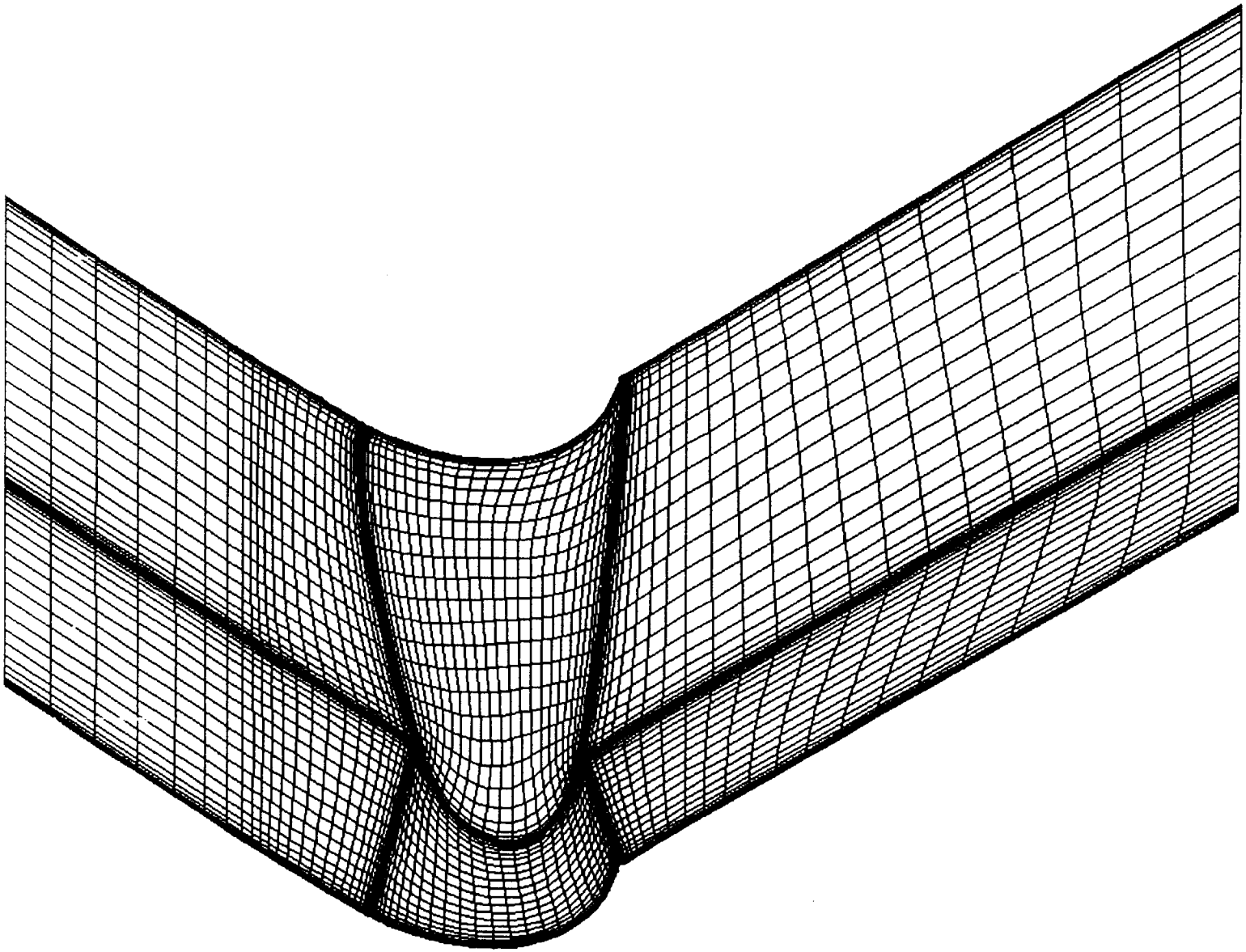

FIGURE 4 - TIP SECTION GRID (BASELINE GEOMETRY)

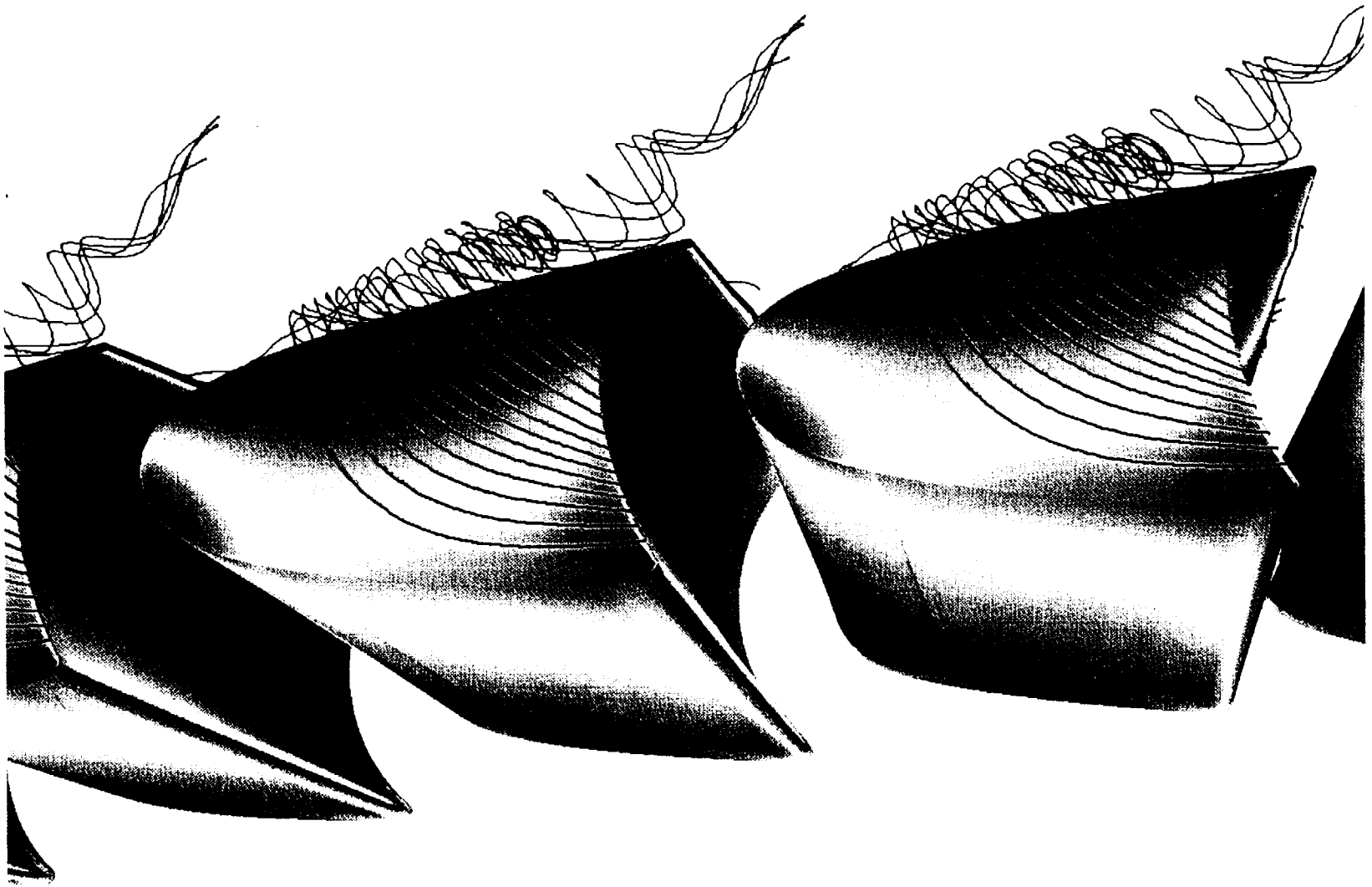

FIGURE 5 - PRESSURE CONTOURS AND PARTICLE TRACES ON THE
BASELINE GGOT BLADE AT THE DESIGN CLEARANCE

FIGURE 6 - TURBINE BLADE GEOMETRY WITH MINI-SHROUD

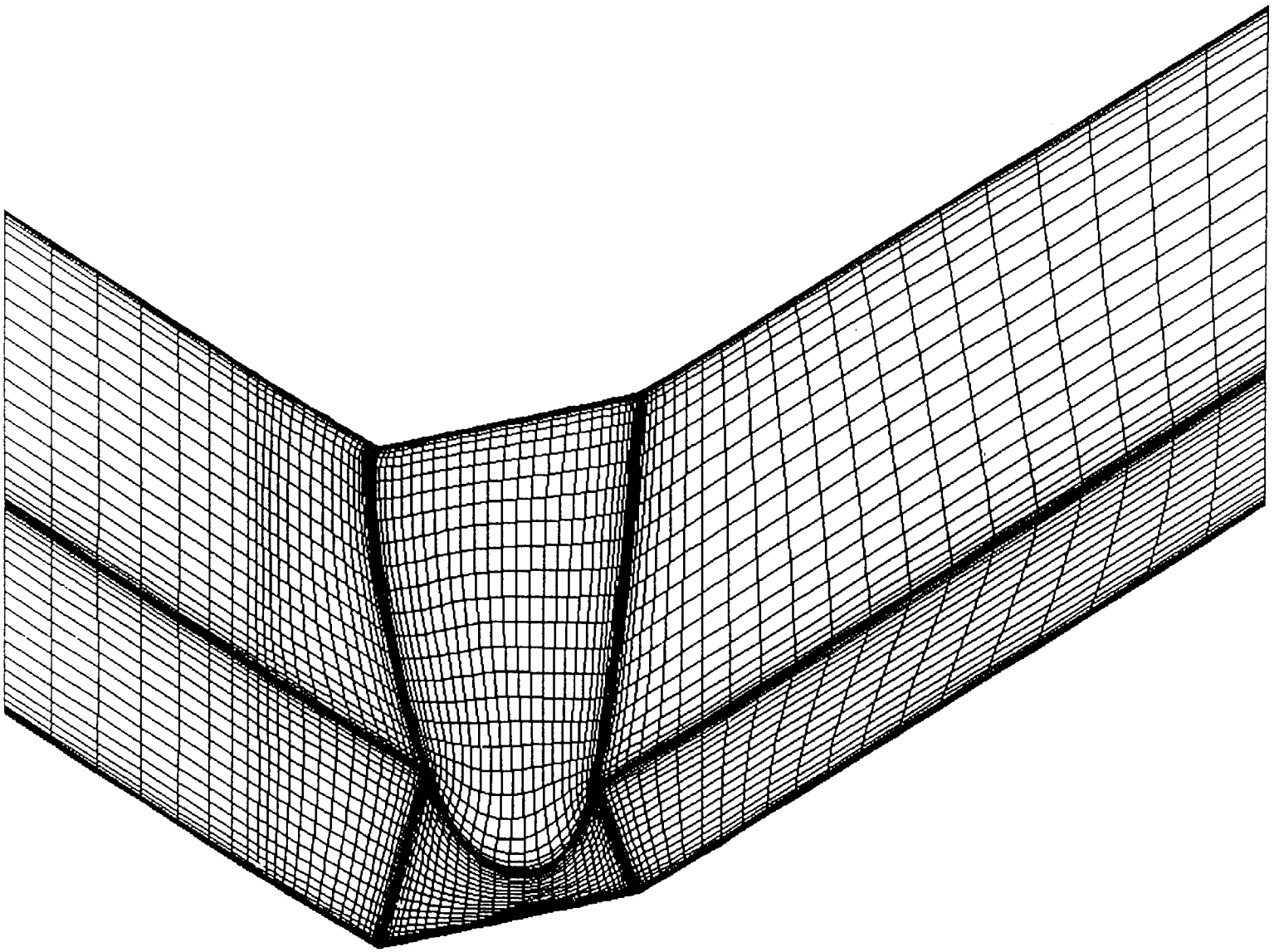

FIGURE 7 - TIP SECTION GRID (GEOMETRY WITH MINI-SHROUD)

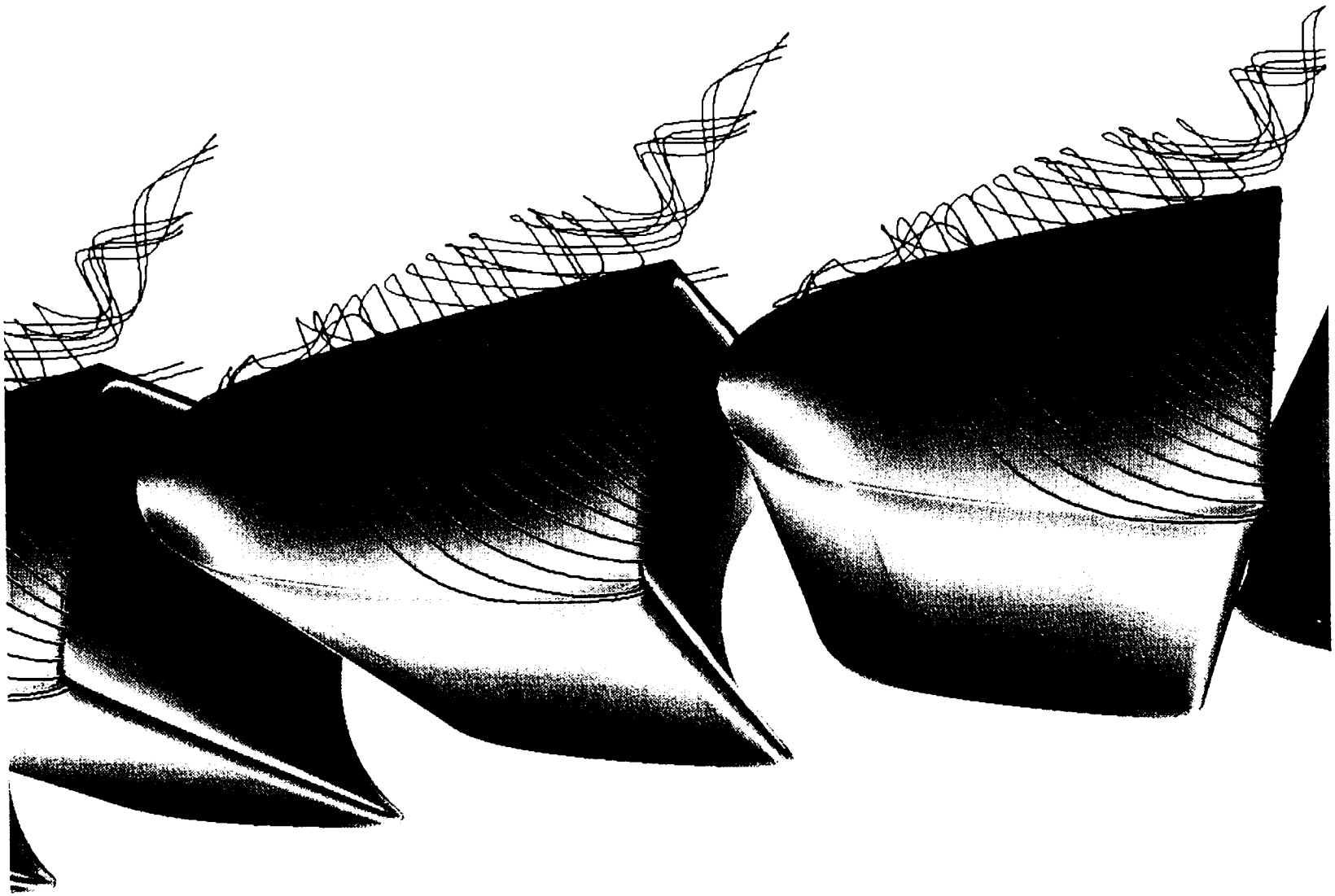

FIGURE 8 - PRESSURE CONTOURS AND PARTICLE TRACES ON THE
GGOT BLADE WITH MINI-SHROUD AT THE DESIGN CLEARANCE

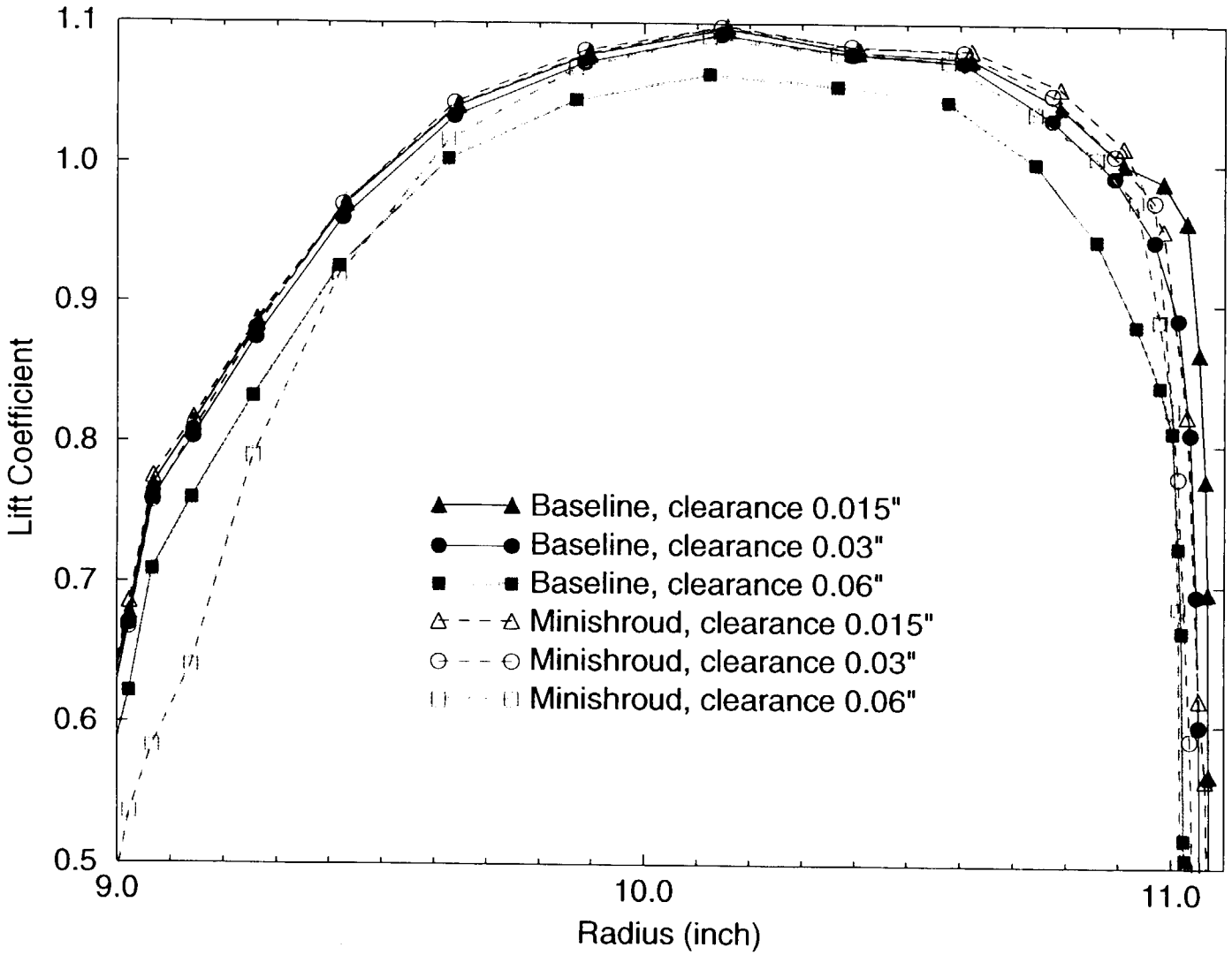

FIGURE 9 - BLADE LIFT COEFFICIENT AS A FUNCTION OF RADIUS

APPENDIX

Baseline Design of the

Gas Generator Oxidizer Turbine (GGOT)

and performance predictions for the associated

Oxidizer Technology Turbine Rig (OTTR)

F.W. Huber
P.D. Johnson
X.A. Montesdeoca

March 23, 1993

Introduction

The work described here is being sponsored by the NASA Marshall Space Flight Center (MSFC), under contract No. NAS8-38865. This report is intended to summarize work completed under a Pratt & Whitney (P&W) subcontract from Scientific Research Associates (SRA) No. S900084-91-0001, Task I. Task I is as follows:

The subcontractor shall provide the aerodynamic design for a baseline turbine with operating characteristics generally consistent with the NLS oxidizer turbopump, and shall provide follow-on support for the mechanical design of the baseline turbine rig. The objectives of this effort are to ensure that the aerodynamic design intent of the baseline turbine is achieved in the hardware, and to provide supporting aerodynamic analyses for the mechanical design effort. These analyses will include calculation of aero loads on vanes and blades, prediction of turbine output torque characteristics, and prediction of flowpath gas state conditions (pressure, temperature, and flowrate) for all turbine operating conditions of interest. Design consultation and review services will be provided to ensure the mechanical design of the flowpath meets aerodynamic design requirements. A report detailing predicted turbine rig performance, torque, and flowpath conditions will be delivered.

Turbine Technology Team

The aerodynamic design of a technology demonstrator gas generator turbine, hereafter referred to as the Gas Generator Oxidizer Turbine (GGOT), was performed within the Consortium for Computational Fluid Dynamics Application in Propulsion Technology, by the Turbine Technology Team (Figure 1). Pratt & Whitney's responsibility was to generate a preliminary turbine design for team member analyses, and to incorporate the results of these analyses into a baseline turbine design, which is the subject of this report (Figure 2). Consortium analyses are continuing in the "advanced concepts" phase. Results from these analyses along with the results from testing of the baseline turbine will be incorporated into an advanced concept turbine design.

Design Table

The design of the GGOT is consistent with the requirements for the U.S. Governments National Launch System (NLS) Oxidizer Turbine Design Table Revision 8A (Figure 3). In order to maximize specific impulse, a gas generator cycle with minimized turbine flowrate was chosen, which leads to high values of turbine specific work. The requirements for high specific work and minimum weight led to the design of a highly loaded single stage oxidizer turbine which utilizes inlet and exit volutes to provide optimum performance.

Aerodynamic Design Process

The aerodynamic design of the baseline GGOT was initiated with Pratt & Whitney's generation of a preliminary turbine flowpath elevation along with stator and rotor airfoil

contours. The process used to produce this preliminary configuration started with turbine meanline flowpath parametric analyses to optimize overall geometry such as blade height, flowpath diameter, and average blading reaction (Figure 4). Next, streamline analyses were conducted to optimize the radial distribution of flow properties. The results of the streamline studies were used to create first pass 2D airfoil sections at a number of spanwise locations for both stator and rotor. These sections were radially faired to build 3D models which were then analyzed in multi-stage 3D Euler and Navier-Stokes flow solvers. Numerous iterations involving airfoil contour refinement were performed to arrive at the preliminary design.

Once the preliminary design was completed, Turbine Technology Team members selected various areas for more detailed analyses. These included a 2D unsteady Navier-Stokes analysis of the turbine stage and 3D Navier-Stokes analyses of the vane alone, blade alone, turbine stage, and blade tip leakage details. The results from these studies were then incorporated into the design to define the baseline turbine (Figure 5).

Inlet Volute Design

The aerodynamic design of the baseline inlet volute manifold was accomplished using a Computer Aided Design (CAD) program to generate trial contours, which were then analyzed with a 3D Navier-Stokes flow solver. The design features a circular cross section, with an approximately linear decrease in thru-flow area in the circumferential direction (Figures 6A-6C). A decreasing area volute was selected over a geometrically simpler constant area toroid for several reasons: predicted reduction in the inlet radial side load by 80%, reduction in weight, and the creation of a highly swirled and uniform exit flow which enables a reduction in stator count. 3D Navier-Stokes pressure distributions indicate that the inlet volute should experience a minimal transverse static pressure gradient at the aerodynamic design point (Figure 7).

Turbine Stage Design

The baseline oxidizer turbine is a single stage configuration which rotates in a clockwise direction when viewed from the aft looking upstream (Figure 8). This highly loaded turbine uses a mixture of oxygen and hydrogen gases to deliver over 1900 horsepower at a flow rate of 60.4 lbm/s. The turbine stator airfoil contour design has been integrated with that of the inlet volute (Figure 9A-9G). This integration of flowpath components has significantly reduced stator turning, and the number of stators required. 3D Euler analysis predicts that the stator will smoothly accelerate the flow from a Mach number of 0.35 to 1.05 through a combination of minimal turning and endwall convergence at the aerodynamic design point (Figure 10A-10E).

In an effort to improve performance while reducing cost, this turbine has been designed with reduced thru-flow velocities and increased blade reaction, relative to previous gas generator turbine experience. This causes the required blade turning angle to increase to an average of 157 degrees (Figure 11A-11G). While this level of gas turning is beyond traditional design experience, 3D Euler analysis predicts that the rotor will smoothly accelerate the flow from a Mach number of 0.80 to 1.05 (Figure 12A-12E).

Numerous independent CFD analyses performed by Turbine Technology Team members have consistently confirmed the prediction of smooth airfoil velocity distributions. This design concept is predicted to improve turbine stage efficiency by as much as 2%, while reducing the required blade count by 50% relative to traditional designs.

Exit Volute Design

The aerodynamic design of the baseline exit volute manifold was accomplished using the same methods and similar criteria as the inlet volute manifold. However, the challenge of designing the exit volute is compounded by the higher Mach number and diffusing flowfield. To ensure turbine operation over the entire test matrix, two exit volutes were designed. One exit volute was designed with an oversized square cross-section to ensure that the flow did not choke at off-design operation (Figure 13A-13C). The other exit volute was designed with a round cross-section to smoothly collect the turbine exit flow at the aerodynamic design point and provide optimum efficiency (Figure 14A-14C). The exit volute is positioned 139 degrees counter-clockwise relative to the inlet volute when viewed from the top of the engine configuration looking down (Figure 15).

The turbine exhaust system consists of three regions: an annular diffuser located downstream of the rotor, a volute manifold with an increasing flow area, and a conical pipe diffuser for static pressure recovery (Figure 16). The annular diffuser reduces the Mach number by approximately 5% while acting as a short buffer zone between the turbine and exit volute. The volute flowpath has an approximately linear increase in area in the circumferential direction to minimize the static pressure gradient. A conical diffuser, located at the exit volute exit reduces the Mach number to a level required by the downstream ducting and engine nozzle.

3D Navier-Stokes pressure distributions indicate that the square oversized exit volute will experience a substantial static pressure gradient (Figure 17A-17B). However, this design will allow the turbine to operate over the entire test matrix, dropping the flow Mach number from 0.80 to 0.60 at the aerodynamic design point. 3D Navier-Stokes pressure distributions indicate that the round, aerodynamically designed, exit volute will experience a minimal transverse static pressure gradient (Figure 18A-18B).

Oxidizer Technology Turbine Rig

The Oxidizer Technology Turbine Rig (OTTR, Figure 19) is a 50% scale model of the GGOT previously described. The OTTR, like the hot engine design, is an integrated turbine system consisting of an inlet volute, a turbine stage, and an exhaust volute and diffuser. Aerodynamic performance evaluation of the OTTR will be performed in MSFC's Turbine Test Equipment (TTE) facility.

Similarity requirements were used to define the "cold" turbine test article operating conditions (Figure 20). Testing at reduced inlet pressure and temperature facilitates the collection of quality data, but requires the scaling of other parameters to maintain flow similarity. Scaling was done as follows:

Pressure Ratio : $(Ptin / Ptex)$

Speed Parameter : $(N D / \sqrt{z R Ttin})$

Flow Parameter : $(4 \dot{W} \sqrt{z R Ttin} / \pi D^2 Pt_{IN})$

Where,

Ptin	Inlet Total Pressure
Ptex	Exit Total Pressure
N	Shaft Speed
D	Rotor Mean Diameter
z	Compressibility
R	Gas Constant
Ttin	Inlet Total Temperature
$\dot{W}$	Weight Flow

Pressure ratio and speed parameter will be set when testing the OTTR, while flow parameter will be an output. Reynolds number, another similarity parameter will not be matched but evaluated as follows:

Reynolds Number : $(Ps V X / z R Ts \mu)$

Where,

Ps	Local Static Pressure
V	Local Velocity
X	Airfoil Axial Chord
Ts	Local Temperature
μ	Fluid Viscosity

Reynolds number is predicted to be a secondary influence on turbine performance (Figure 21). To evaluate this effect, the following turbulent boundary layer Reynolds number correlation can be used (Glassman):

Correlation:
$$\frac{(1-\eta)_{GGOT}}{(1-\eta)_{OTTR}} = \left\{ \frac{Rn_{OTTR}}{Rn_{GGOT}} \right\}^{0.042}$$

Where,

η	Turbine Efficiency
Rn	Average of Vane & Blade Exit Reynolds Numbers

The value of the exponent was derived from Pratt & Whitney's extensive turbine test data base.

OTTR Performance Predictions

OTTR test objectives include measurement of turbine performance at the aerodynamic

design point (ADP) and at off-design conditions (Figure 22). Nominal inlet conditions for testing of this turbine will be 100 psia and 560 R. Design point pressure ratio and speed at these inlet conditions will be 1.60 and 3710 rpm, respectively. The off-design envelope will include pressure ratios from 1.20 to 1.80, and speeds from 1000 to 5000 rpm.

Turbine performance, such as efficiency and flow characteristics, will be mapped and compared to predictions (Figures 23 and 24). Other performance parameters such as flowpath pressures, temperatures, Mach numbers, and air angles, as well as turbine power output will also be assessed (Figure 25A-25E).

The performance of the total turbine system will be evaluated and compared to design intent. Losses will be measured for the various components to determine where design goals are being accomplished and where improvements can be made (Figure 26A-26B). Also, detailed flow measurements including laser velocimitry will be used to pin-point areas of potential improvement.

Summary

The design of the Gas Generator Oxidizer Turbine (GGOT), and the associated test article, the Oxidizer Technology Turbine Rig (OTTR) are being done in support of turbine research and development within the Turbine Technology Team, which is part of the Consortium for Computational Fluid Dynamics Application in Propulsion Technology. The baseline OTTR will undergo performance evaluation testing in MSFC's short duration experimental turbine test facility. The baseline test results will be integrated with analytical results of ongoing team studies to define an "advanced concept" oxidizer turbine system having potential for further performance and cost benefits. This turbine design is the result of a successful team working relationship, in which organizations with various turbine backgrounds have worked together in a complementary and synergistic manner. Turbine geometric data sets (including the inlet volute, vane, blade, and exit volute) may be obtained via the Turbine Technology Team Coordinator, Mail Stop ED-32, National Aeronautics and Space Administration, George C. Marshall Space Flight Center, MSFC, AL 35812.

FIGURE 1

OXIDIZER TURBINE BASELINE DESIGN

Consortium for CFD Application in Propulsion Technology

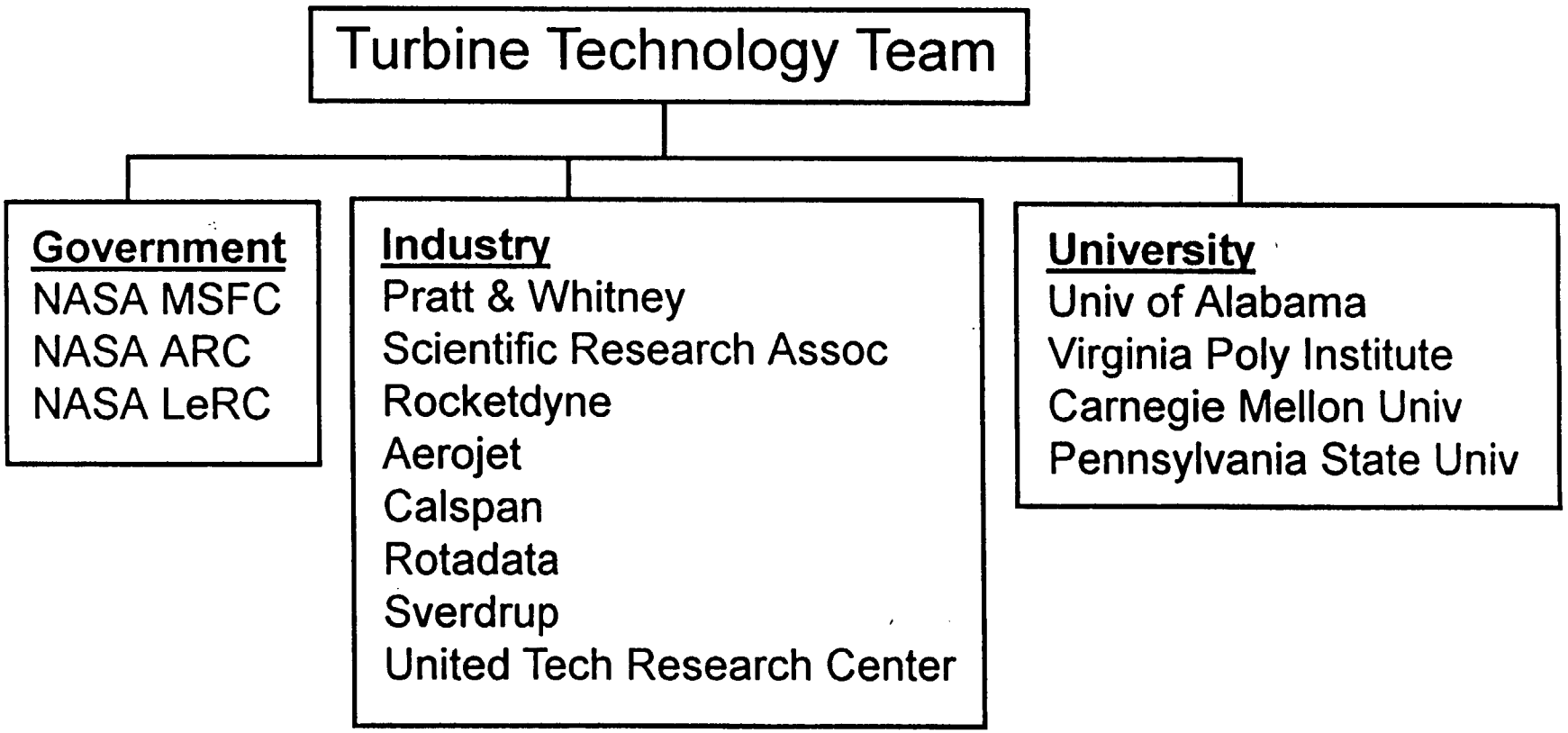

FIGURE 2
OXIDIZER TURBINE BASELINE DESIGN

Turbine Technology Team - Oxidizer Turbine Baseline Design Completed

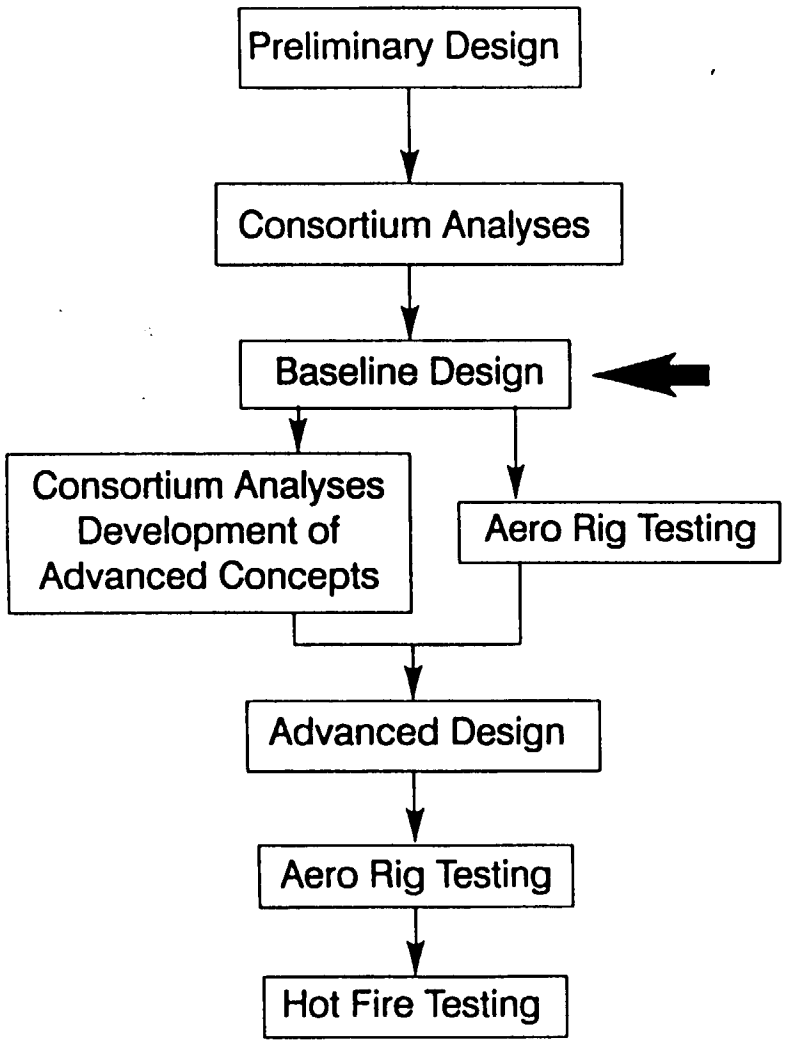

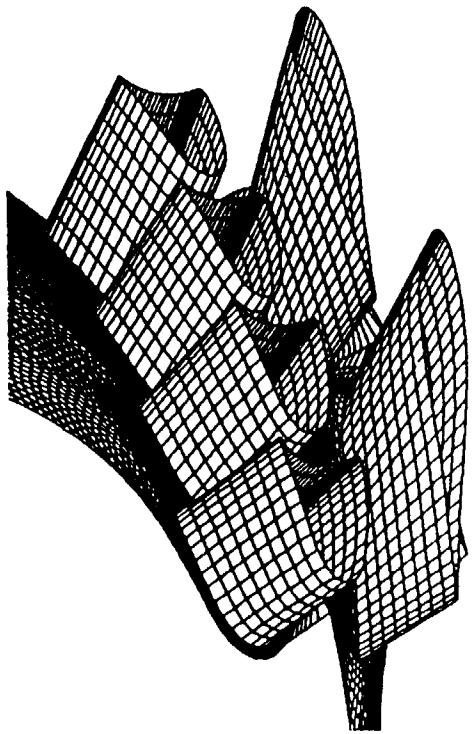

FIGURE 3
OXIDIZER TURBINE BASELINE DESIGN

Hot T/P Design Requirements (NLS Design Table Revision 8A)

Working Fluid	O2/H2
Gas Constant (ft-lbf/°R-lbm)	412.62
Ratio of Specific Heats	1.37
Inlet Pressure (psia)	542.8
Inlet Temperature (°R)	1307.0
Shaft Speed (rpm)	7880.0
Pressure Ratio	1.60
Flow Rate (lbm/s)	60.42
Power (Hp)	19020.
Efficiency (Turbine T-T)	72.7

FIGURE 4
OXIDIZER TURBINE BASELINE DESIGN

Aerodynamic Design Process

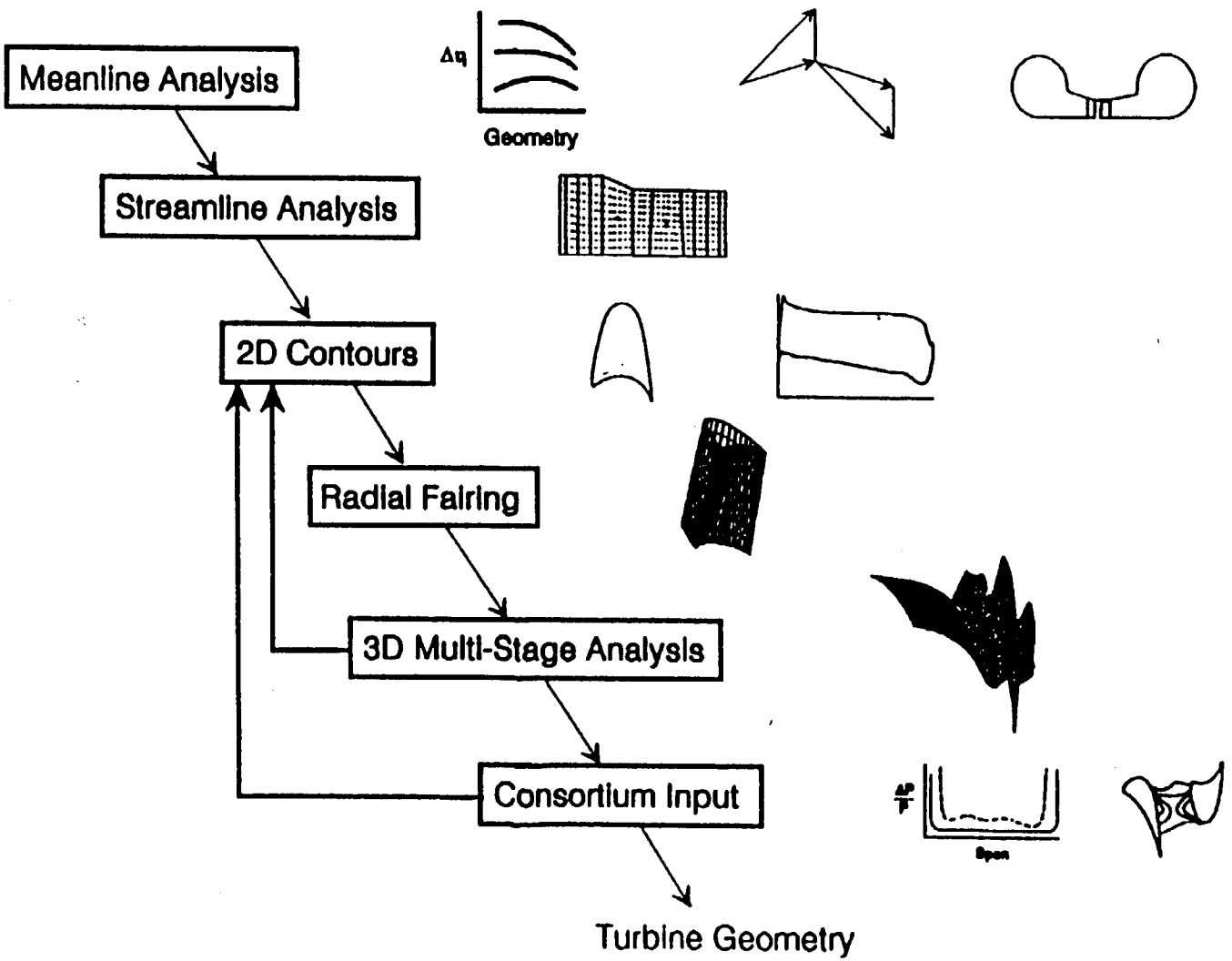

FIGURE 5
OXIDIZER TURBINE BASELINE DESIGN

Full Scale Turbine Flowpath

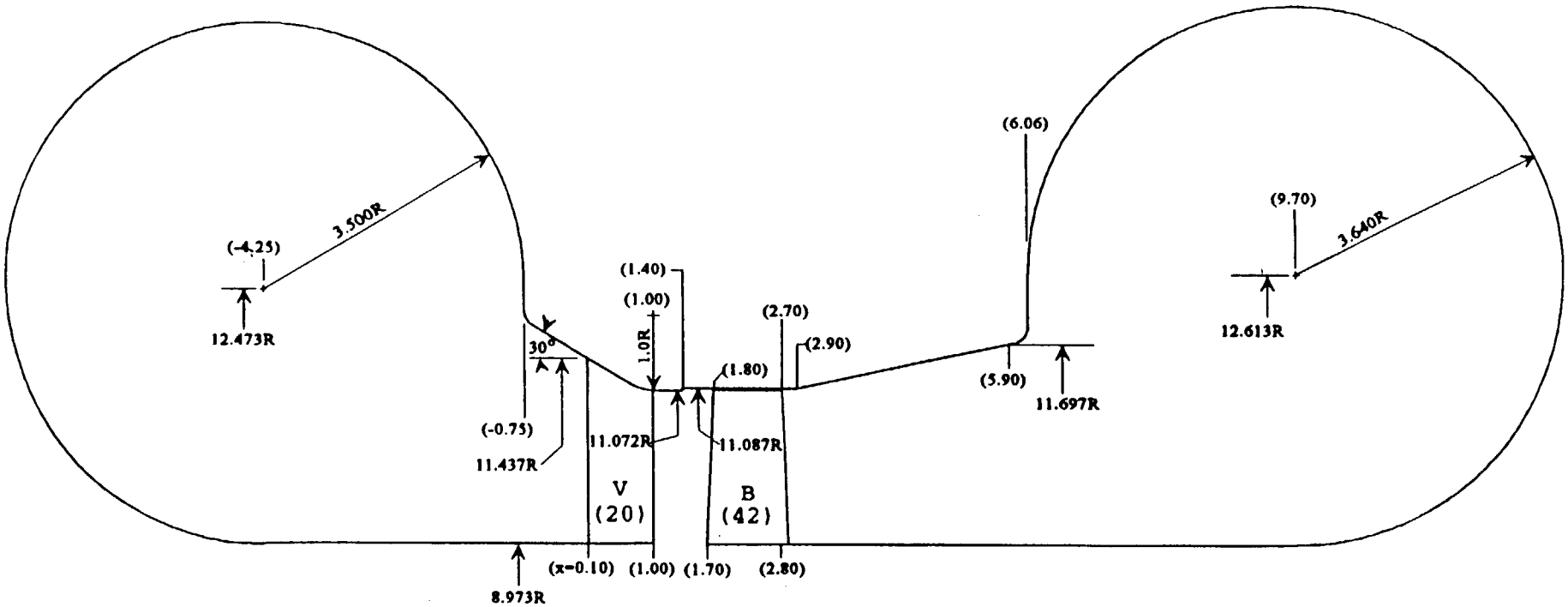

Axial Location - ( )

FIGURE 6A
OXIDIZER TURBINE BASELINE DESIGN

Inlet Volute - 50% Scale OTTR Flowpath

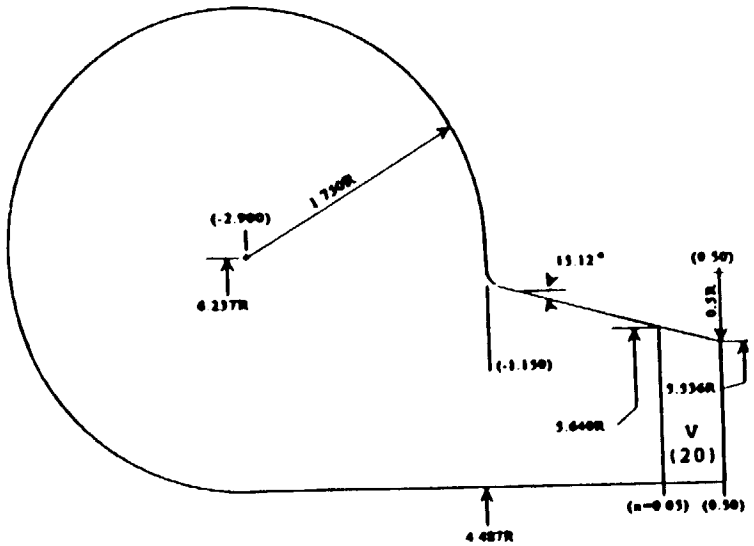

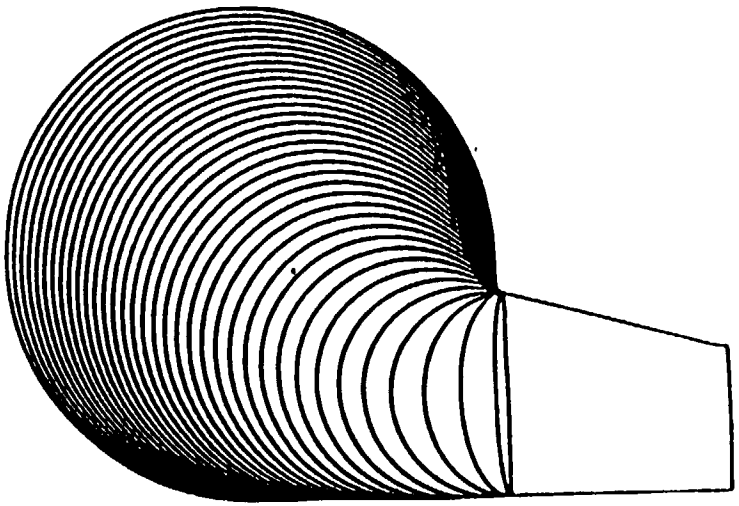

Axial Location - ( )

FIGURE 6B
OXIDIZER TURBINE BASELINE DESIGN

Inlet Volute - Unigraphics Wire Frame Mesh

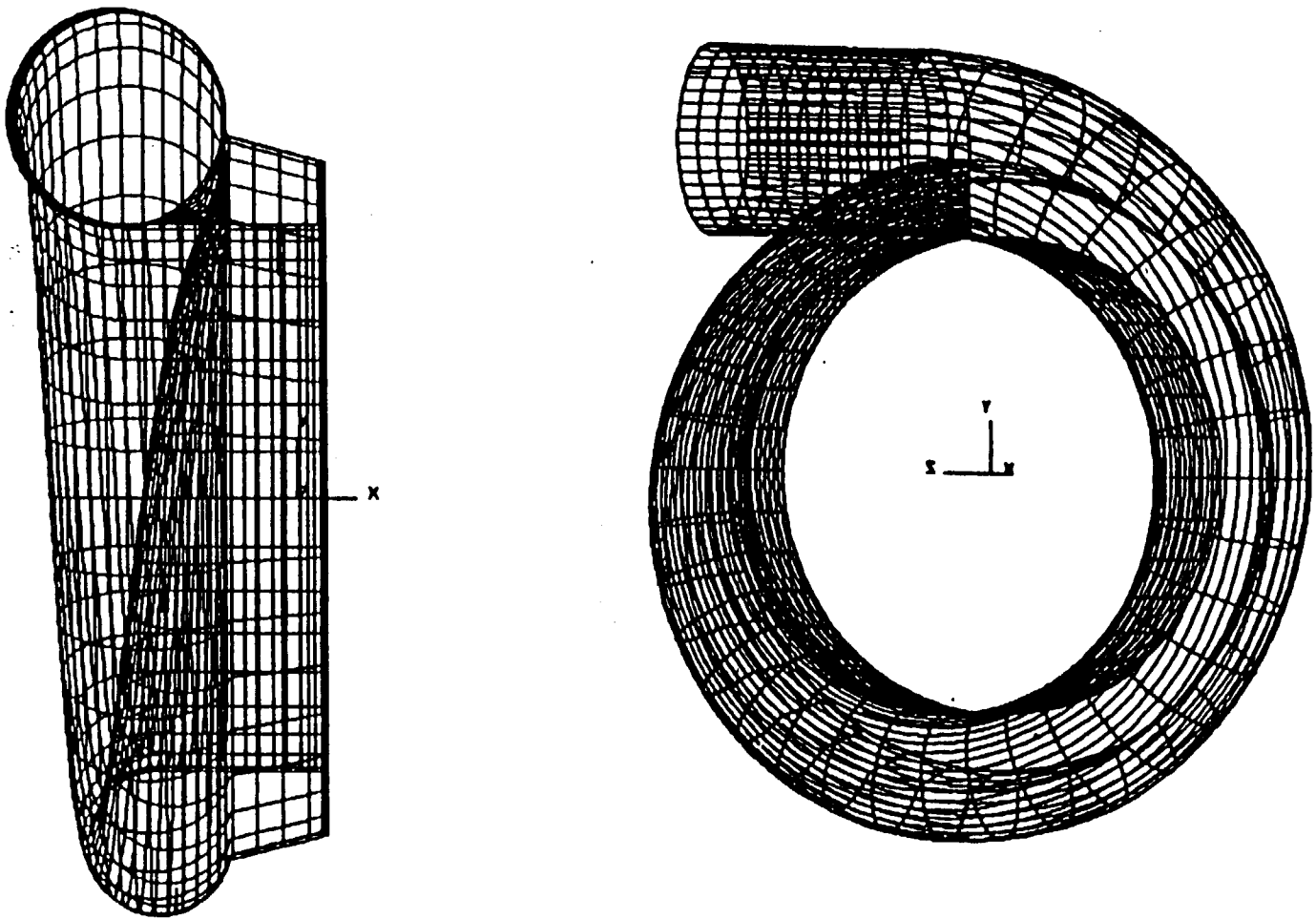

FIGURE 6C
OXIDIZER TURBINE BASELINE DESIGN

Inlet Volute - Geometry Definition

Geometry

22+ Cross-Sections

IGES File on Diskette

-- "BASELINE-INLET-VOLUTE.IGES"

Euler Results

PLOT3D Files

-- " BASELINE-INLET-VOLUTE.Q"

-- " BASELINE-INLET-VOLUTE.XYZ"

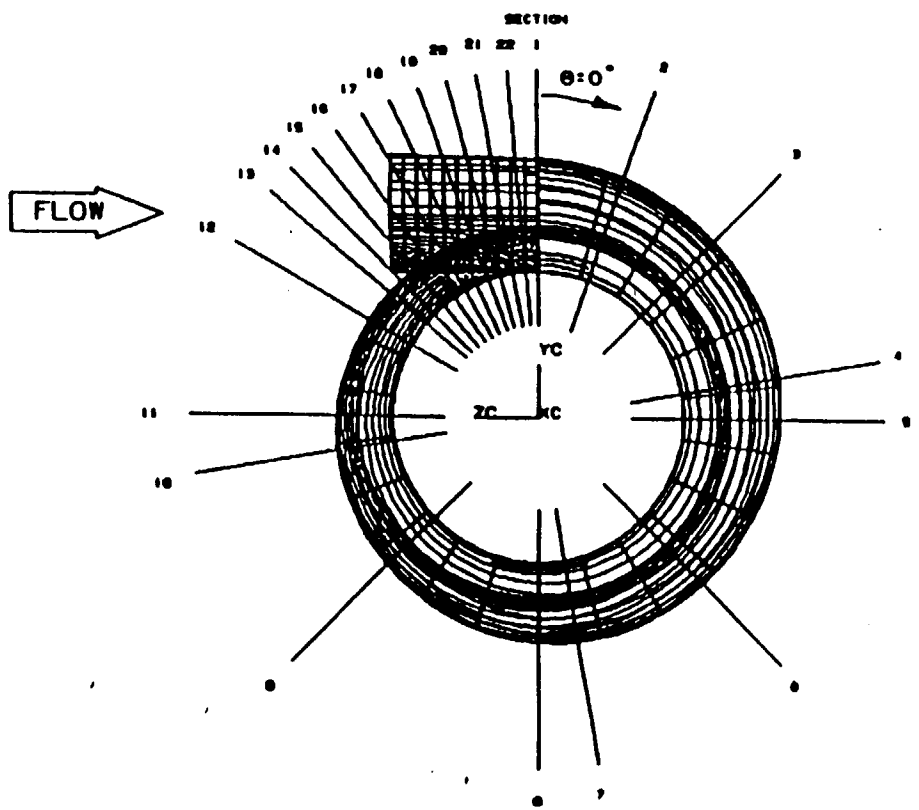

VIEW IS AFT OF TURBINE LOOKING FORWARD

FIGURE 7
OXIDIZER TURBINE BASELINE DESIGN

Inlet Volute - Predicted Static Pressure Distribution at Vane Inlet Plane

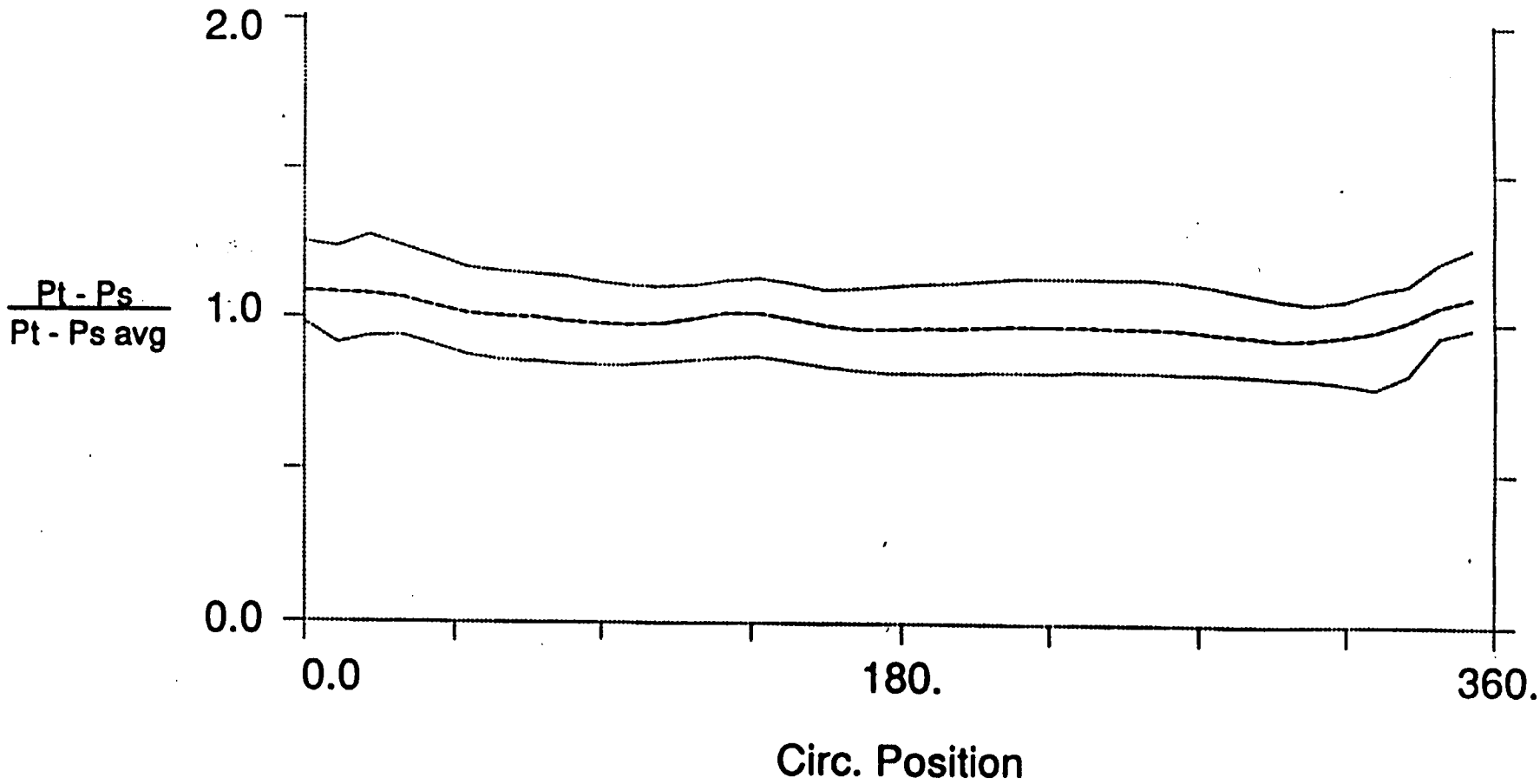

FIGURE 8
OXIDIZER TURBINE BASELINE DESIGN

Single Stage Oxidizer Turbine - 3D Computational Grid Viewed from Front

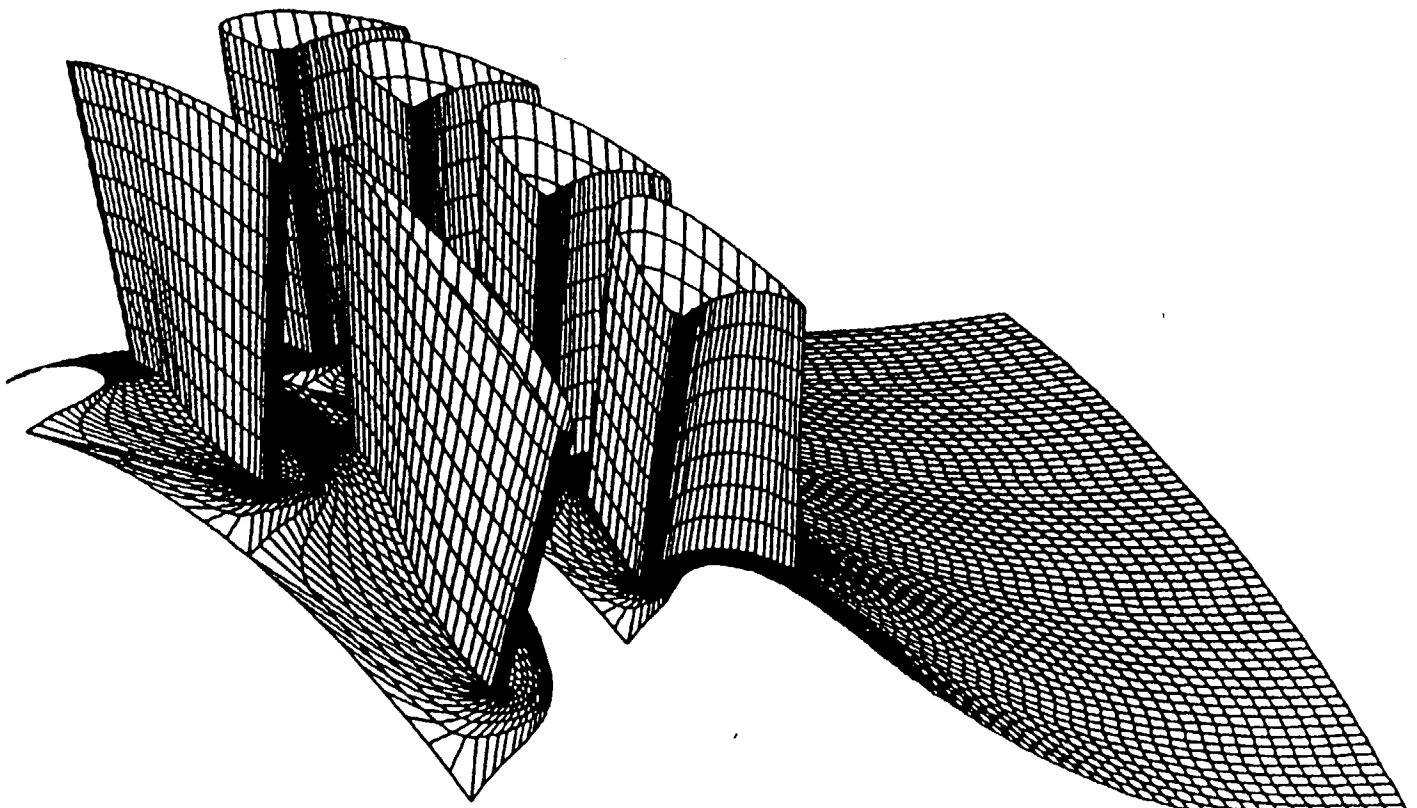

FIGURE 9A
OXIDIZER TURBINE BASELINE DESIGN

Vane Elevation

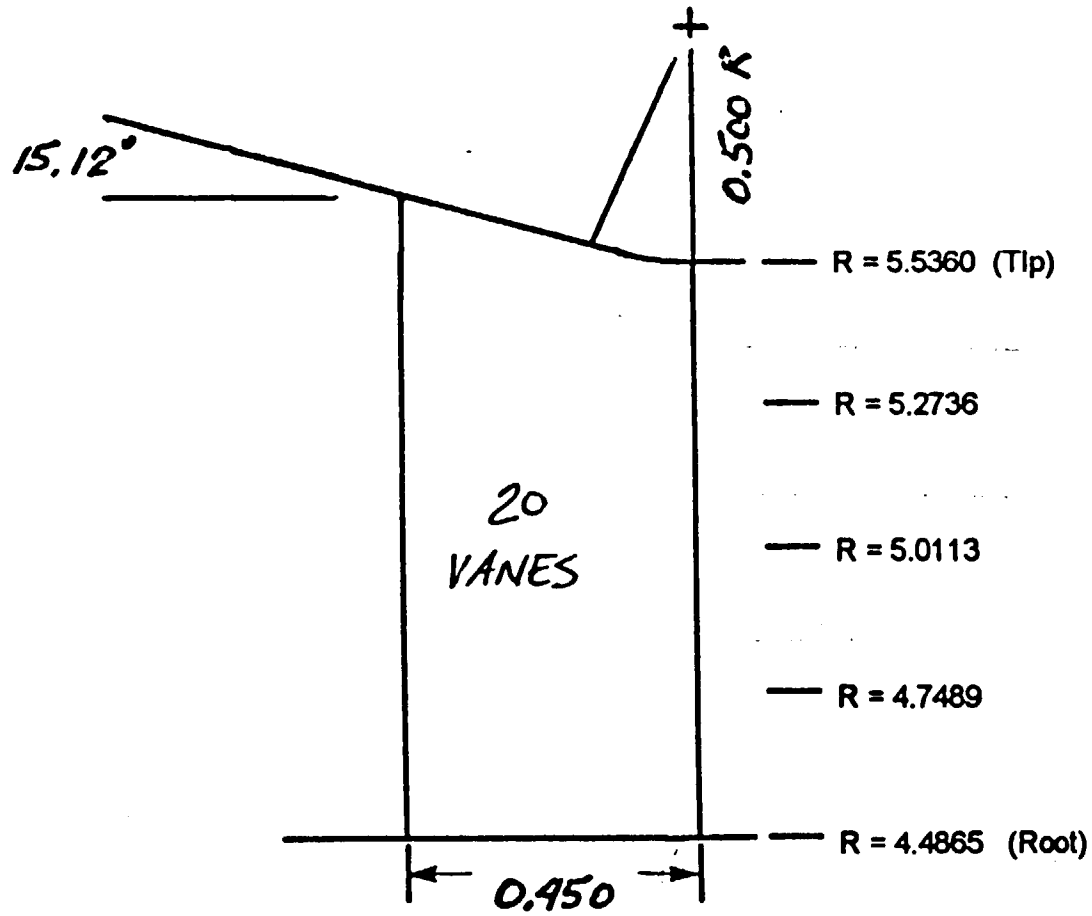

NOTES:
1. Reference Drawing 80M52760 For Machining Details
2. Number of Vanes is 20.
3. Vane is Curved Line Faired Through Defining Sections.

FIGURE 9B
OXIDIZER TURBINE BASELINE DESIGN

Vane - Stacked Airfoil Sections

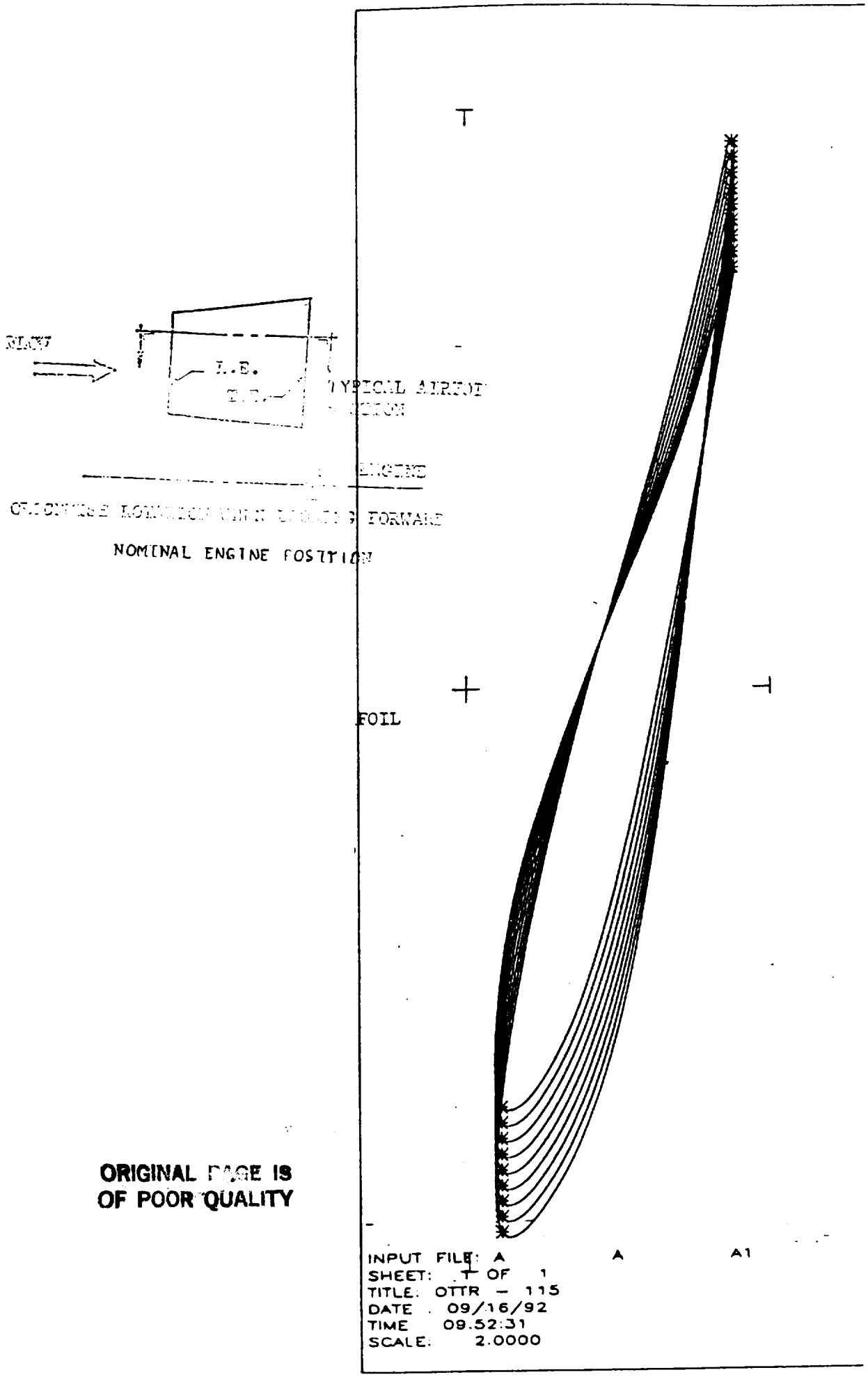

ORIGINAL PAGE IS
OF POOR QUALITY

FIGURE 9C
OXIDIZER TURBINE BASELINE DESIGN

Vane - Section at Radius=4.4865

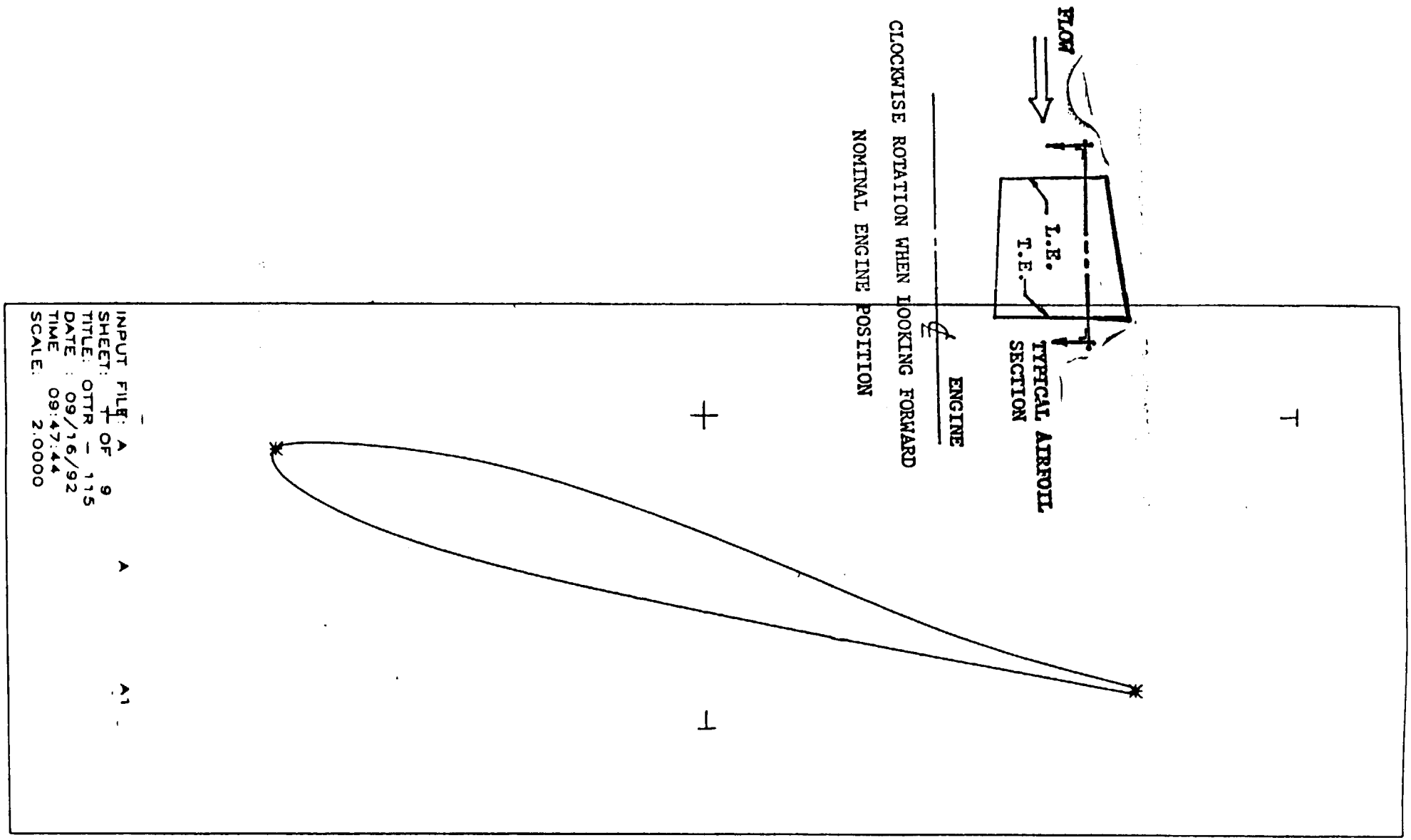

FIGURE 9D
OXIDIZER TURBINE BASELINE DESIGN

Vane - Section at Radius=4.7489

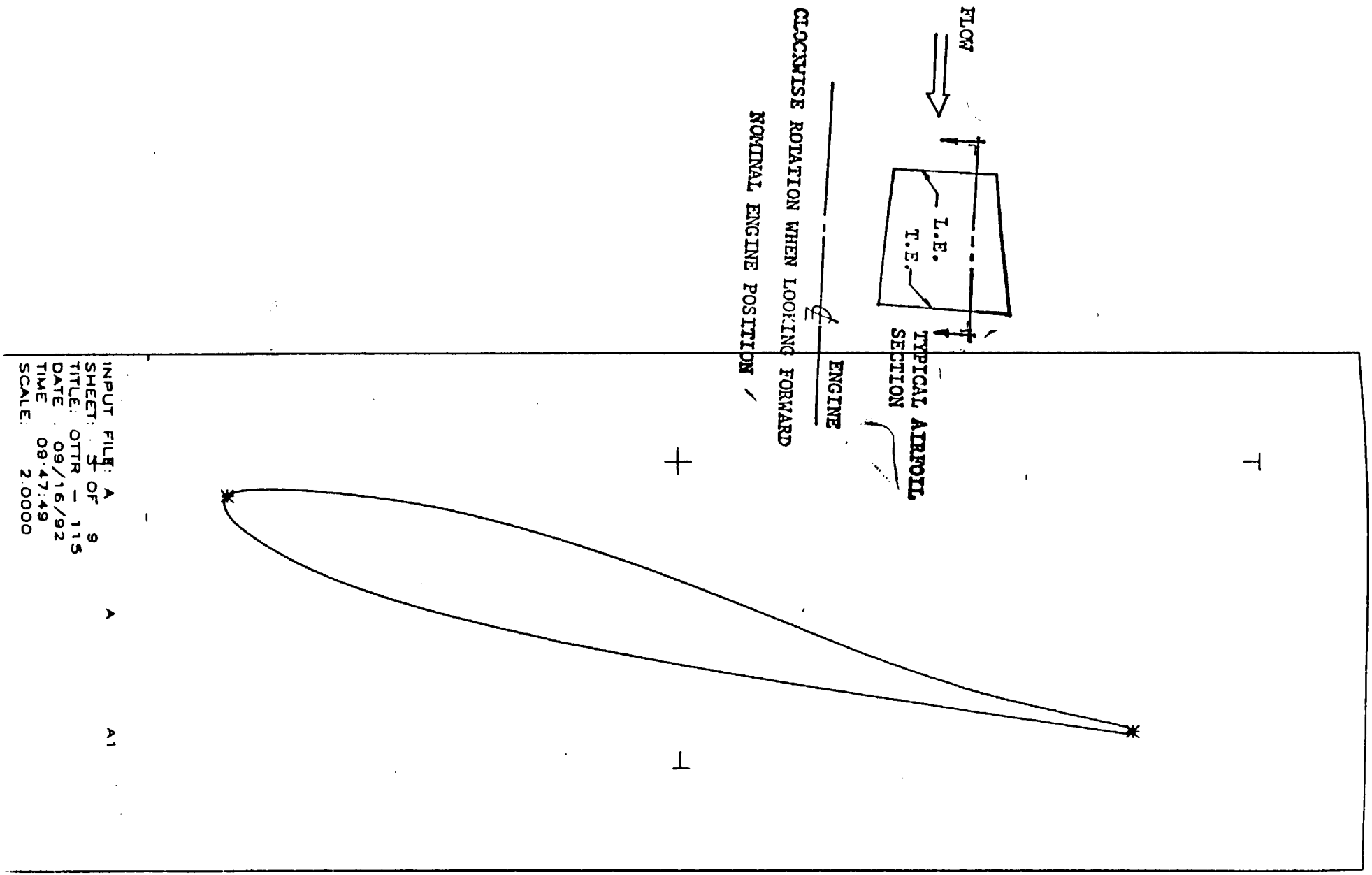

FIGURE 9E
OXIDIZER TURBINE BASELINE DESIGN

Vane - Section at Radius=5.0113

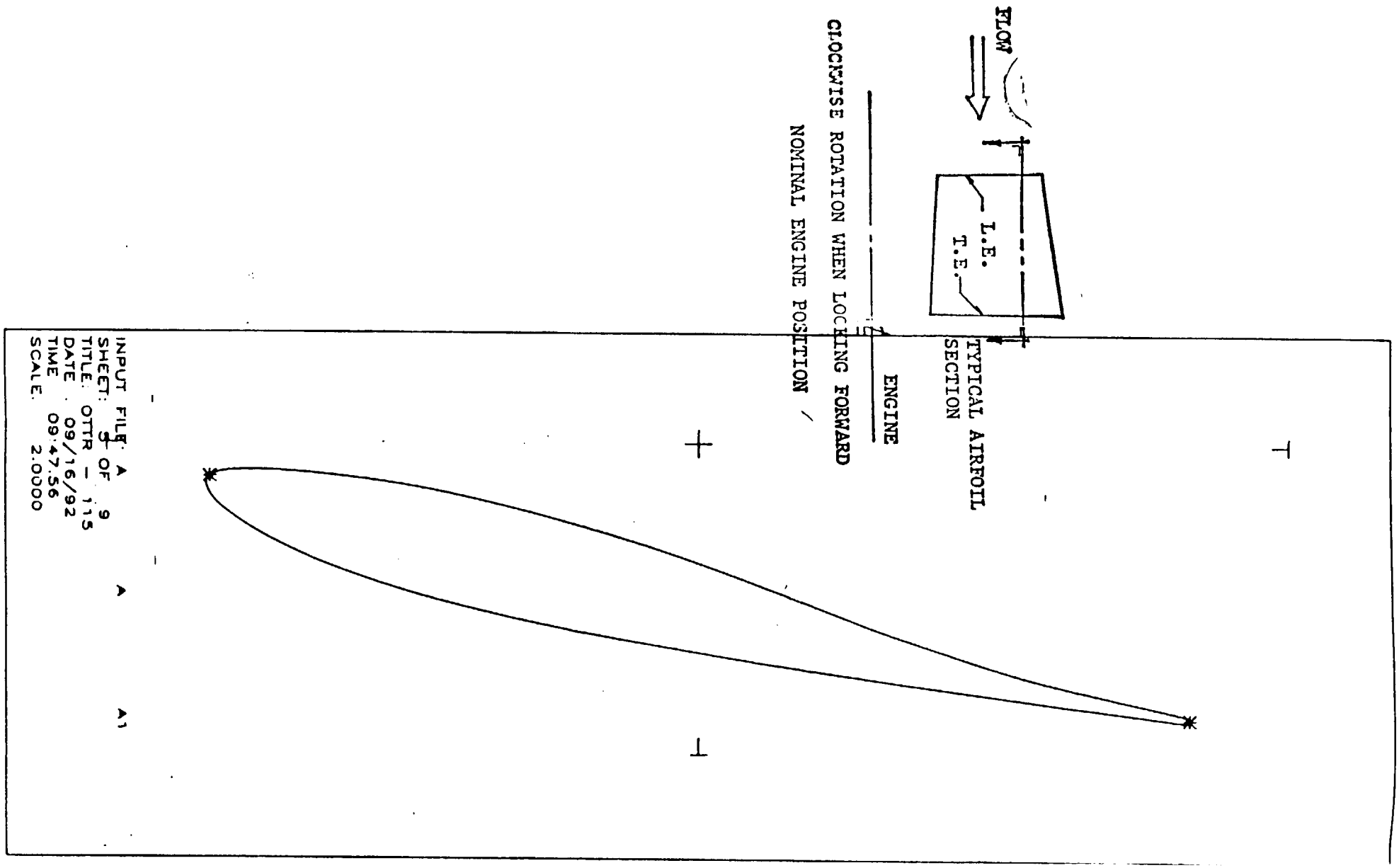

FIGURE 9F
OXIDIZER TURBINE BASELINE DESIGN

Vane - Section at Radius=5.2736

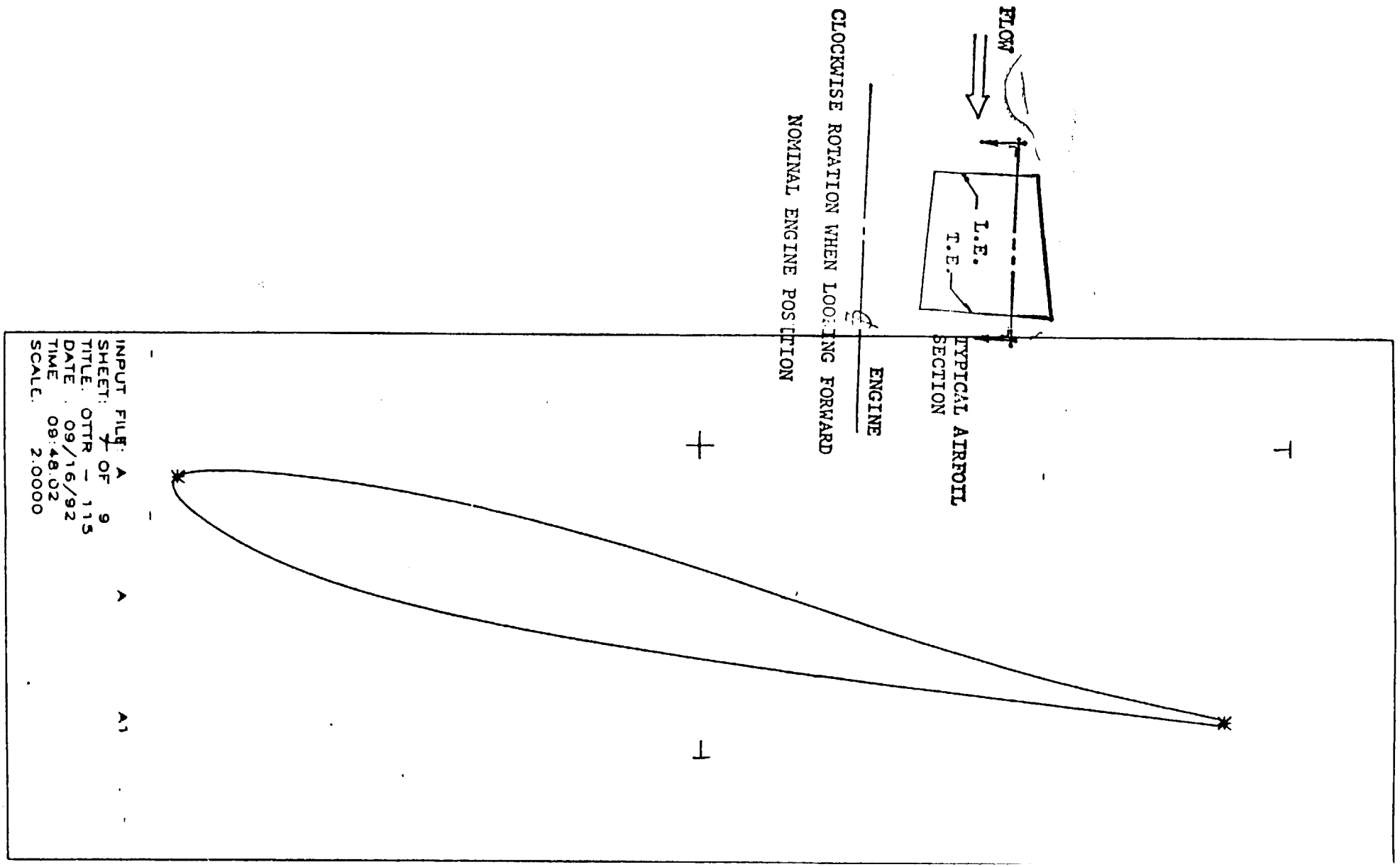

FIGURE 9G
OXIDIZER TURBINE BASELINE DESIGN

Vane - Section at Radius=5.5360

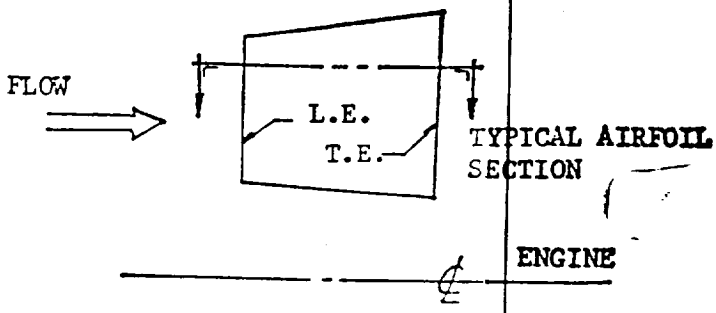

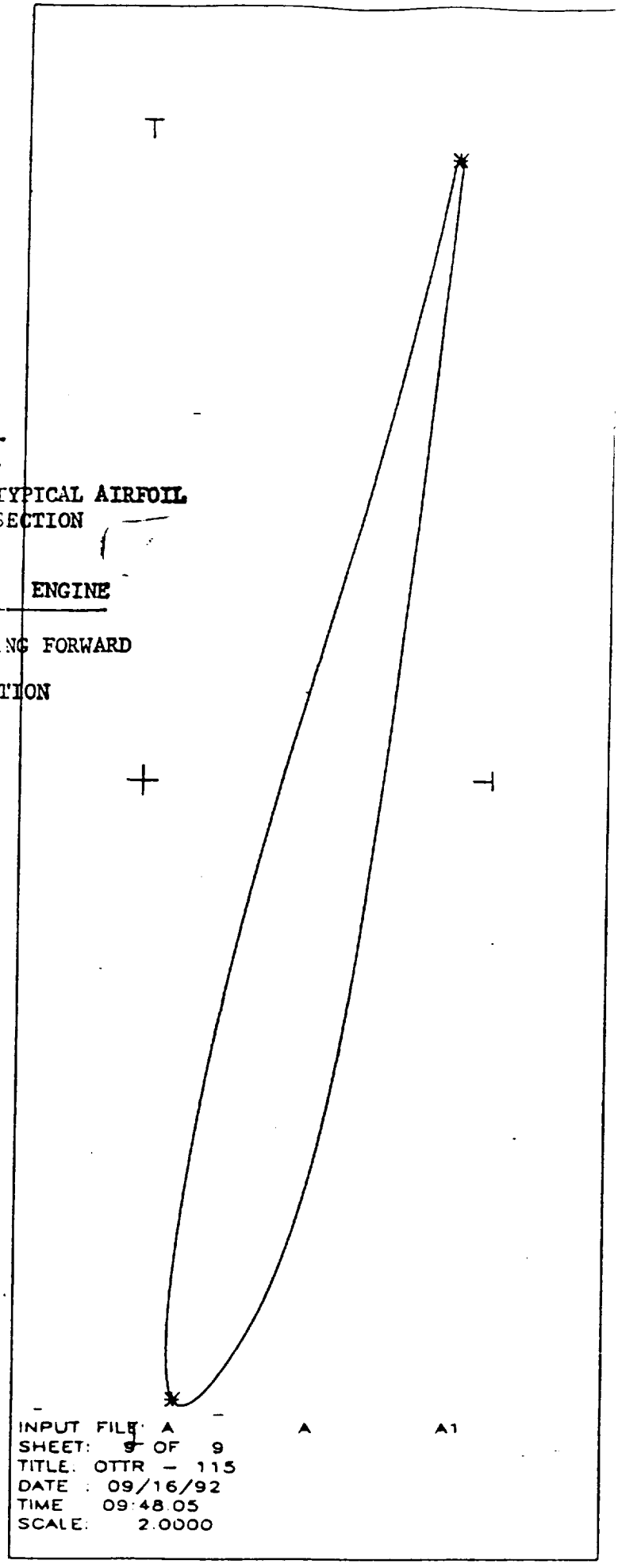

FIGURE 10A
OXIDIZER TURBINE BASELINE DESIGN

Vane - Pressure Distribution at 0% Span

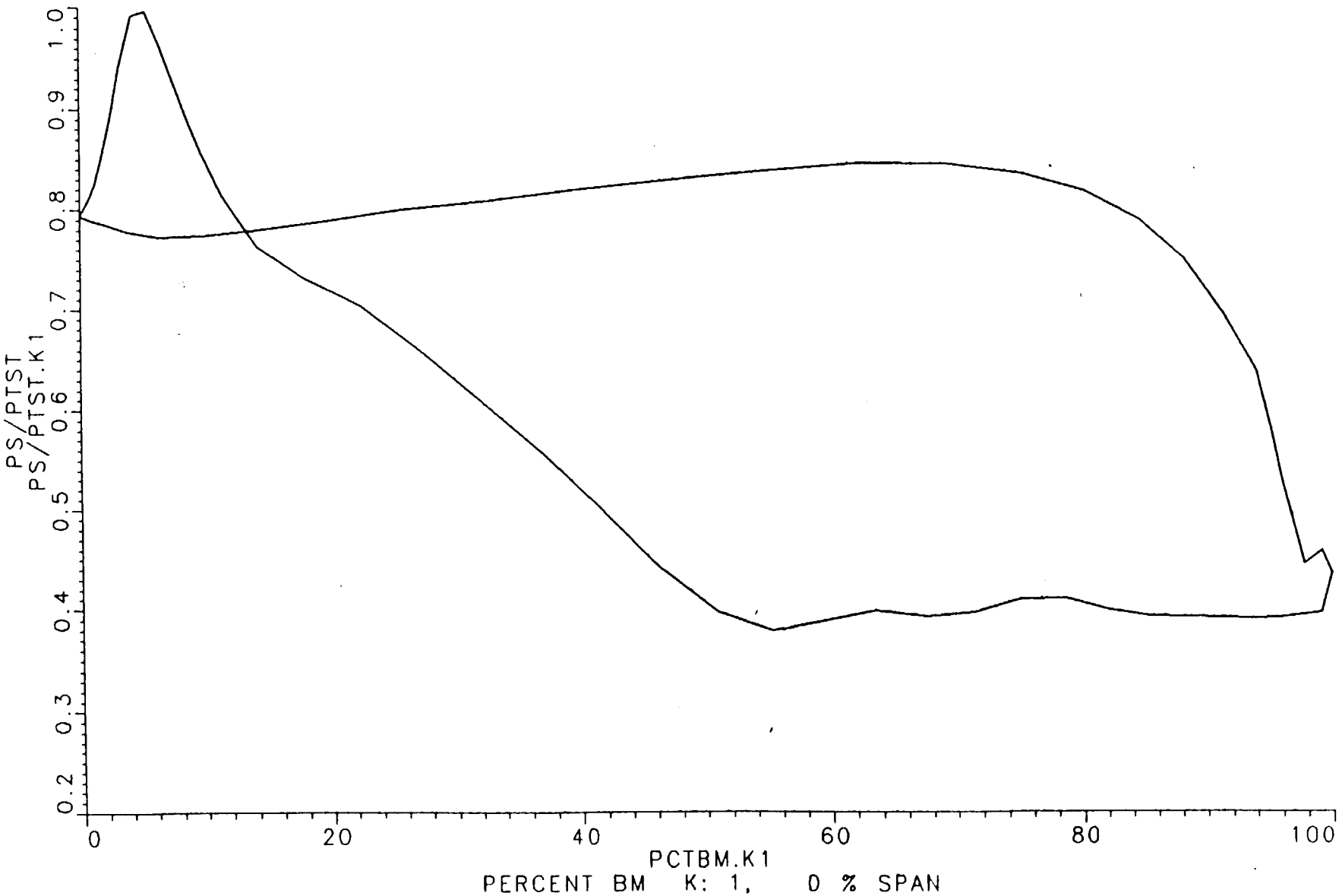

FIGURE 10B
OXIDIZER TURBINE BASELINE DESIGN

Vane - Pressure Distribution at 25% Span

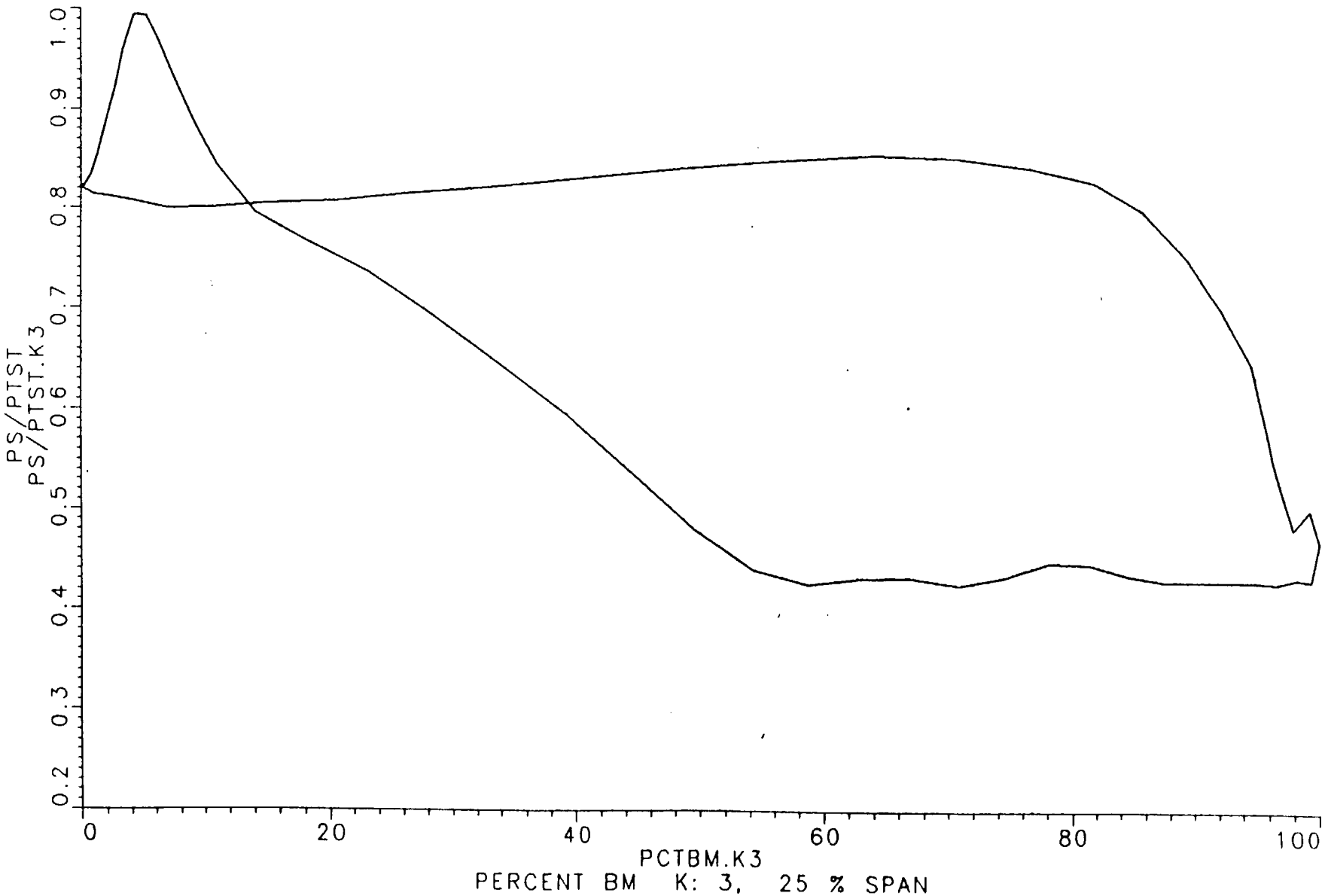

FIGURE 10C
OXIDIZER TURBINE BASELINE DESIGN

Vane - Pressure Distribution at 50% Span

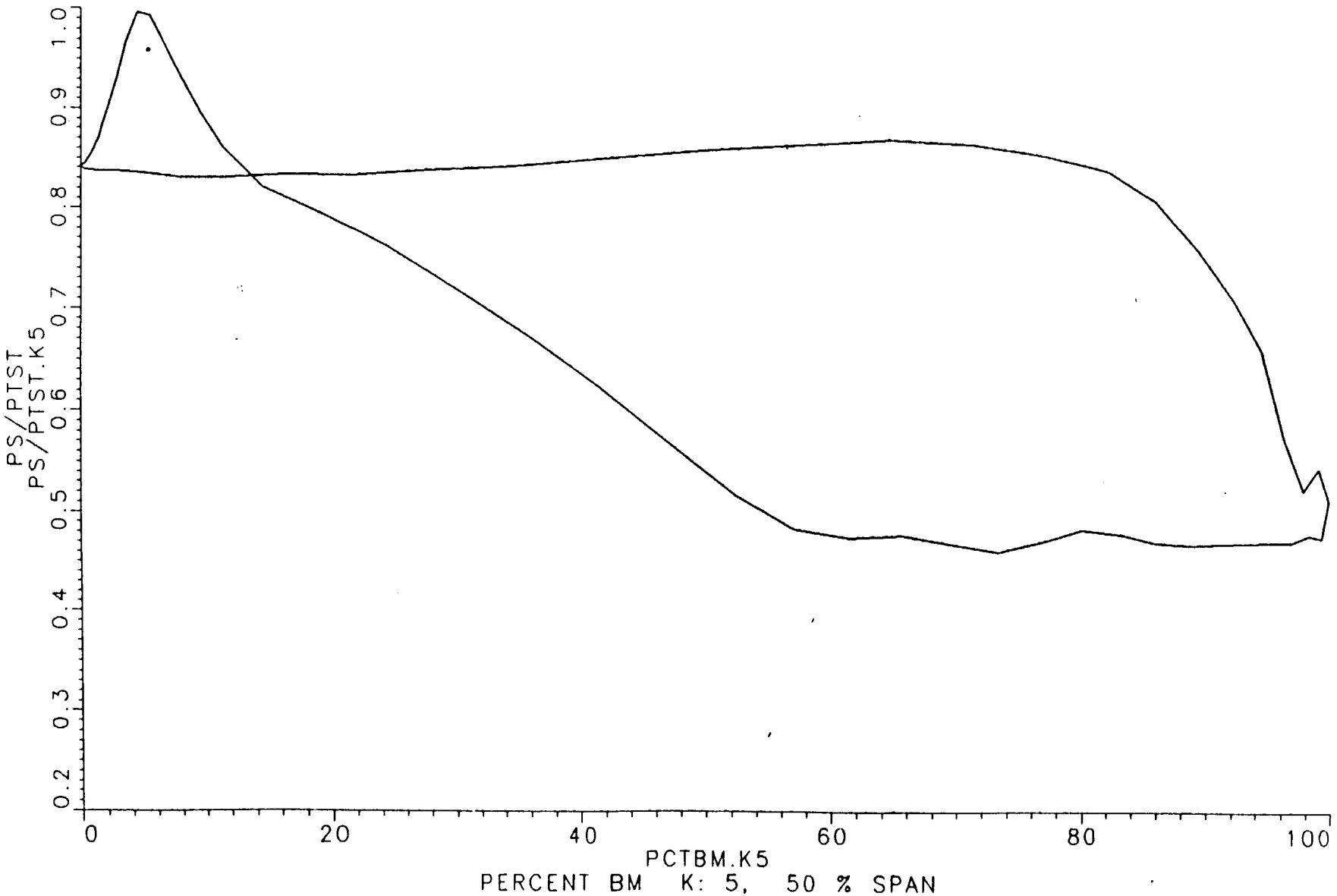

FIGURE 10D
OXIDIZER TURBINE BASELINE DESIGN

Vane - Pressure Distribution at 75% Span

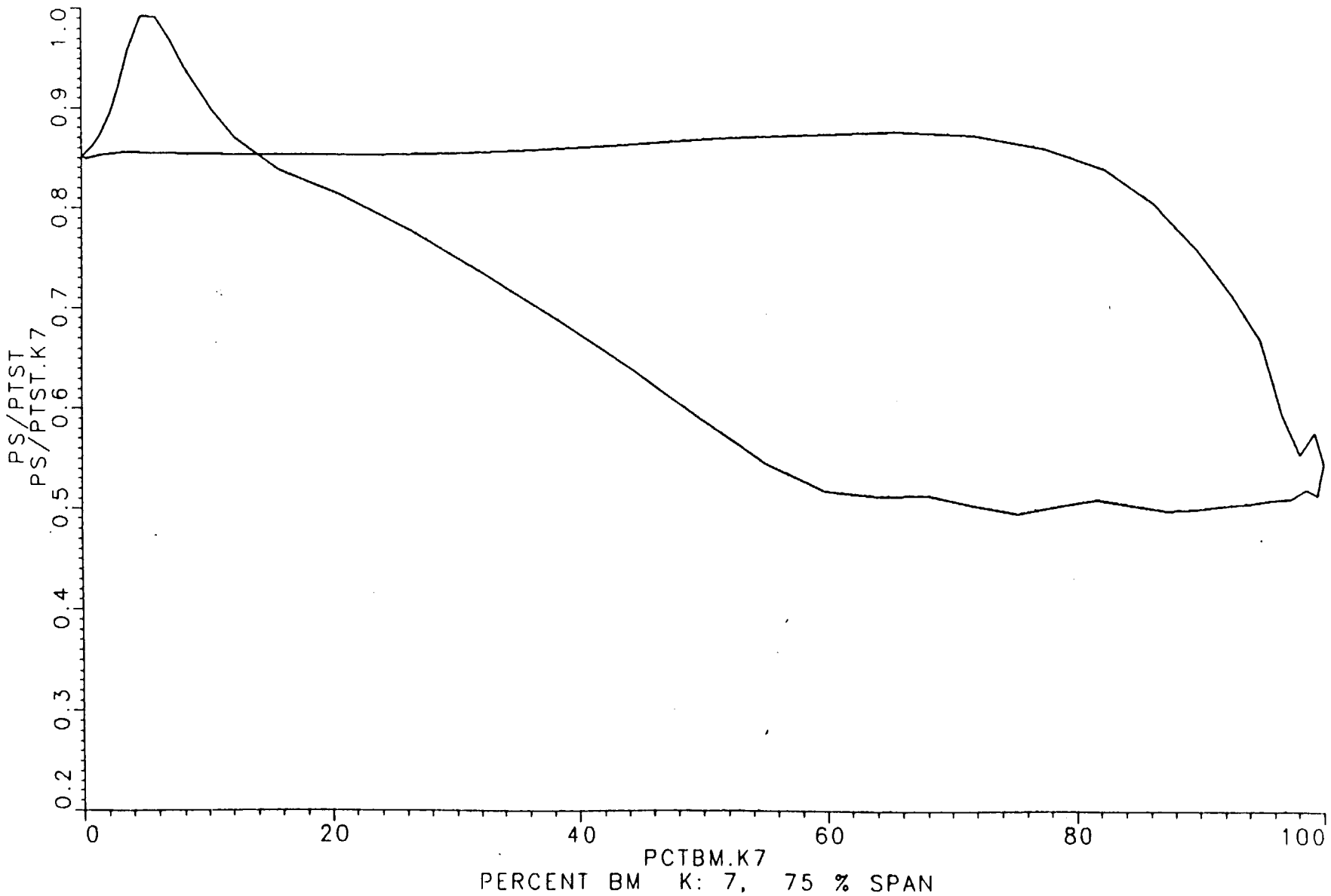

FIGURE 10E
OXIDIZER TURBINE BASELINE DESIGN

Vane - Pressure Distribution at 100% Span

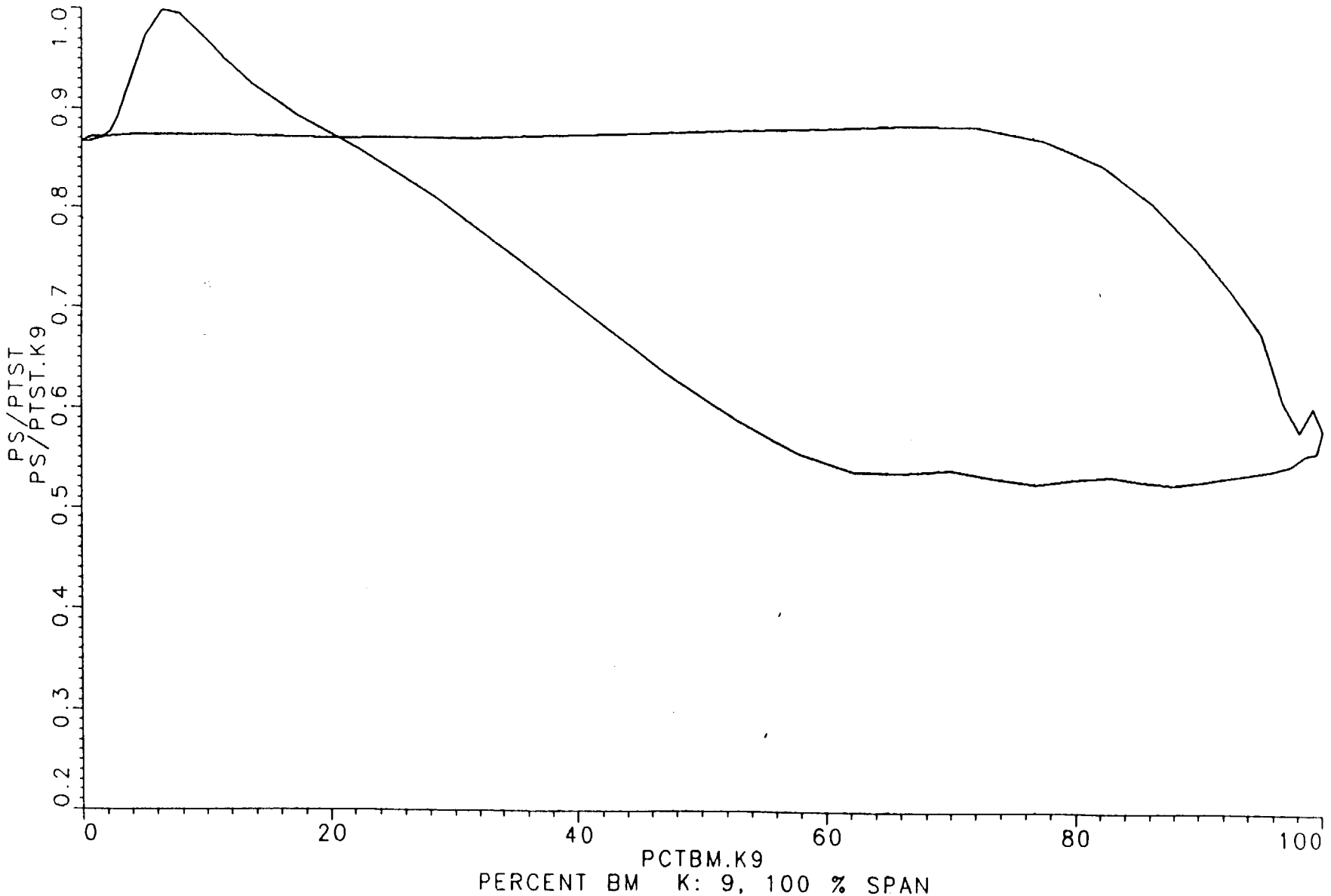

FIGURE IIA
OXIDIZER TURBINE BASELINE DESIGN

Blade Elevation

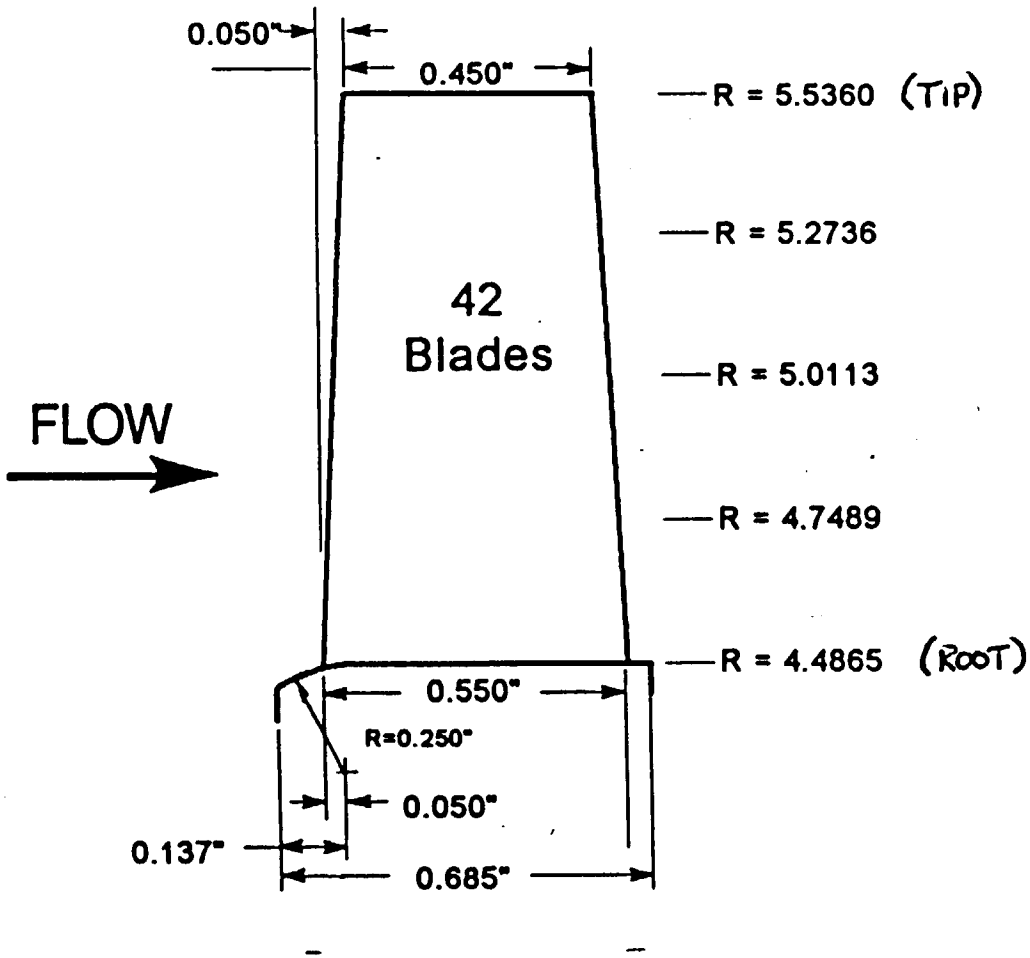

NOTES:
1. Reference Drawing 80M52752 For Machining Details
2. Number of Blades is 42
3. Blade is Curve Line Faired Through Defining Sections
4. Rotation is Clockwise when viewed from Aft looking Forward

FIGURE 11B
OXIDIZER TURBINE BASELINE DESIGN

Blade - Stacked Airfoil Sections

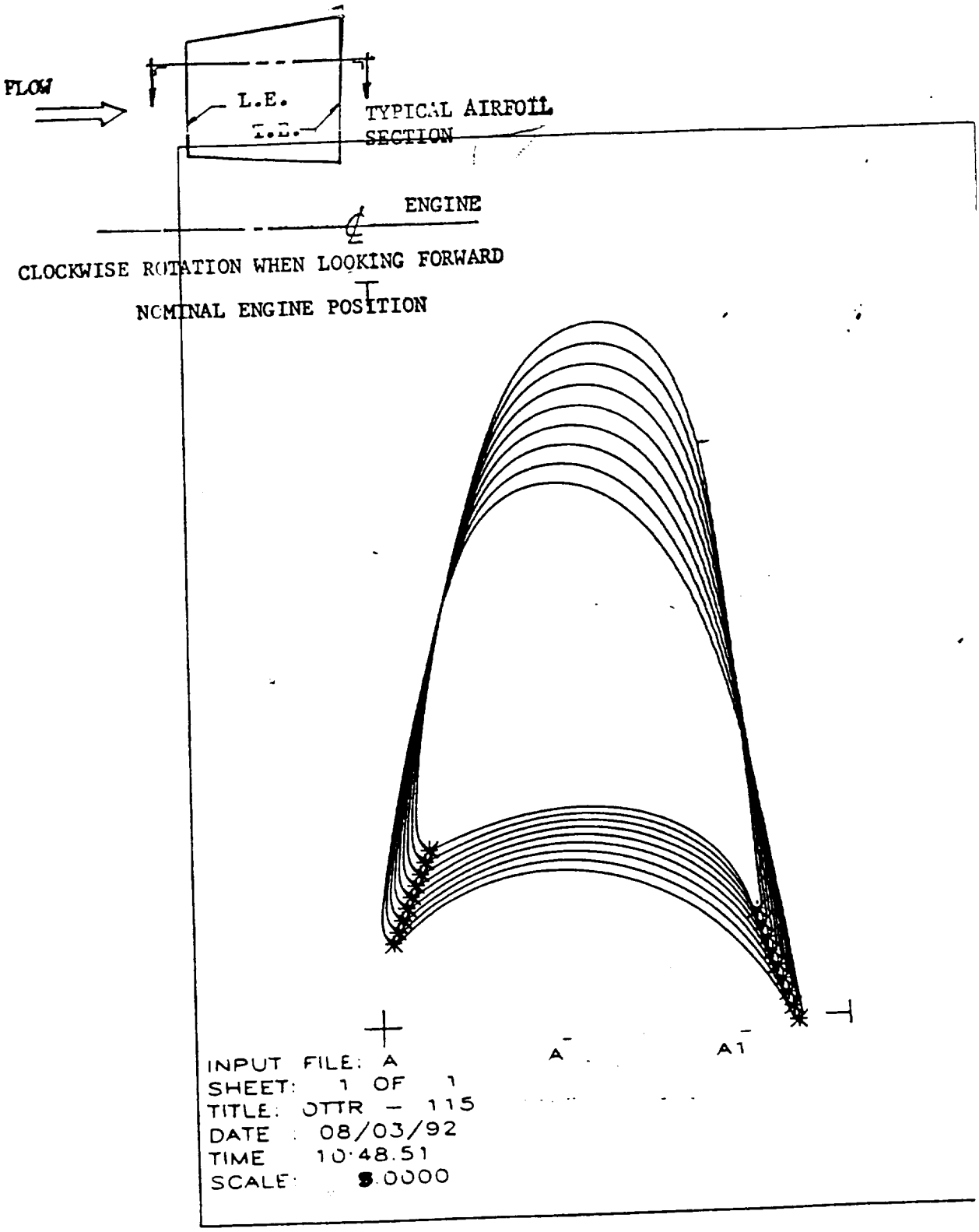

FIGURE IIC
OXIDIZER TURBINE BASELINE DESIGN

Blade - Section at Radius=4.4865

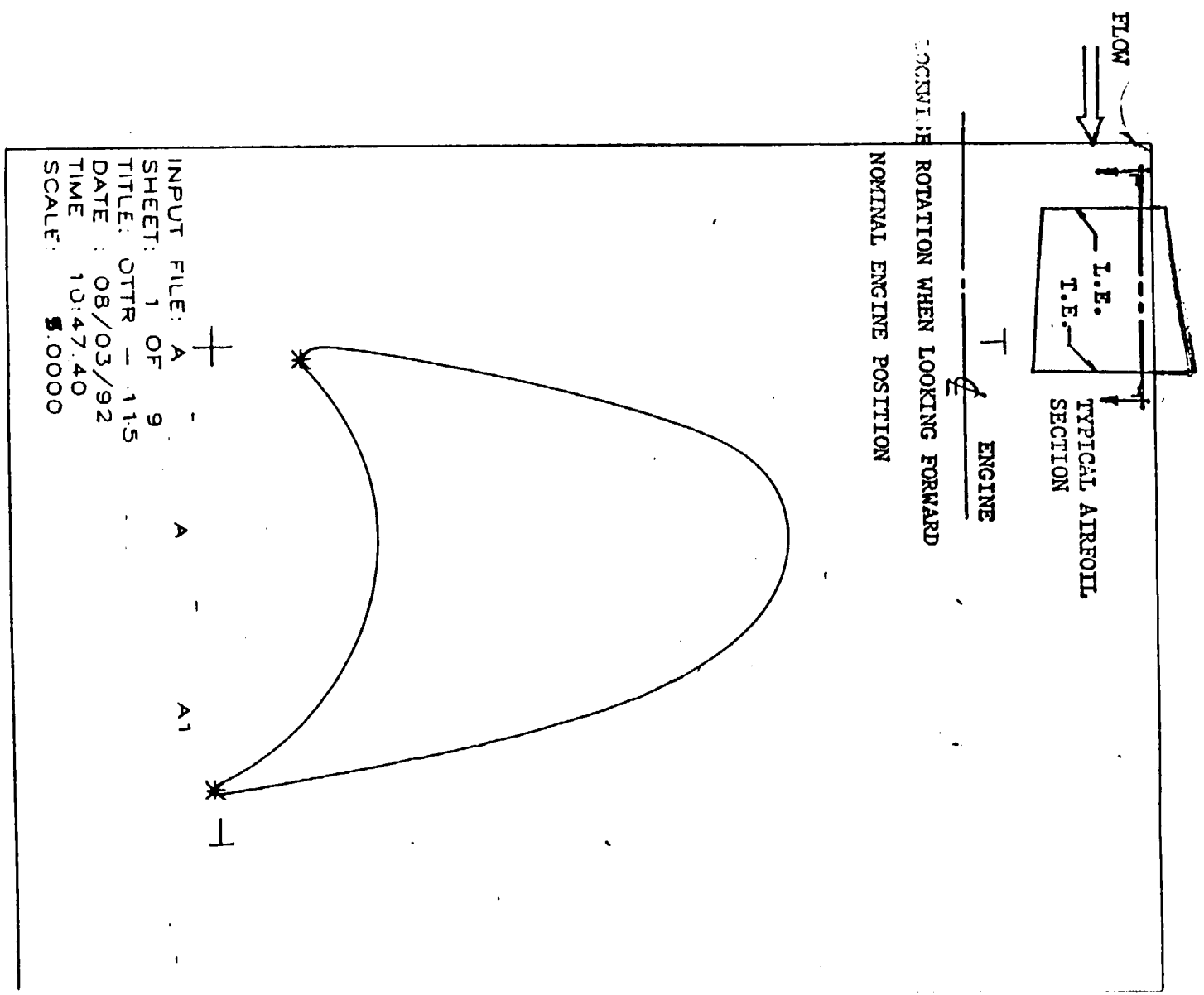

FIGURE IID
OXIDIZER TURBINE BASELINE DESIGN

Blade - Section at Radius=4.7489

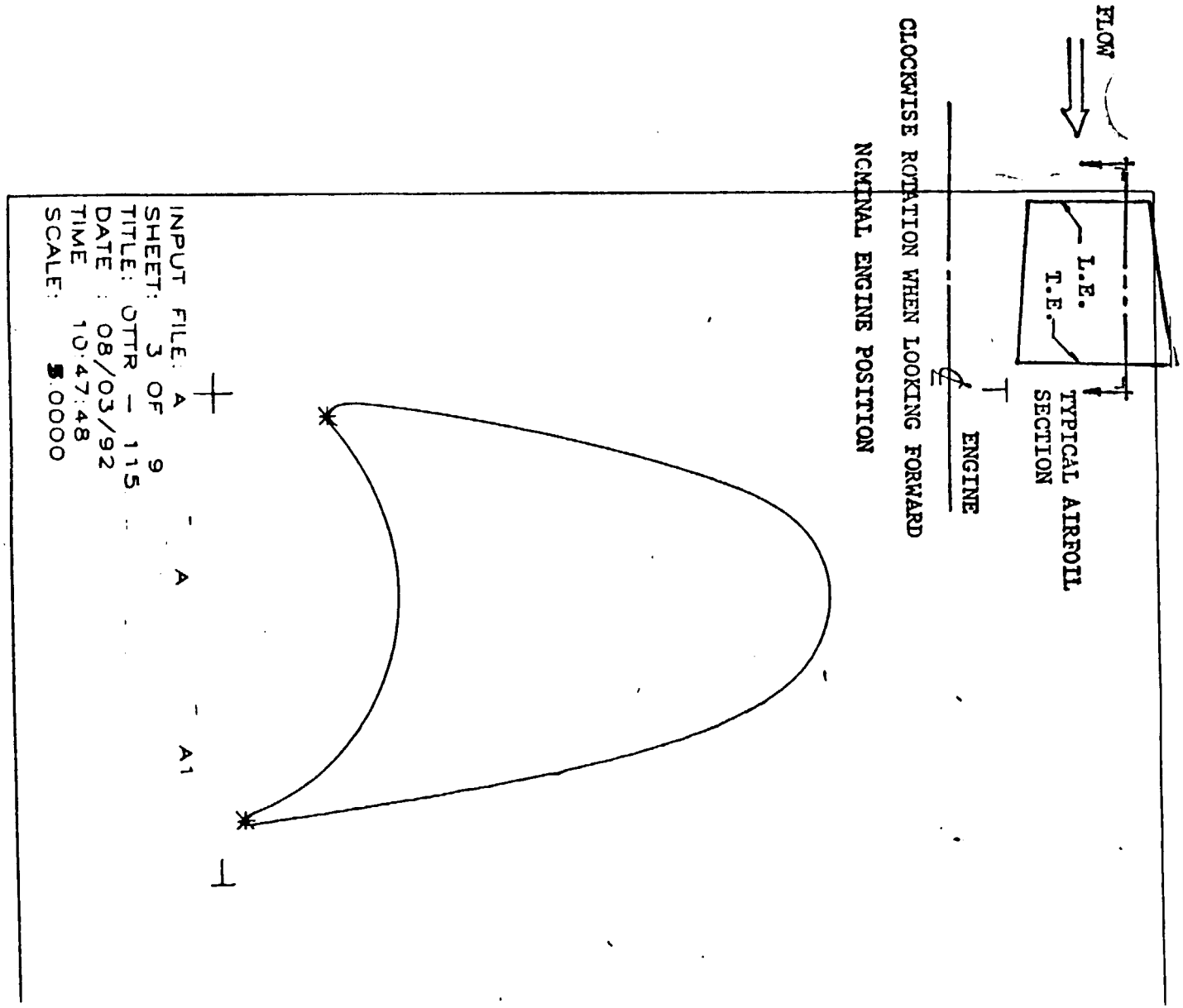

FIGURE IIE
OXIDIZER TURBINE BASELINE DESIGN

Blade - Section at Radius=5.0113

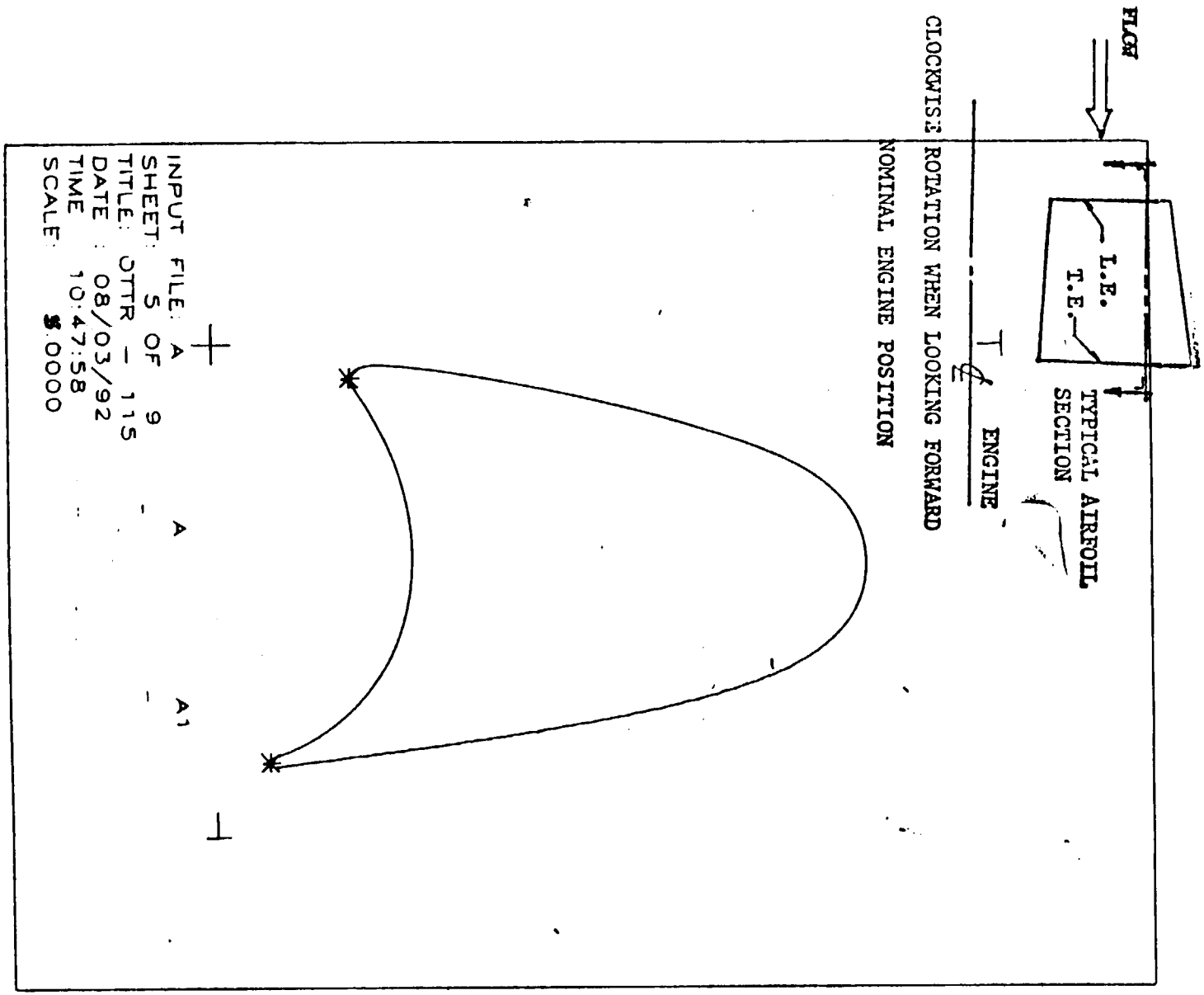

FIGURE IIF
OXIDIZER TURBINE BASELINE DESIGN

Blade - Section at Radius=5.2736

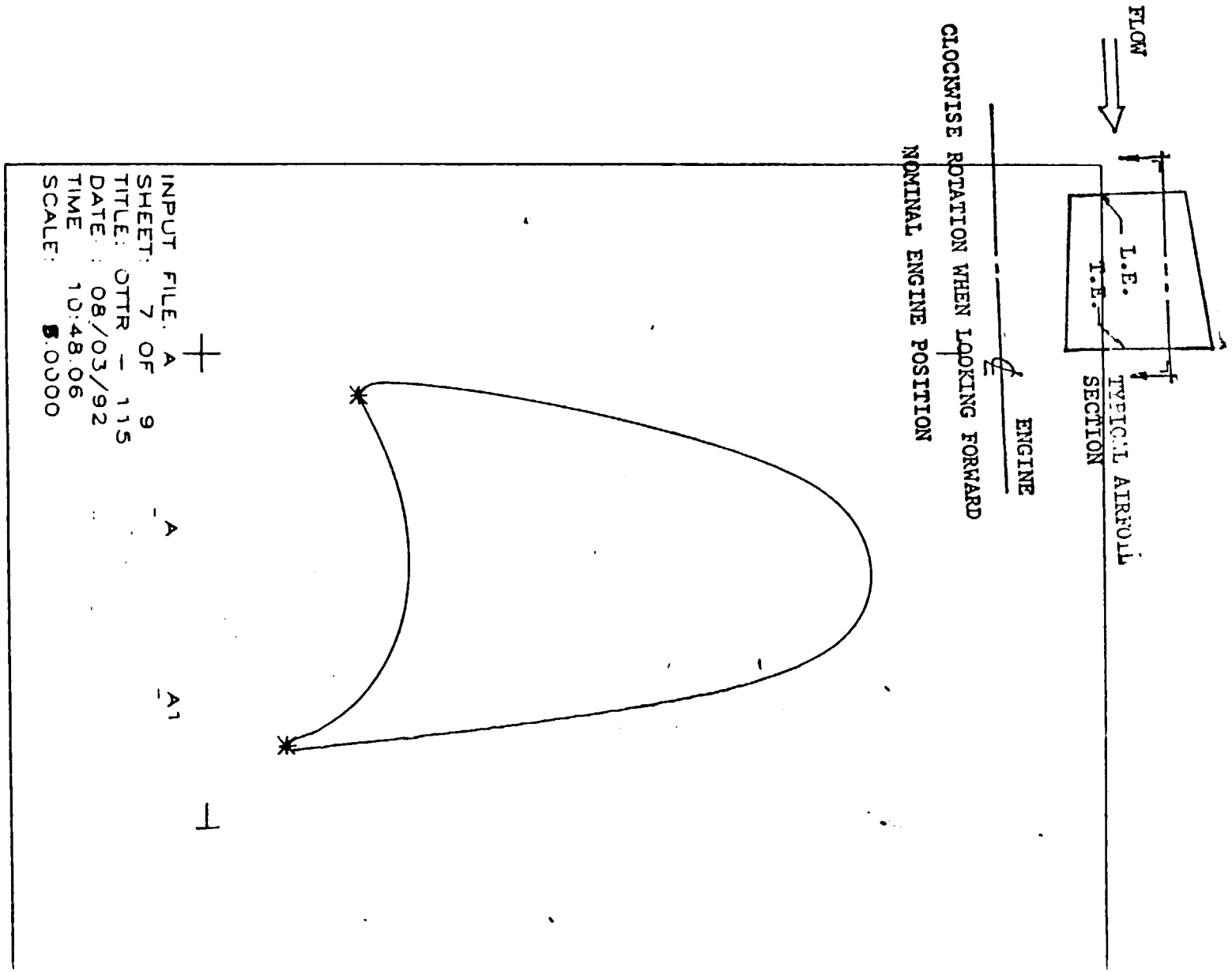

FIGURE 11G
OXIDIZER TURBINE BASELINE DESIGN

Blade - Section at Radius=5.5360

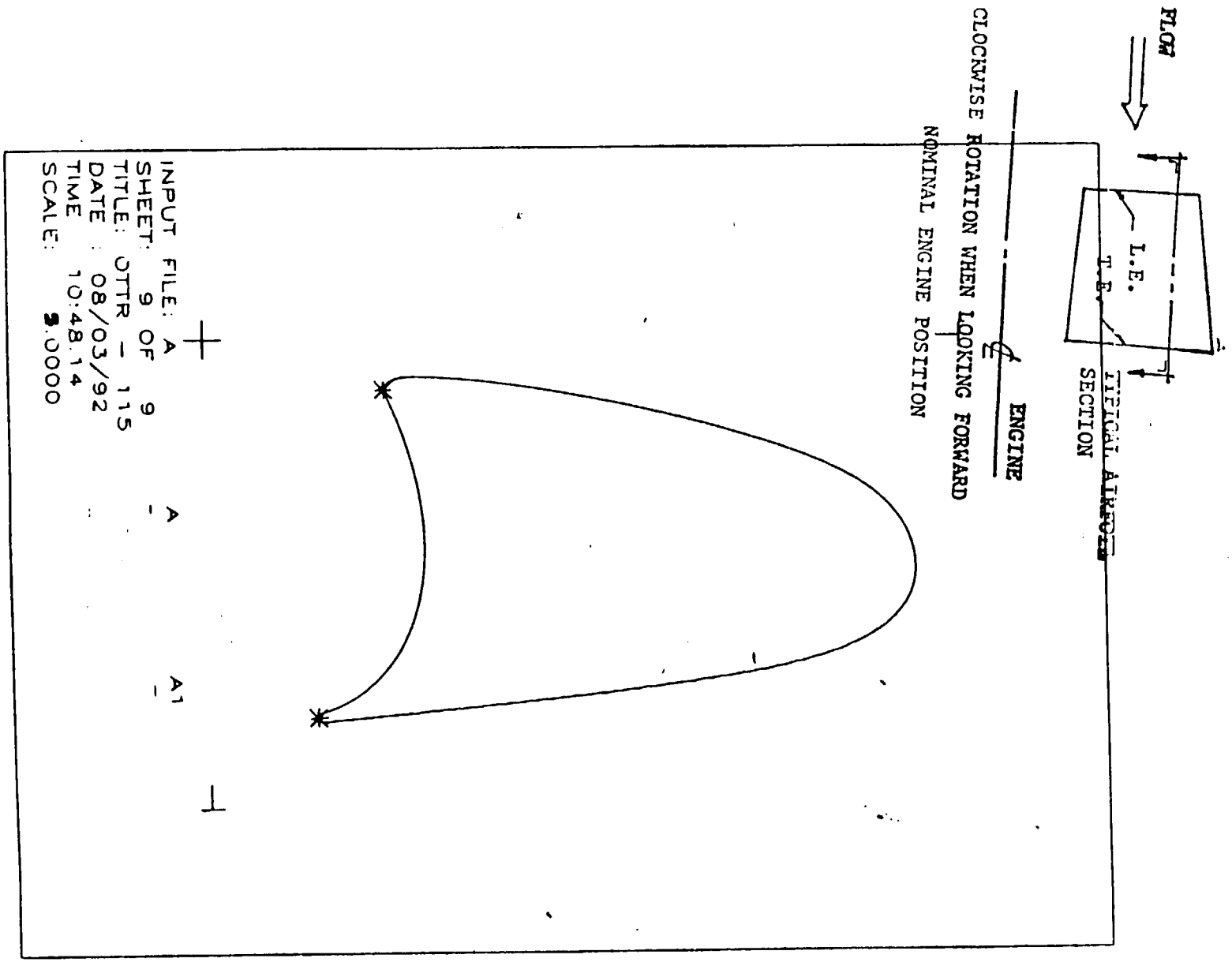

FIGURE 12A
OXIDIZER TURBINE BASELINE DESIGN

Blade - Pressure Distribution at 0% Span

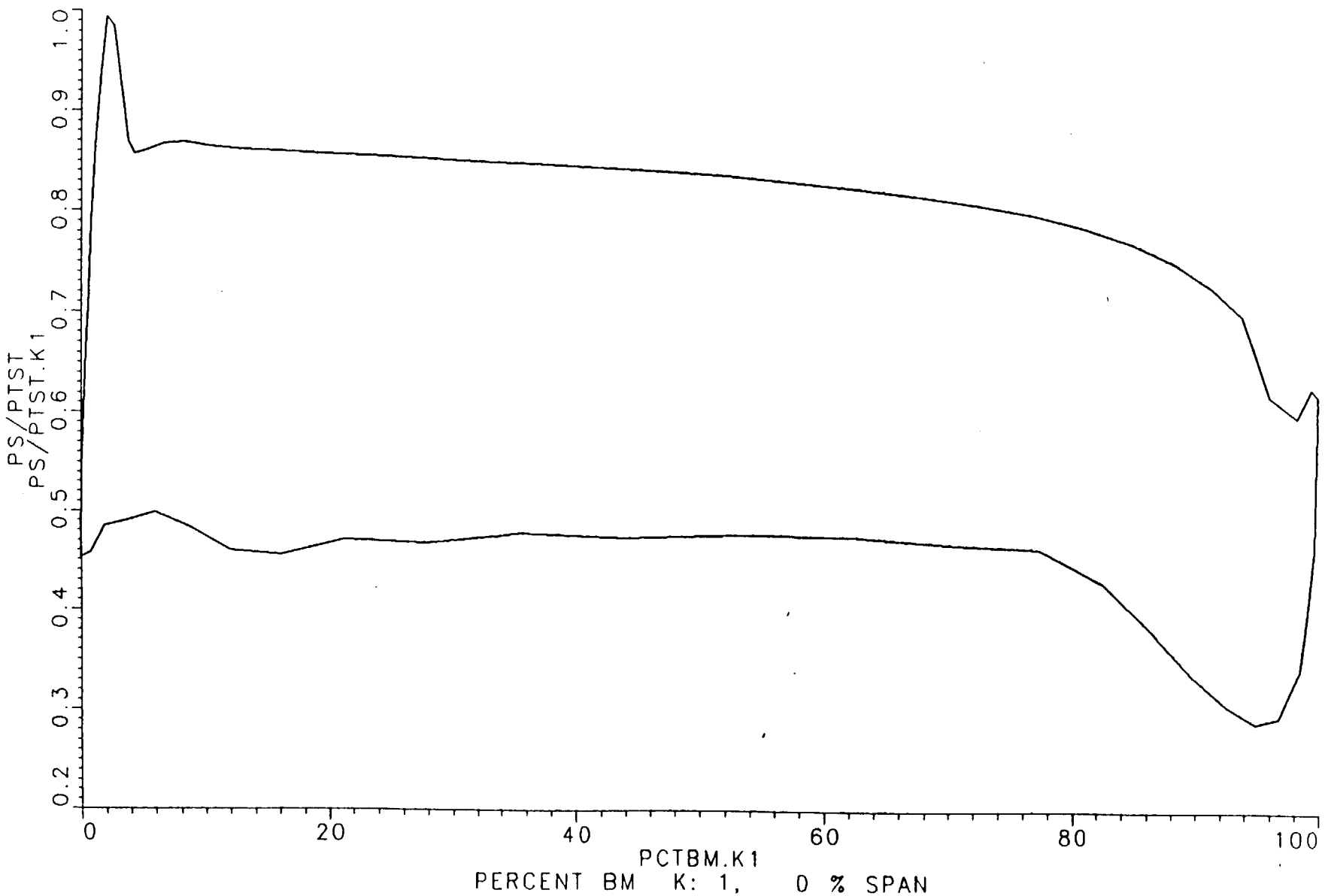

FIGURE 12B
OXIDIZER TURBINE BASELINE DESIGN

Blade - Pressure Distribution at 25% Span

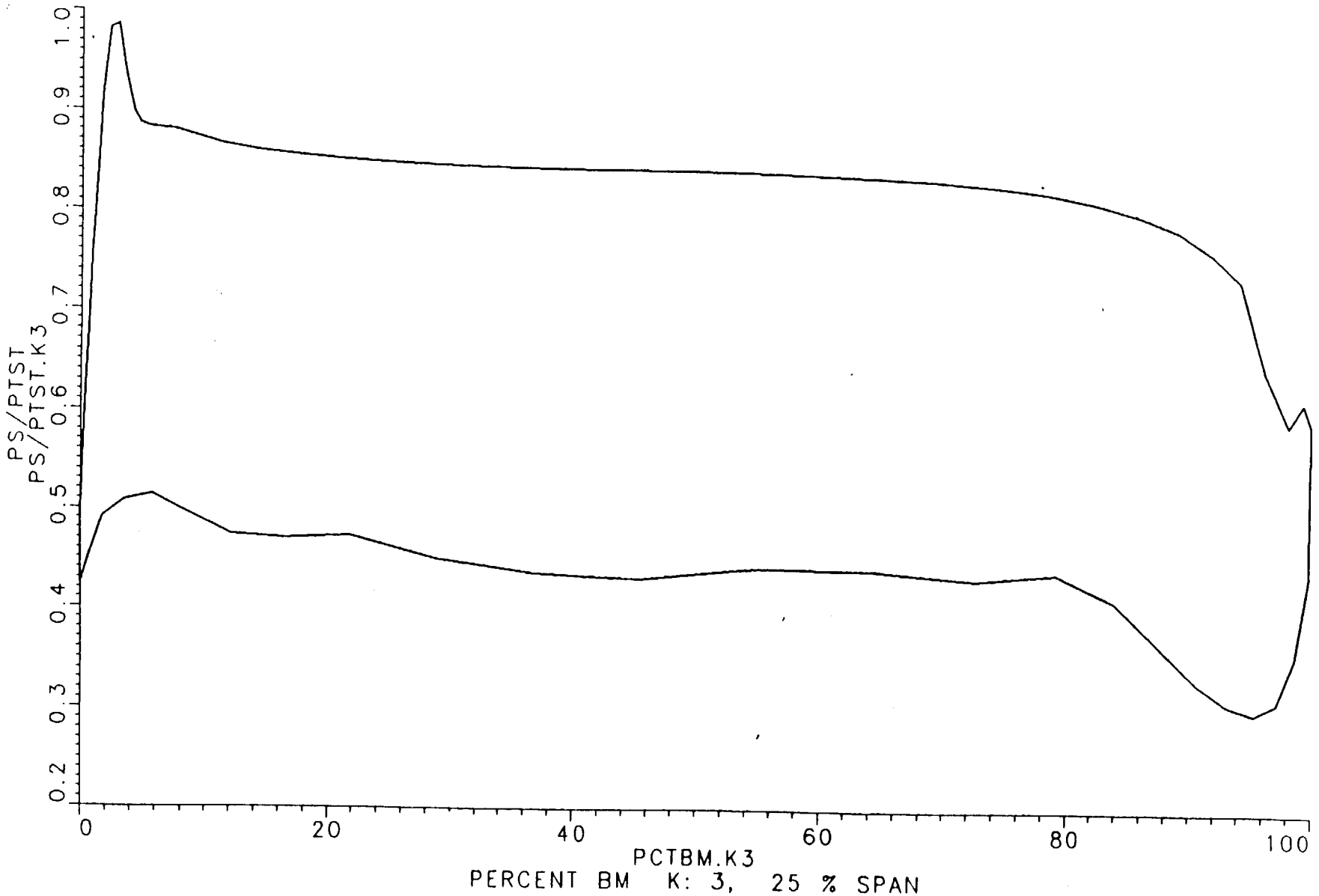

FIGURE 12C
OXIDIZER TURBINE BASELINE DESIGN

Blade - Pressure Distribution at 50% Span

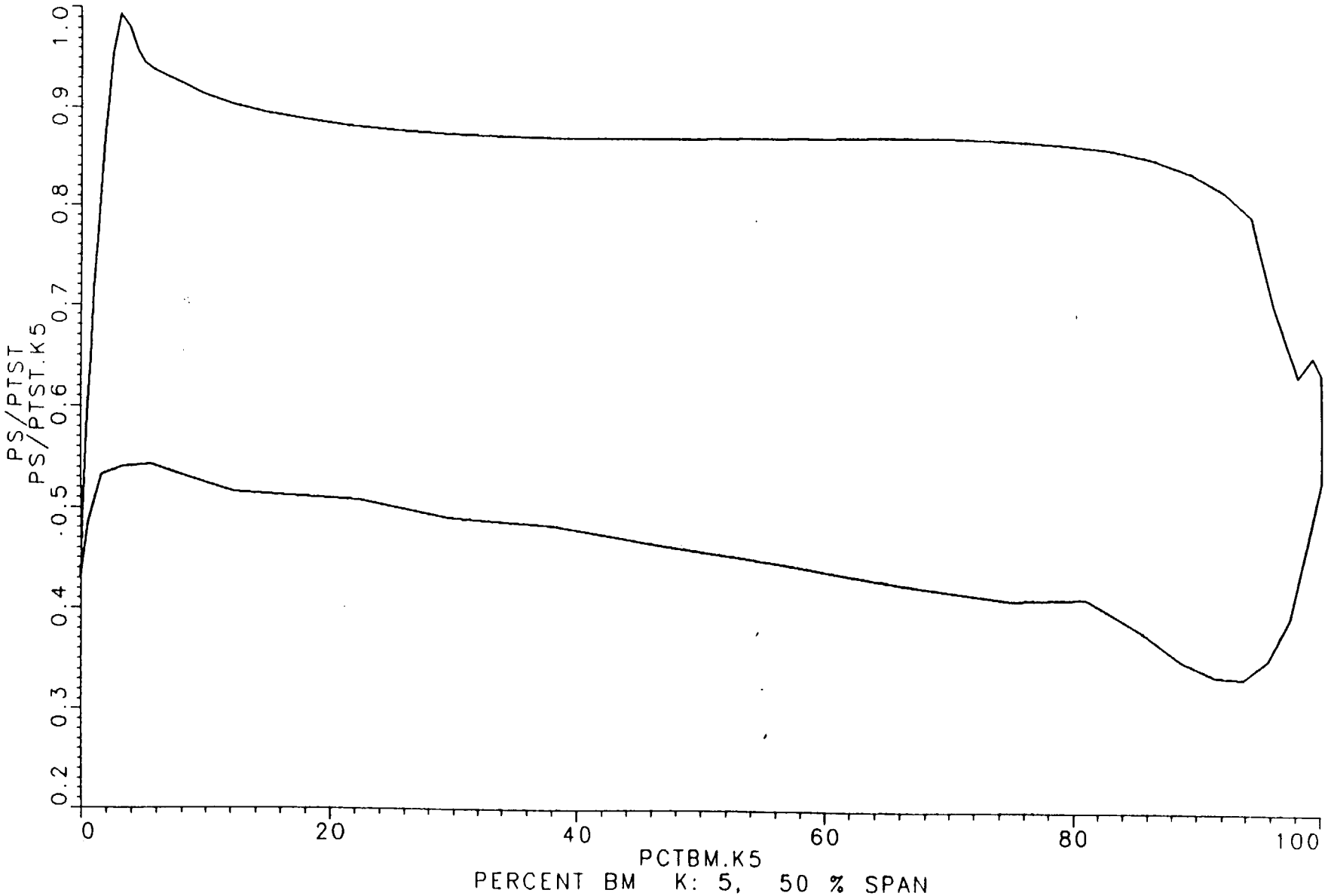

FIGURE 12D
OXIDIZER TURBINE BASELINE DESIGN

Blade - Pressure Distribution at 75% Span

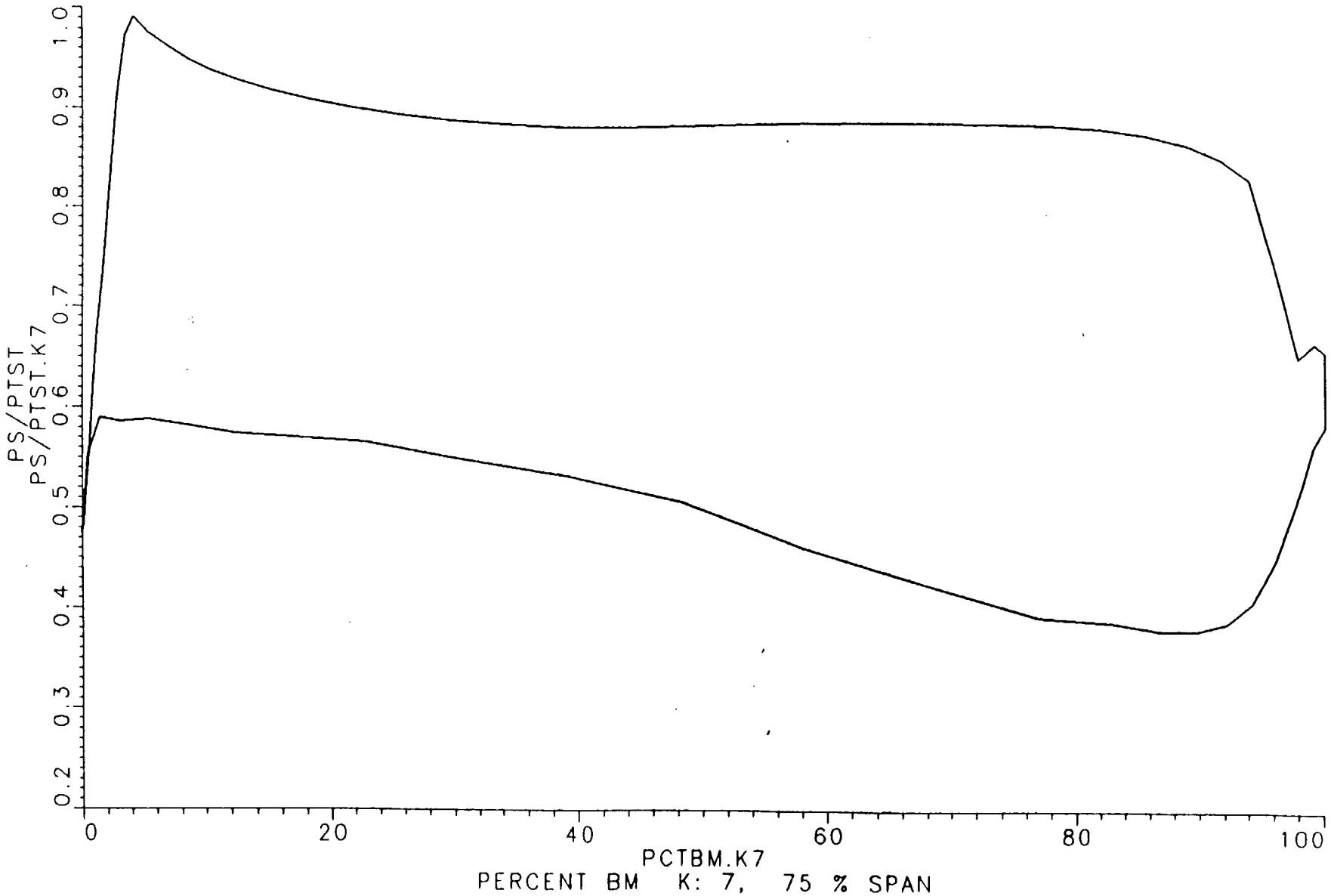

FIGURE 12E
OXIDIZER TURBINE BASELINE DESIGN

Blade - Pressure Distribution at 100% Span

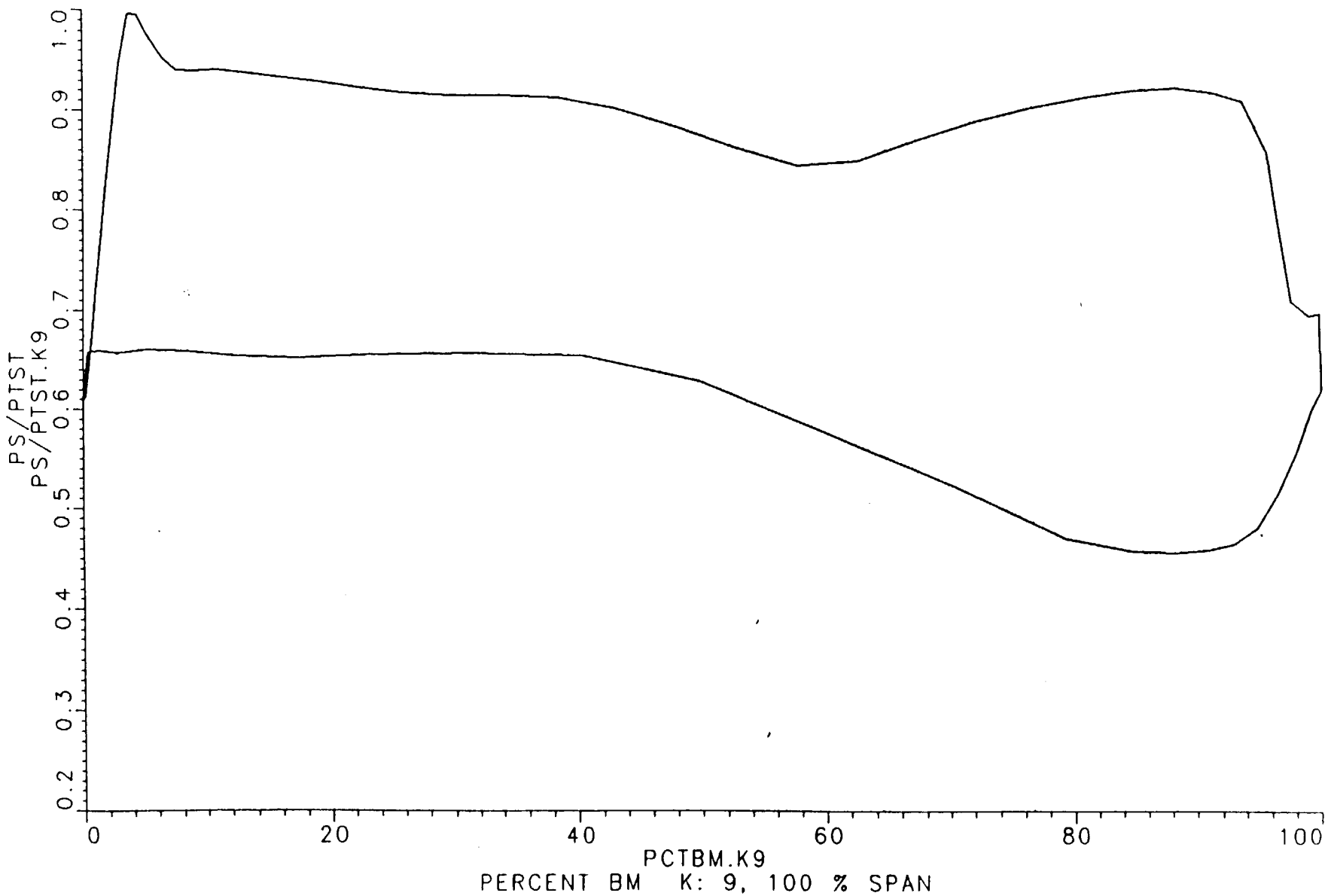

FIGURE 13A
OXIDIZER TURBINE BASELINE DESIGN

Square Exit Volute - 50% Scale OTTR Flowpath

NOTE:
- Corners A, B, and C need to be rounded to manufacturing minimums (0.25" radius or less)
- Tongue leading edge profile needs to be rounded (View X-X)

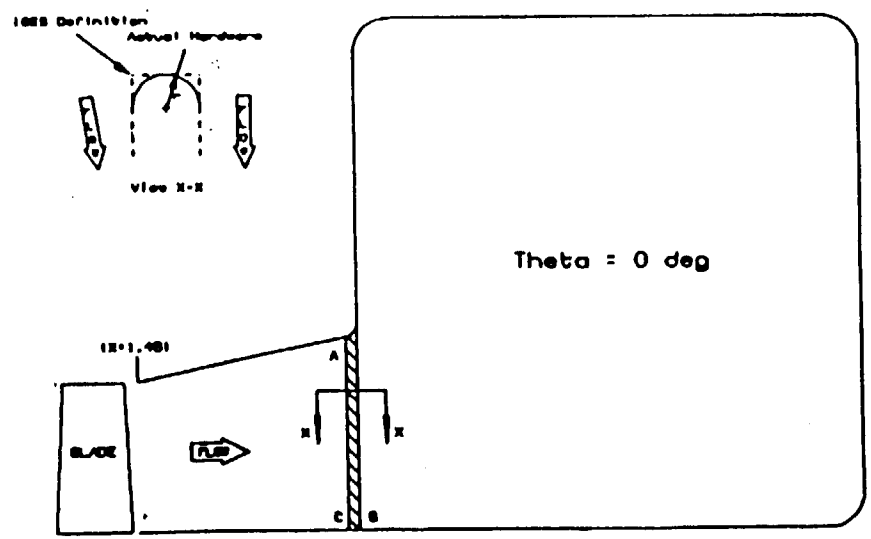

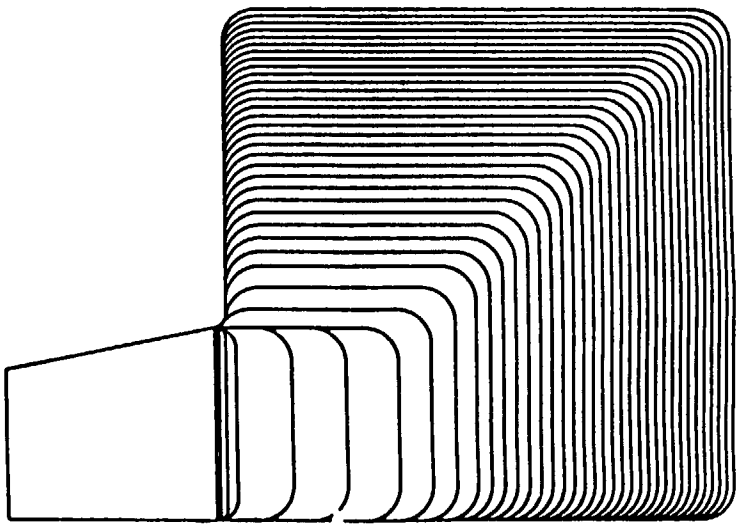

FIGURE 13B
OXIDIZER TURBINE BASELINE DESIGN

Square Exit Volute - Unigraphics Wire Frame Mesh

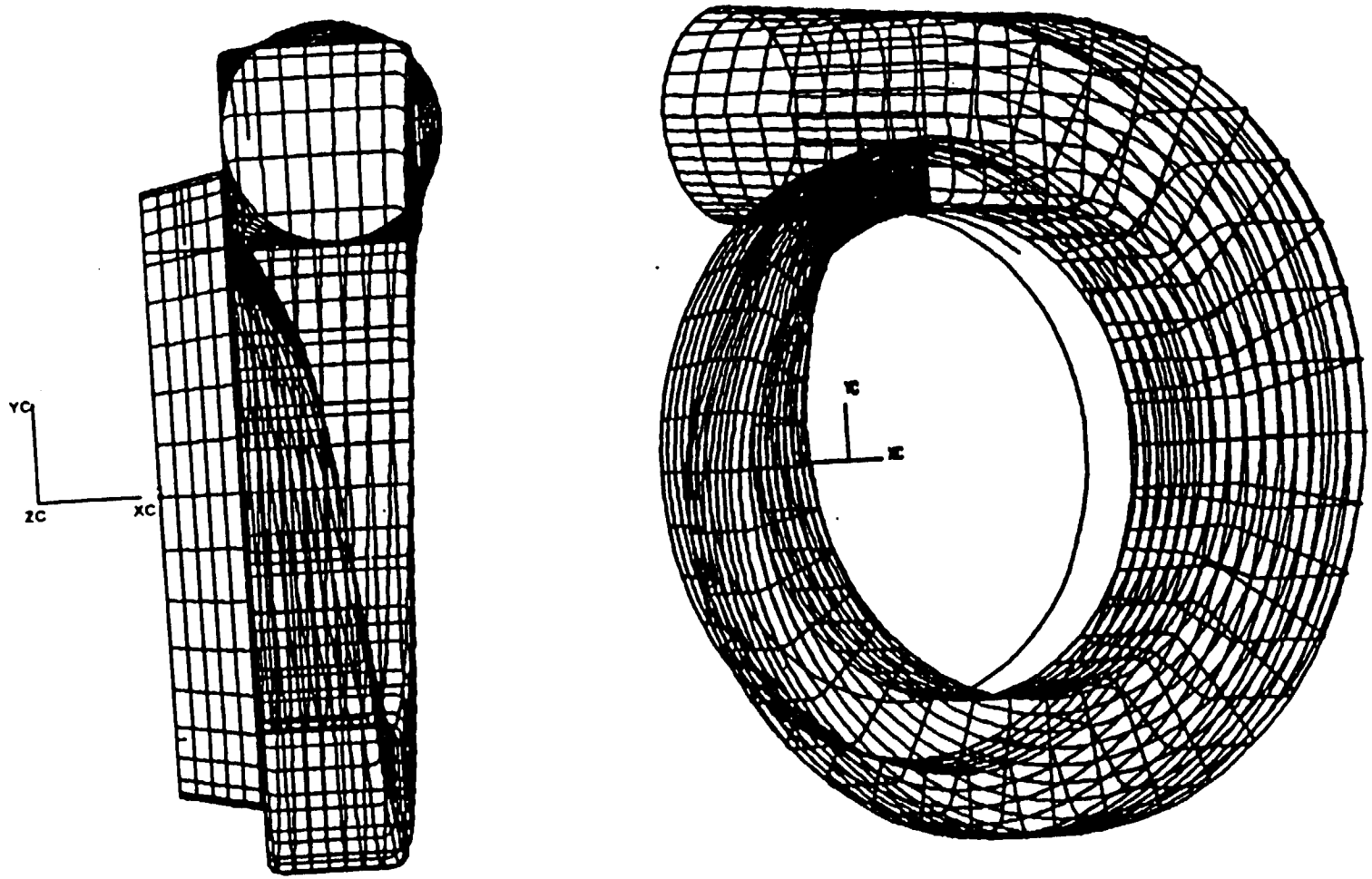

FIGURE 13C
OXIDIZER TURBINE BASELINE DESIGN

Square Exit Volute - Geometry Definition

Geometry

22+ Cross-Sections

IGES File on Diskette

"BASELINE-EXIT-VOLUTE.IGES"

Euler-N/S Results

PLOT3D Files

"BASELINE-SQ-EXIT-VOLUTE.XYZ" (Geometry)
"BASELINE-SQ-EXIT-VOLUTE-DESIGN.Q" (M_1 = 0.82)
"BASELINE-SQ-EXIT-VOLUTE-CHOKED.Q" (Choked)

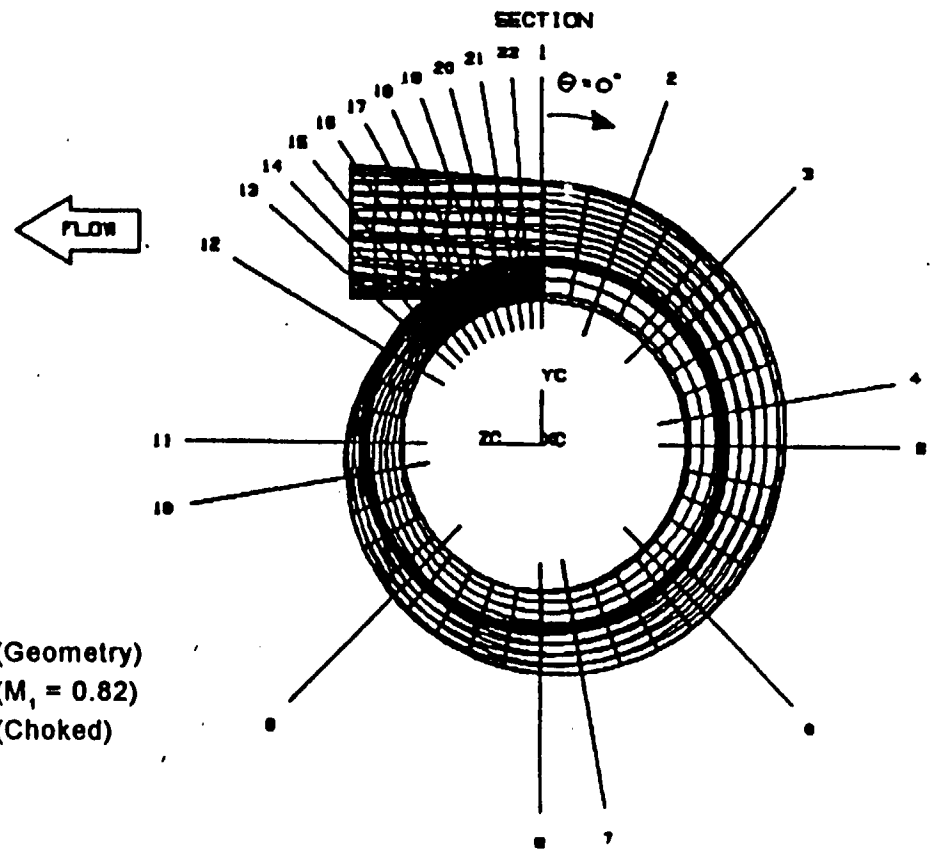

FIGURE 14A
OXIDIZER TURBINE BASELINE DESIGN

Round Exit Volute - 50% Scale OTTR Flowpath

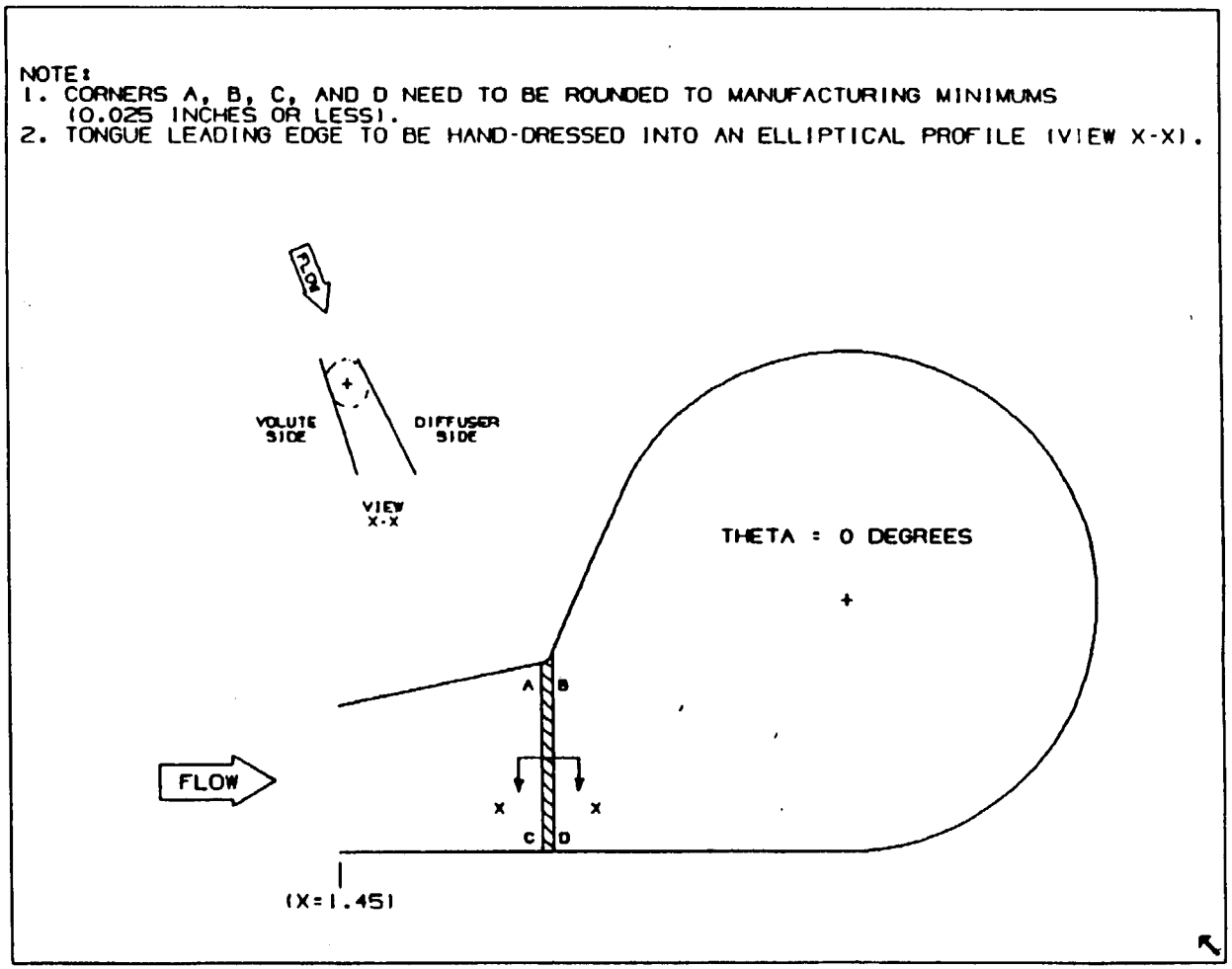

FIGURE 14B
OXIDIZER TURBINE BASELINE DESIGN

Round Exit Volute - Unigraphics Wire Frame Mesh

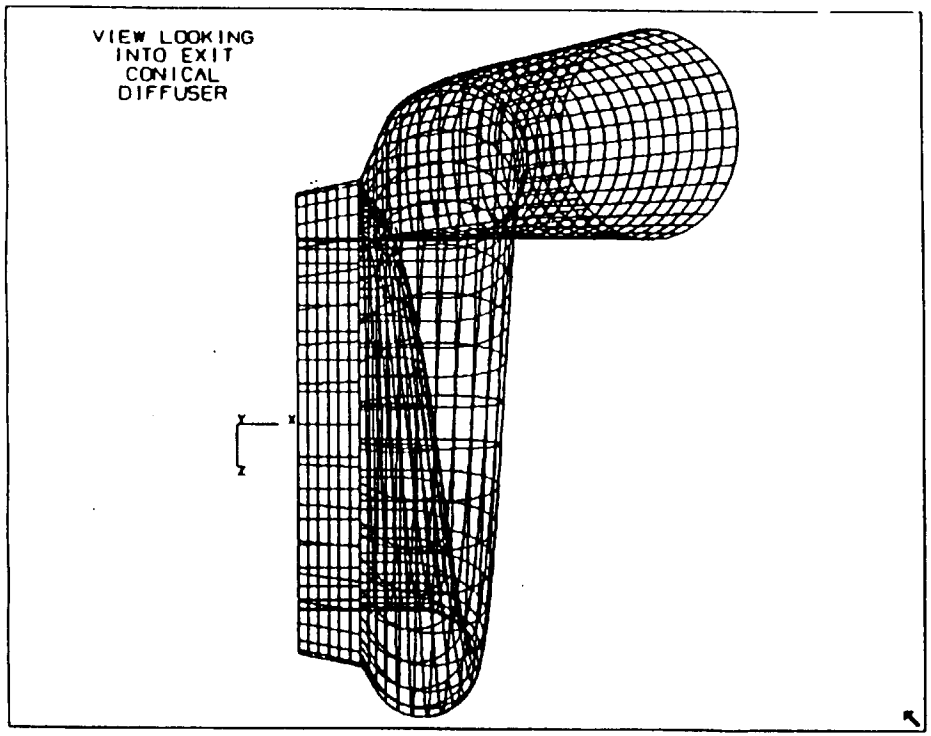

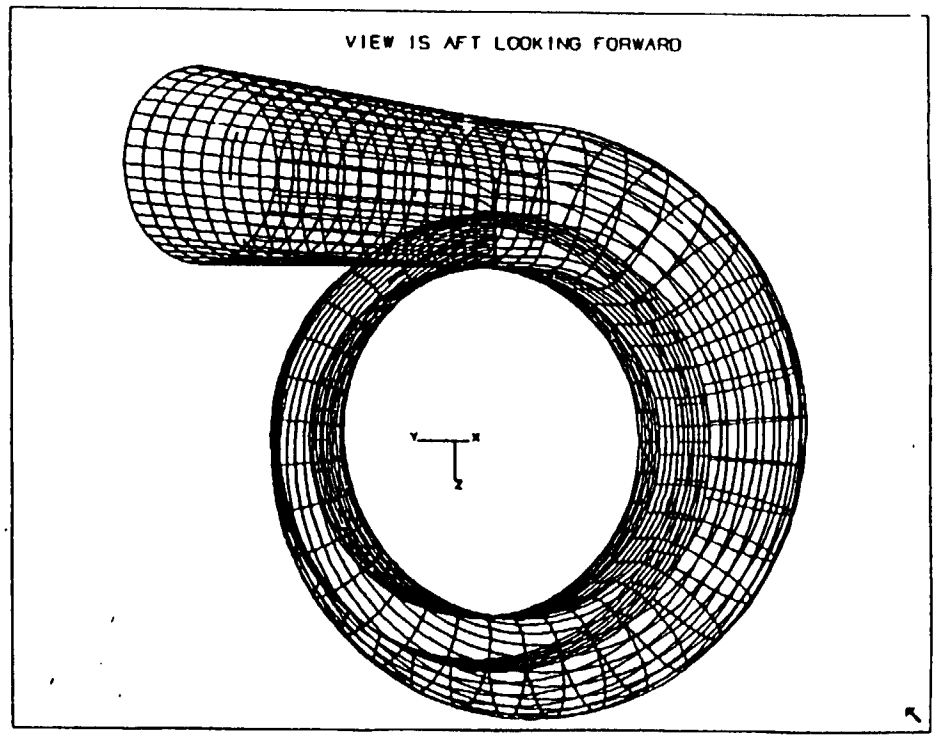

FIGURE 14C
OXIDIZER TURBINE BASELINE DESIGN

Round Exit Volute - Geometry Definition

Geometry

22+ Cross-Sections

IGES File on Diskette

"BASELINE-CIRCULAR-EXIT-VOLUTE.IGES"

Euler-N/S Results

PLOT3D Files

"BASELINE-CIRC-EXIT-VOLUTE.XYZ"

"BASELINE-CIRC-EXIT-VOLUTE-DESIGN.Q"

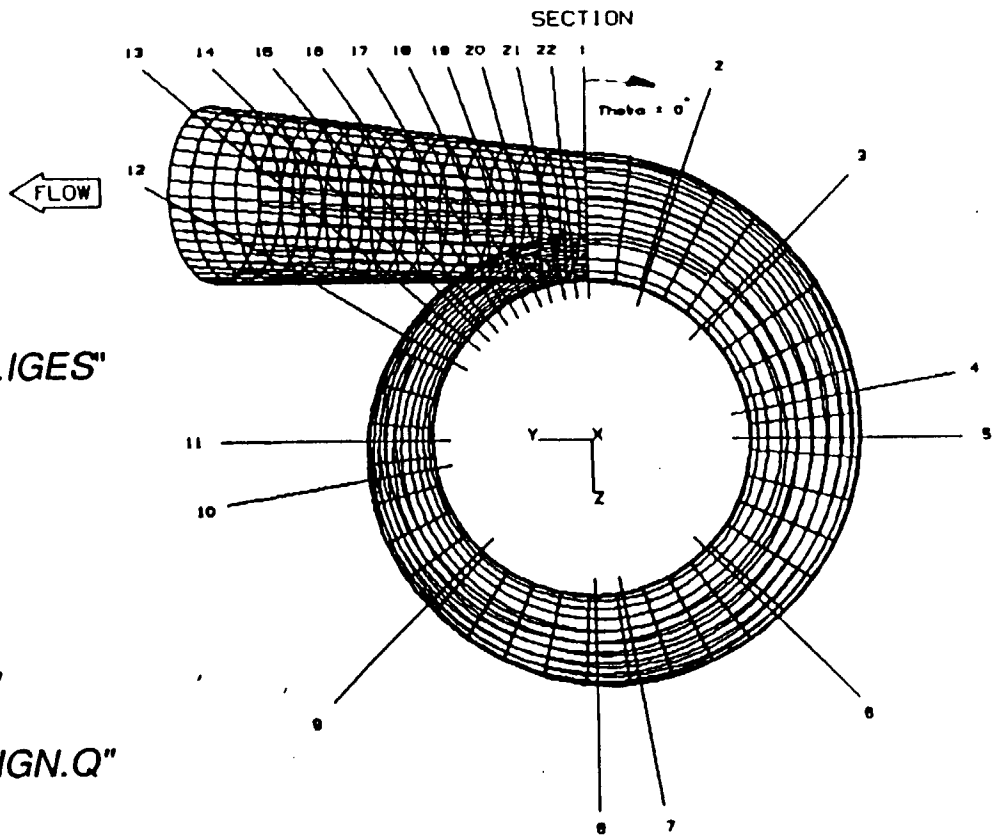

VIEW IS AFT OF TURBINE LOOKING FORWARD

FIGURE 15
OXIDIZER TURBINE BASELINE DESIGN

Inlet Volute & Exit Volute Relative Position

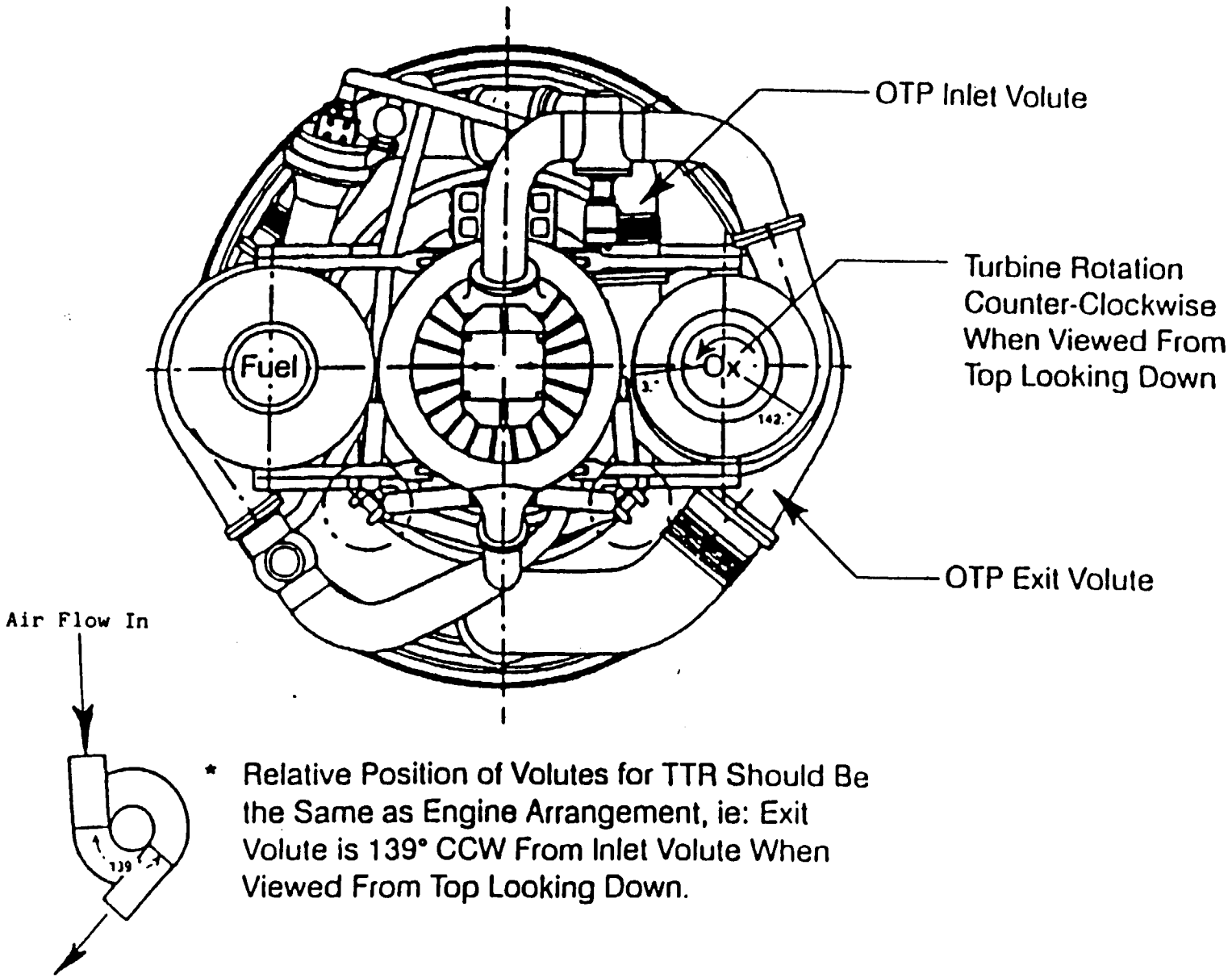

* Relative Position of Volutes for TTR Should Be the Same as Engine Arrangement, ie: Exit Volute is 139° CCW From Inlet Volute When Viewed From Top Looking Down.

FIGURE 16

OXIDIZER TURBINE BASELINE DESIGN

Exit Conical Diffuser

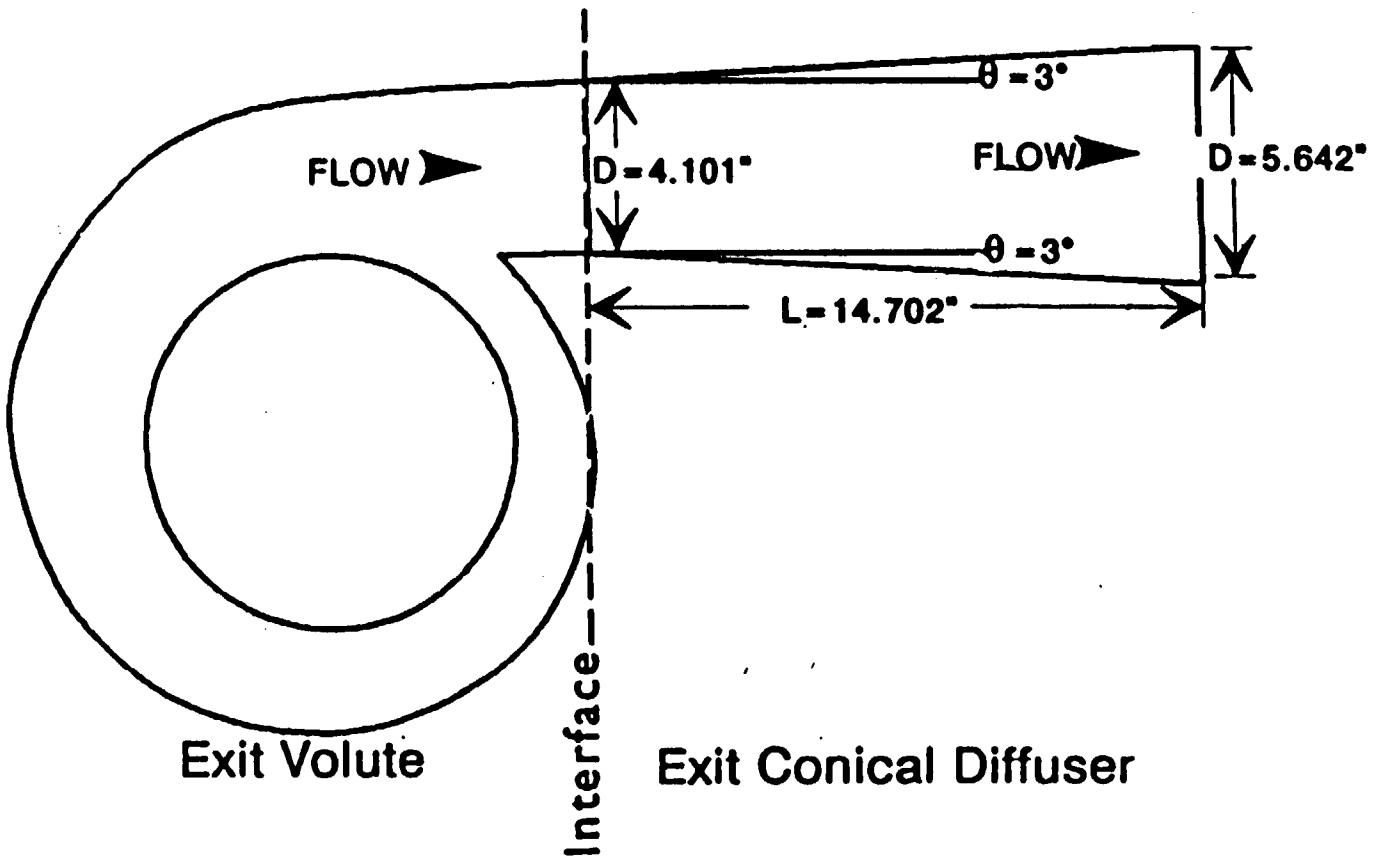

FIGURE 17A
OXIDIZER TURBINE BASELINE DESIGN

Square Exit Volute - Static Pressure Distribution at Blade Exit Plane (M=1.20)

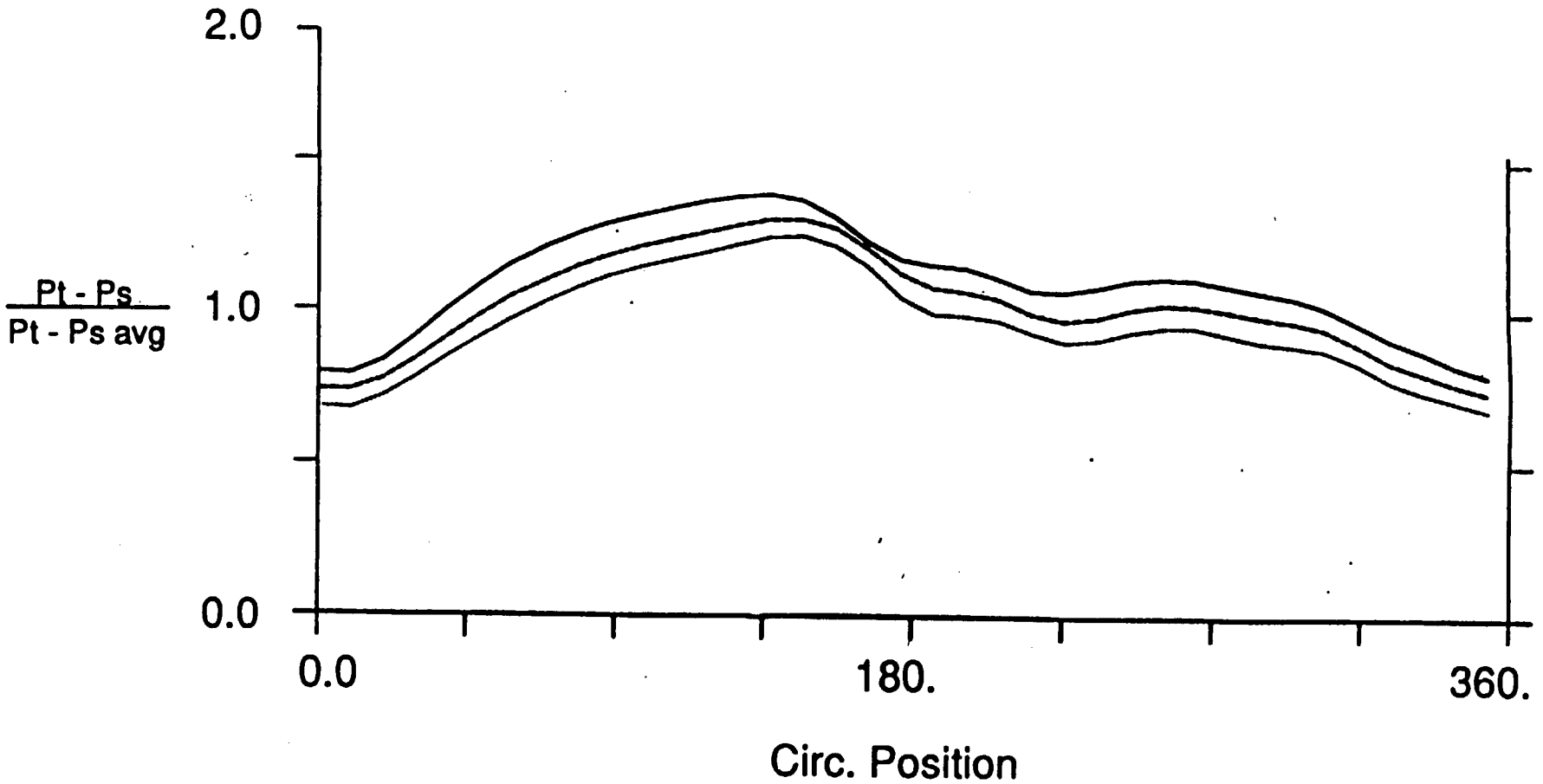

FIGURE 17B

OXIDIZER TURBINE BASELINE DESIGN

Square Exit Volute - Predicted Flow Patterns

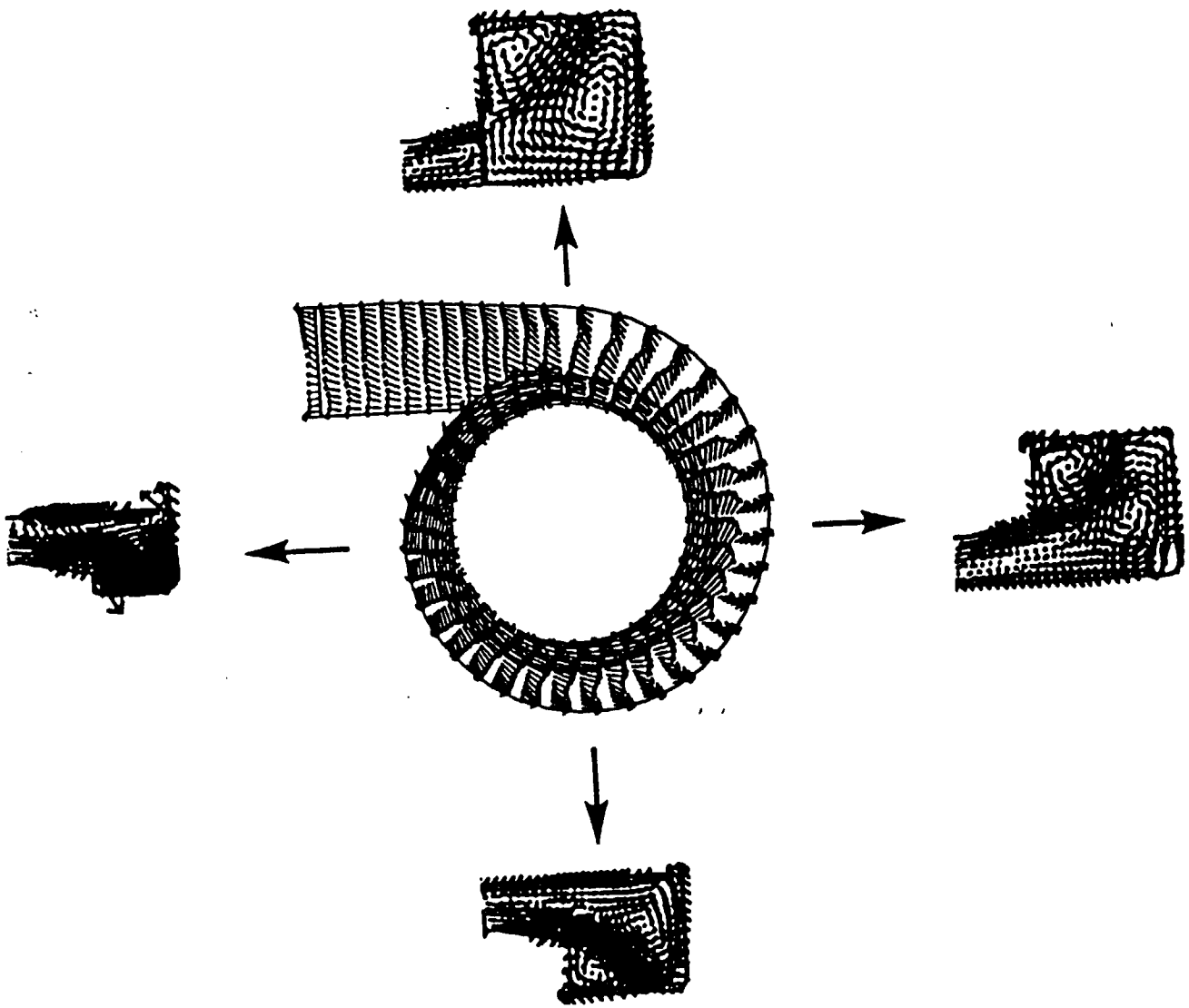

FIGURE 18A
OXIDIZER TURBINE BASELINE DESIGN

Round Exit Volute - Static Pressure Distribution at Blade Exit Plane (M=0.82)

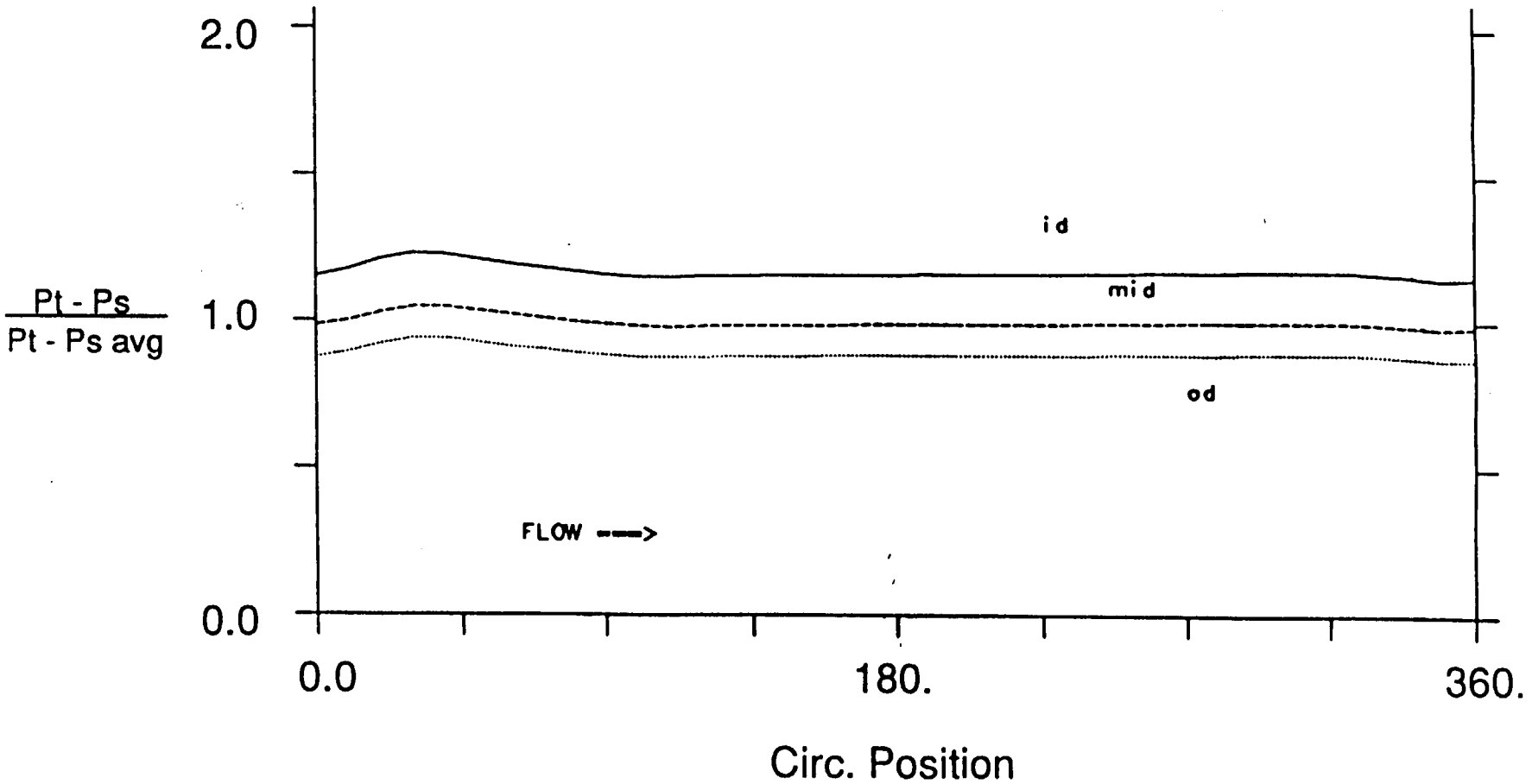

FIGURE 18B
OXIDIZER TURBINE BASELINE DESIGN

Round Exit Volute - Predicted Flow Patterns

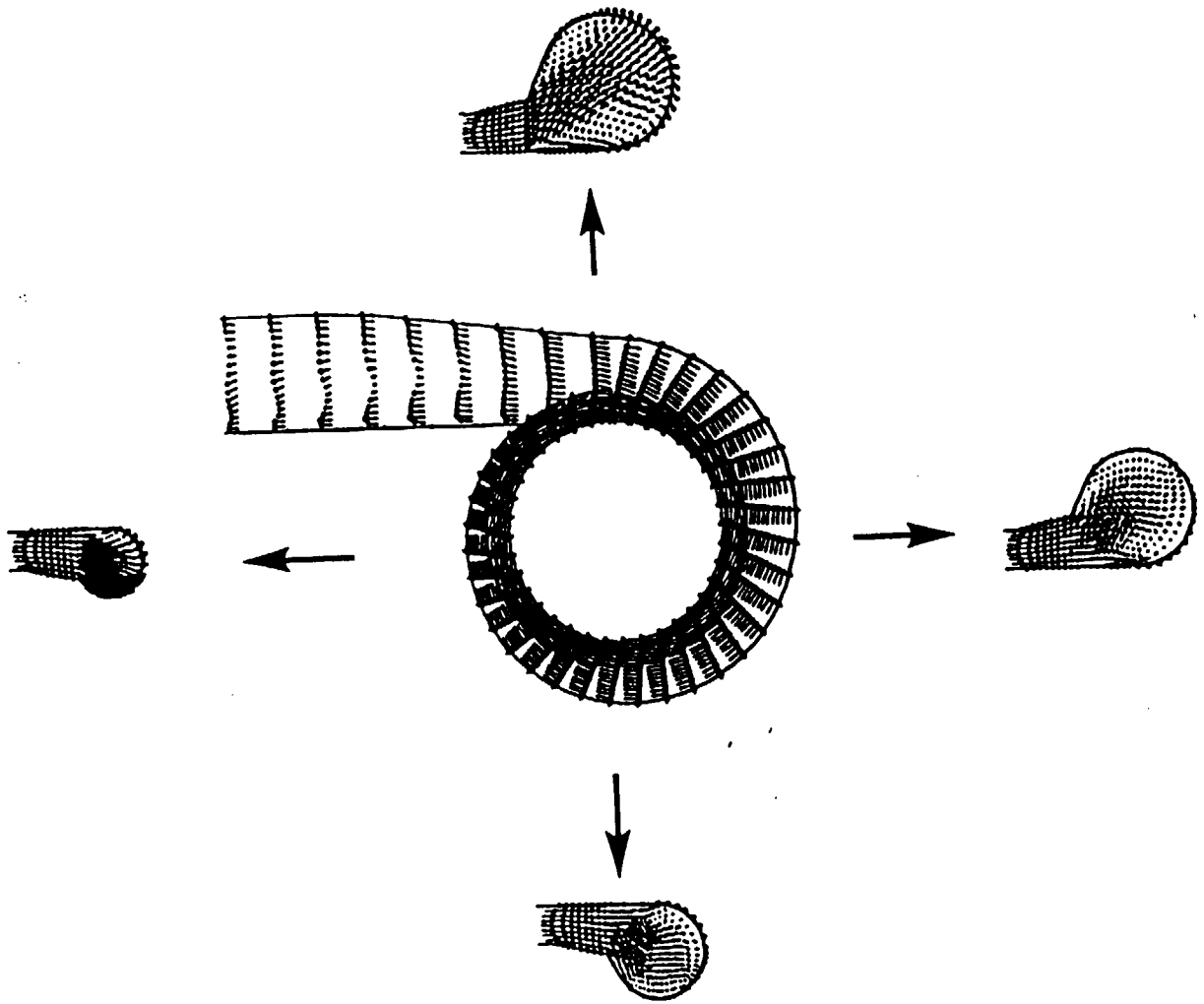

FIGURE 19
OXIDIZER TURBINE BASELINE DESIGN

Oxidizer Technology Turbine Rig (OTTR) Flowpath (50% Scale of Hot T/P)

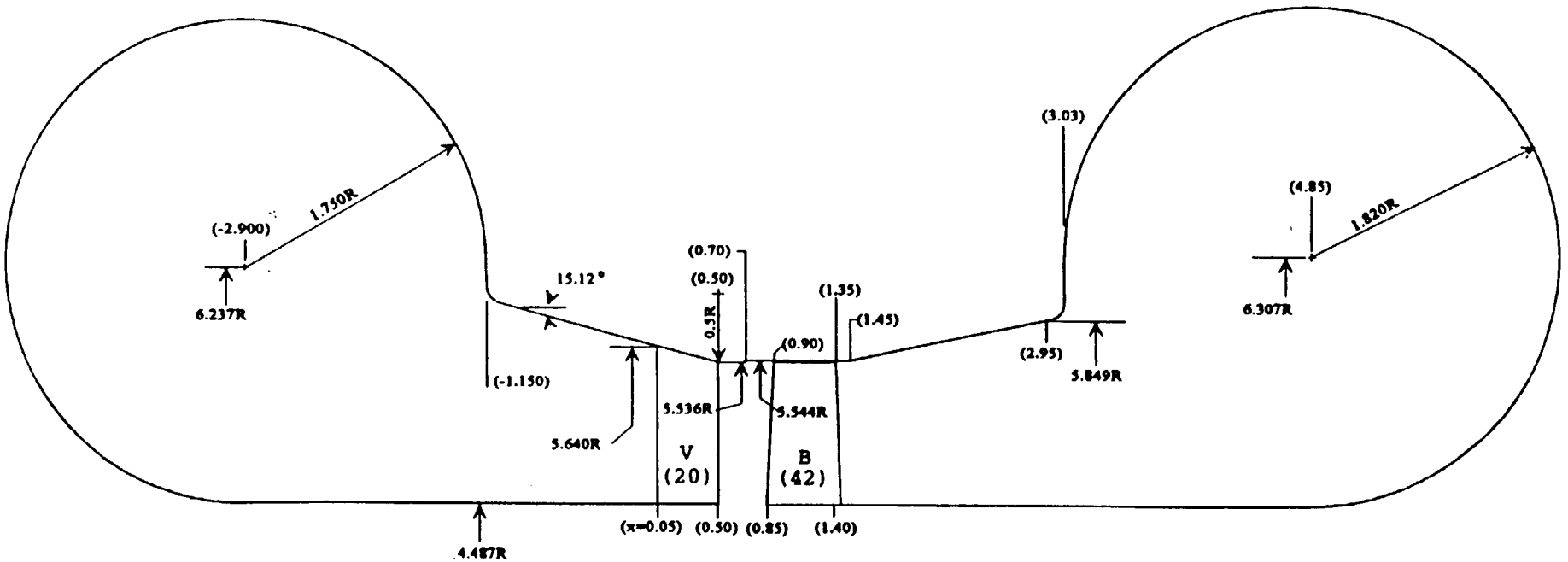

Axial Location - ( )

FIGURE 20
OXIDIZER TURBINE BASELINE DESIGN

OTTR Design Point and Operating Envelope

	Design Point	Operating Envelope
Working Fluid	Air	Air
Gas Constant (ft-lbf/°R-lbm)	53.35	53.35
Ratio of Specific Heats	1.40	1.40
Inlet Pressure (psia)	100.0	30.0 - 200.0
Inlet Temperature (°R)	560.0	560.0
Shaft Speed (rpm)	3710.0	1000.0 - 5000.0
Pressure Ratio	1.60	1.20 - 1.80
Flow Rate (lbm/s)	11.94	2.00 - 24.00
Power (Hp)	205.4	20.0 - 920.0
Efficiency (Turbine T-T)	72.0	24.8 - 87.5

FIGURE 21
OXIDIZER TURBINE BASELINE DESIGN

Predicted Reynolds Number Effect on Efficiency

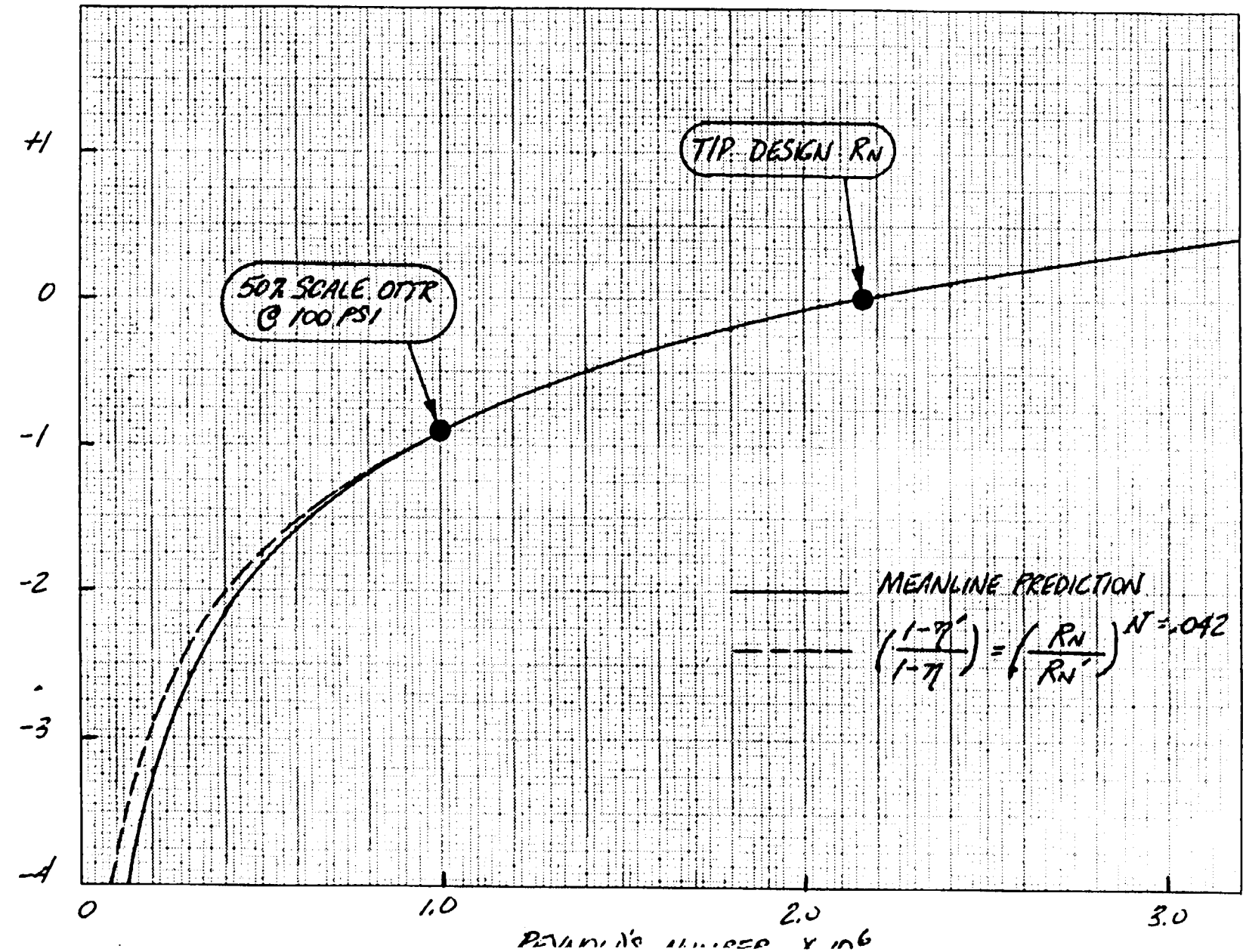

ORIGINAL PAGE IS
OF POOR QUALITY

FIGURE 22

OXIDIZER TURBINE BASELINE DESIGN

OTTR Test Matrix

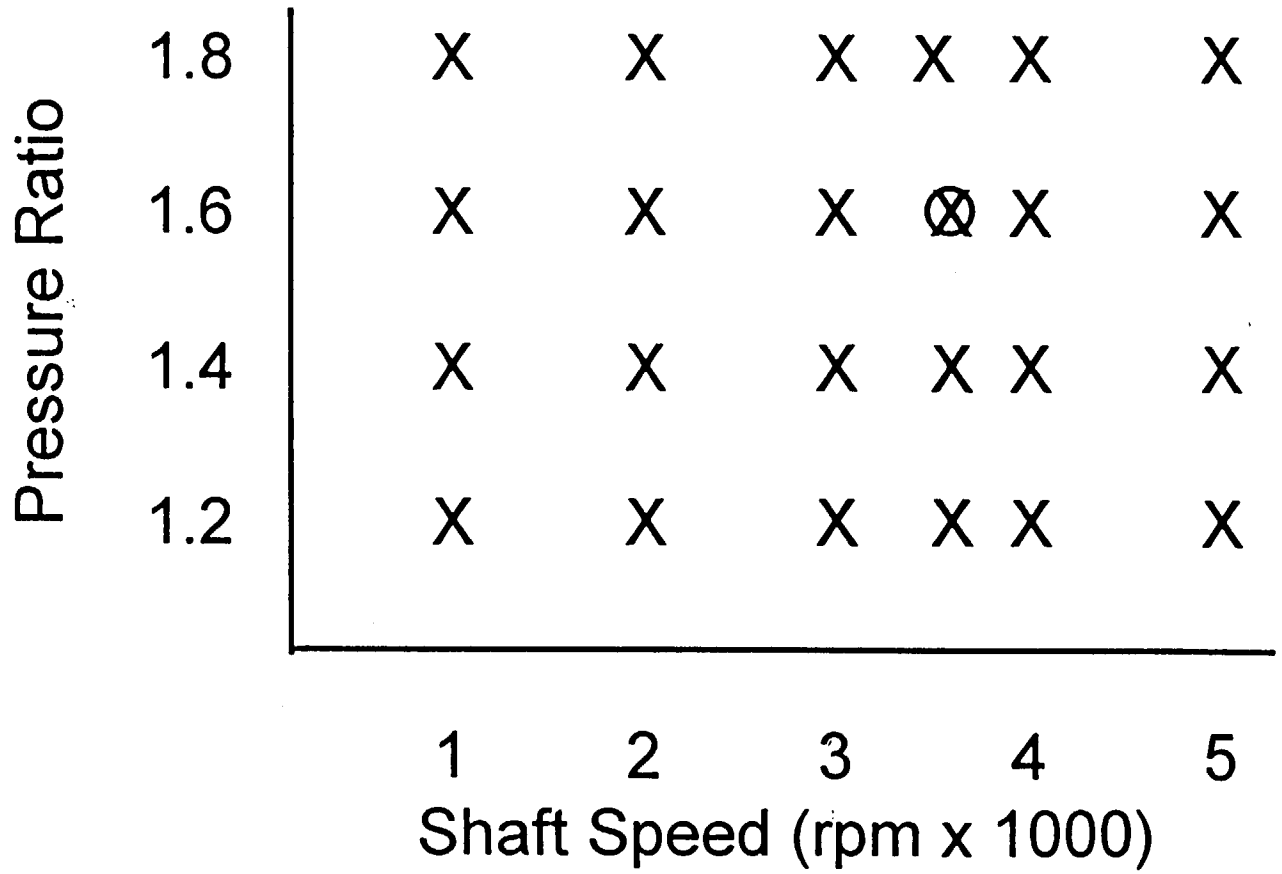

FIGURE 23
OXIDIZER TURBINE BASELINE DESIGN

OTTR - Predicted Efficiency

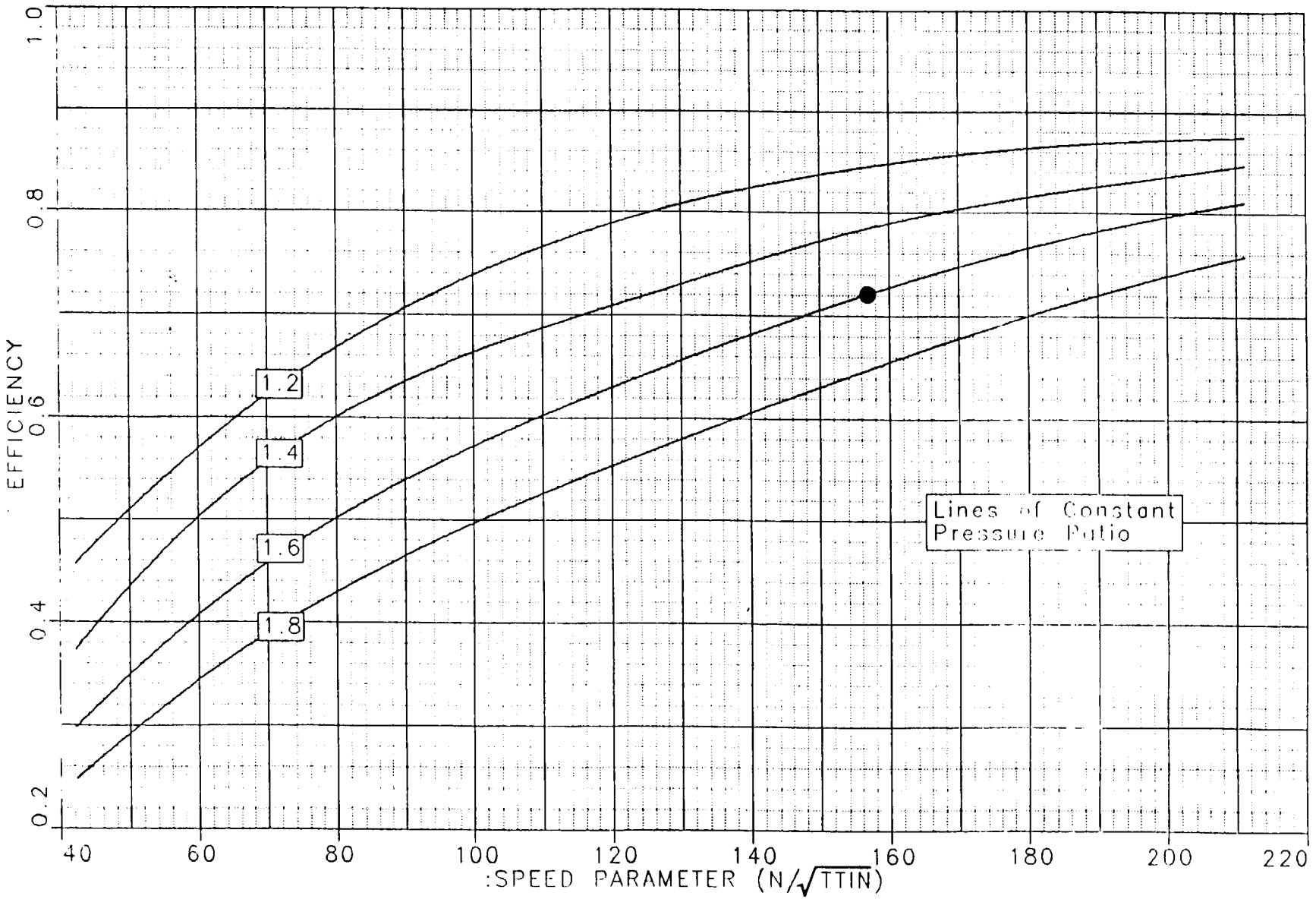

FIGURE 24
OXIDIZER TURBINE BASELINE DESIGN

OTTR - Predicted Flow Parameter

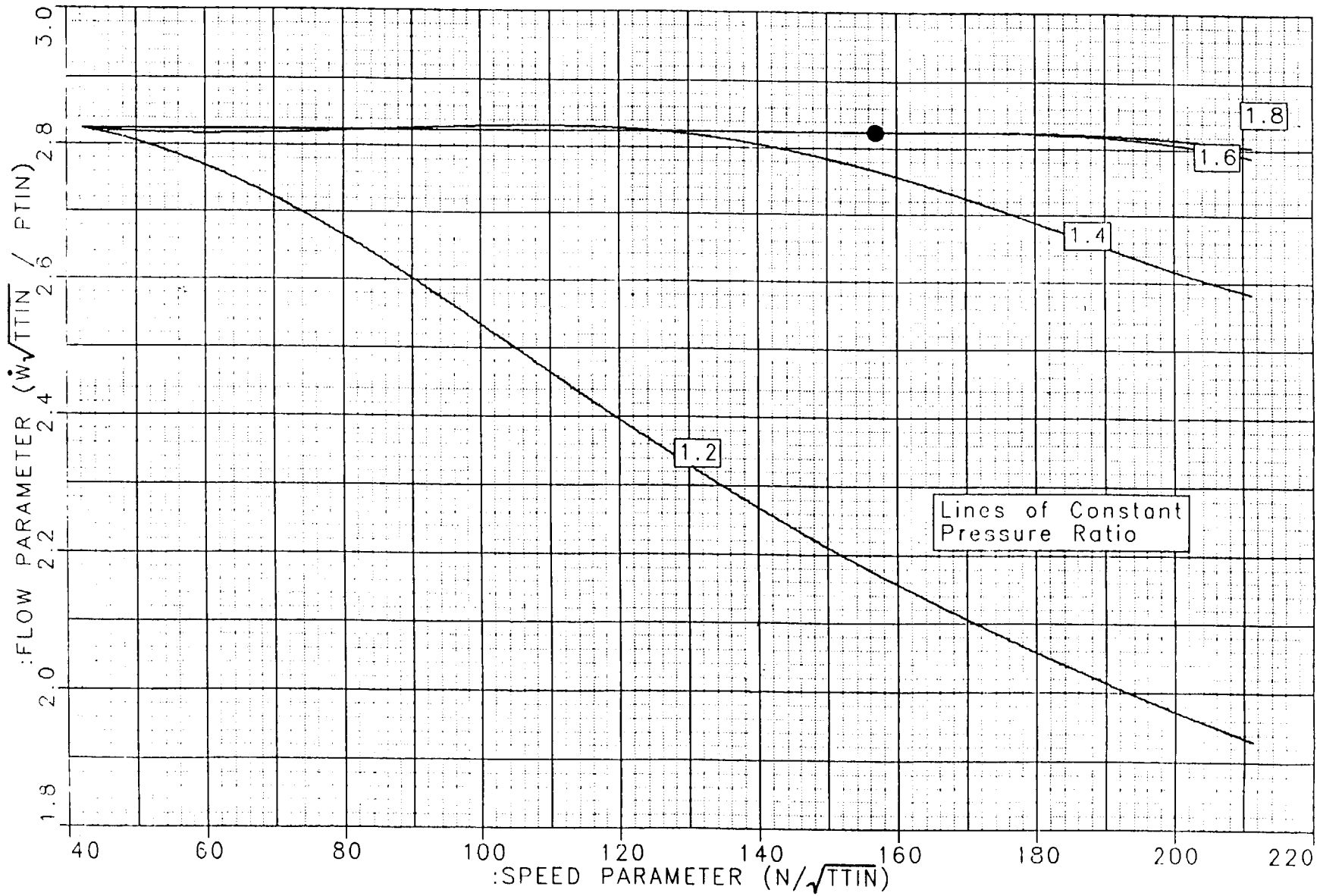

FIGURE 25A
OXIDIZER TURBINE BASELINE DESIGN

OTTR - Predicted Performance at Ptin=100 psia and Ttin=560 °R

PR = 1.2

N	WDOT	SWRLIN	MIN	PSIN	PS1VEX	SWRLEX	MEX	PSEX	PTEX	TTEX	POWER	TORQUE	ETA
1000.0	11.936	75.800	0.330	92.736	48.722	77.327	0.642	63.142	83.333	547.030	52.567	276.123	0.456
2000.0	11.144	75.800	0.305	93.742	69.735	76.353	0.508	69.867	83.333	540.525	73.684	193.525	0.685
3000.0	9.933	75.800	0.269	95.105	78.957	74.543	0.373	75.689	83.333	537.211	76.846	134.554	0.801
3710.0	9.182	75.800	0.247	95.852	82.933	72.547	0.297	78.378	83.333	535.987	74.852	105.979	0.845
4000.0	8.915	75.800	0.239	96.101	84.161	71.495	0.270	79.212	83.333	535.662	73.654	96.722	0.856
5000.0	8.151	75.800	0.217	96.764	87.251	66.260	0.191	81.252	83.333	535.126	68.831	72.312	0.875

PR = 1.4

N	WDOT	SWRLIN	MIN	PSIN	PS1VEX	SWRLEX	MEX	PSEX	PTEX	TTEX	POWER	TORQUE	ETA
1000.0	11.936	75.800	0.330	92.736	16.073	77.098	1.059	35.161	71.429	540.859	77.567	407.445	0.373
2000.0	11.936	75.800	0.330	92.736	30.162	76.784	0.798	46.925	71.429	528.314	128.378	337.172	0.617
3000.0	11.933	75.800	0.330	92.741	53.944	75.714	0.659	53.354	71.429	522.901	150.253	263.084	0.722
3710.0	11.691	75.800	0.322	93.058	62.453	74.869	0.574	57.127	71.429	519.745	159.727	226.150	0.784
4000.0	11.527	75.800	0.317	93.267	65.125	74.440	0.538	58.659	71.429	518.823	161.894	211.550	0.802
5000.0	10.916	75.800	0.298	94.013	71.901	72.510	0.427	63.025	71.429	516.507	161.128	169.275	0.847

PR = 1.6

N	WDOT	SWRLIN	MIN	PSIN	PS1VEX	SWRLEX	MEX	PSEX	PTEX	TTEX	POWER	TORQUE	ETA
1000.0	11.936	75.800	0.330	92.736	16.073	73.212	1.439	18.581	62.500	539.006	85.076	446.891	0.298
2000.0	11.936	75.800	0.330	92.736	28.175	75.099	1.189	26.139	62.500	523.469	147.995	388.696	0.519
3000.0	11.936	75.800	0.330	92.736	42.622	75.570	0.931	35.715	62.500	514.394	184.731	323.454	0.648
3710.0	11.936	75.800	0.330	92.736	50.204	75.233	0.815	40.366	62.500	509.300	205.351	290.748	0.720
4000.0	11.936	75.800	0.330	92.737	52.885	75.006	0.775	42.020	62.500	507.538	212.479	279.028	0.745
5000.0	11.783	75.800	0.325	92.938	60.453	73.920	0.642	47.368	62.500	502.958	228.052	239.584	0.810

PR = 1.8

N	WDOT	SWRLIN	MIN	PSIN	PS1VEX	SWRLEX	MEX	PSEX	PTEX	TTEX	POWER	TORQUE	ETA
1000.0	11.936	75.800	0.330	92.736	16.073	68.749	1.623	12.629	55.556	538.534	86.989	456.935	0.248
2000.0	11.936	75.800	0.330	92.736	28.175	71.355	1.439	16.503	55.556	521.421	156.289	410.479	0.446
3000.0	11.936	75.800	0.330	92.736	42.621	73.447	1.179	23.550	55.556	510.525	200.394	350.877	0.571
3710.0	11.936	75.800	0.330	92.736	50.204	73.888	1.074	26.868	55.556	503.907	227.171	321.641	0.648
4000.0	11.936	75.800	0.330	92.736	52.830	73.980	1.038	28.063	55.556	501.454	237.098	311.358	0.676
5000.0	11.848	75.800	0.327	92.853	58.639	74.058	0.889	33.235	55.556	494.362	263.824	277.164	0.758

FIGURE 25B
OXIDIZER TURBINE BASELINE DESIGN

OTTR - Predicted Performance at Ptin=100 psia and Ttin=560 °R

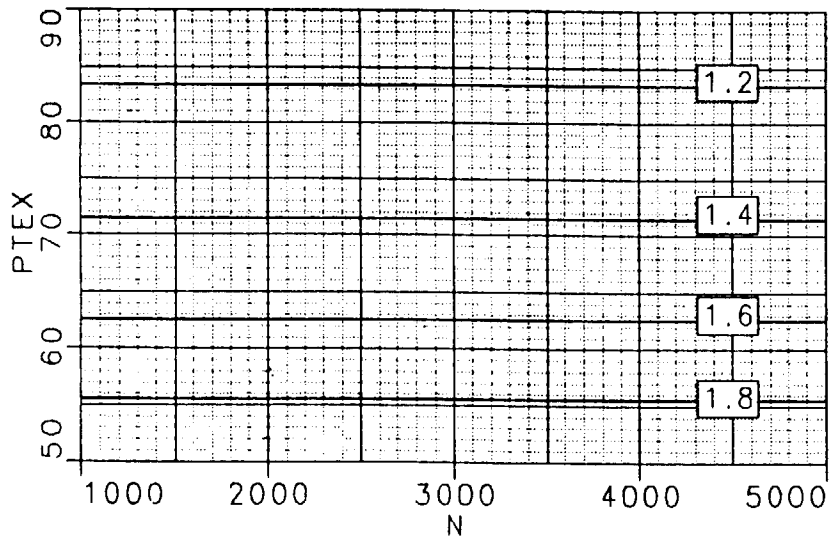

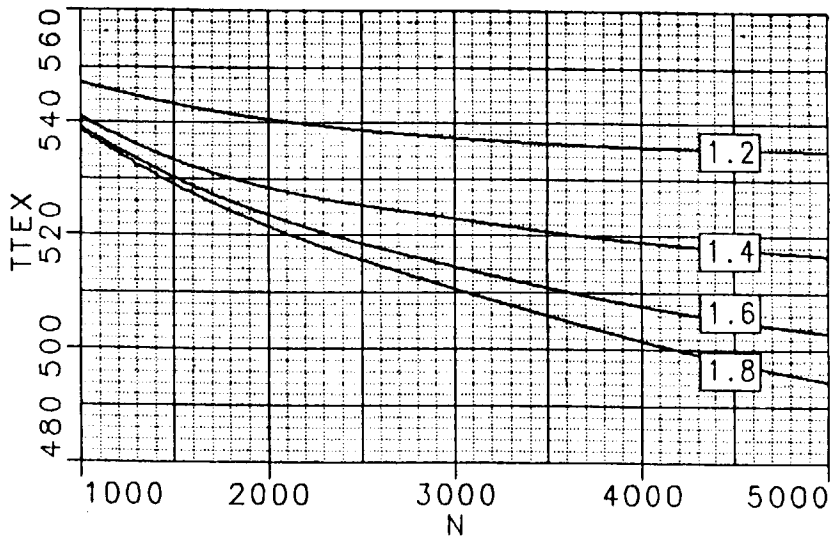

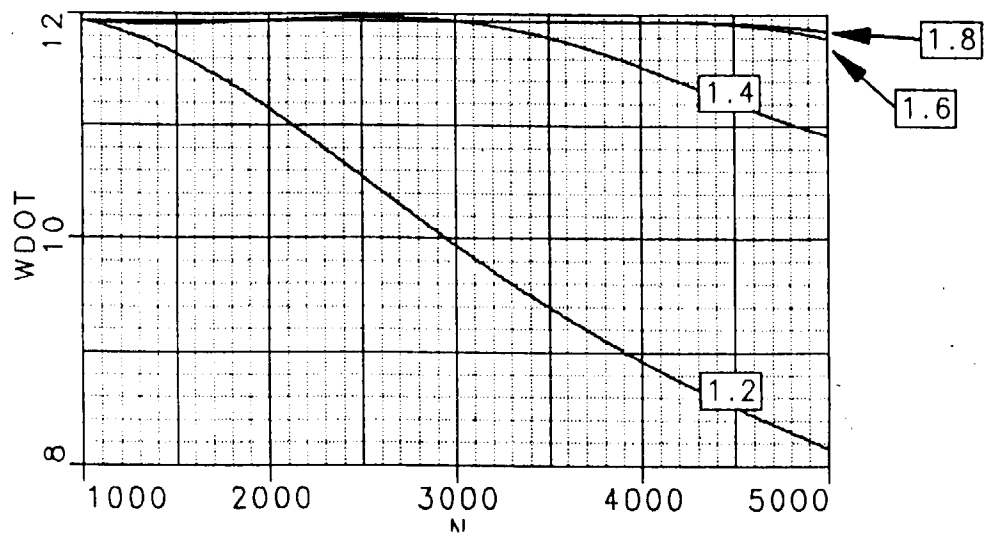

Lines of Constant Pressure Ratio

FIGURE 25C
OXIDIZER TURBINE BASELINE DESIGN

OTTR - Predicted Performance at Ptin=100 psia and Ttin=560 °R

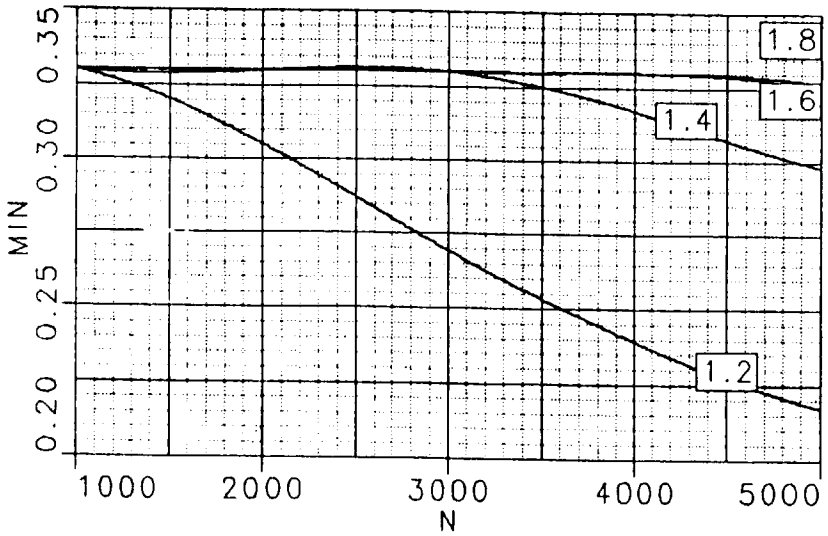

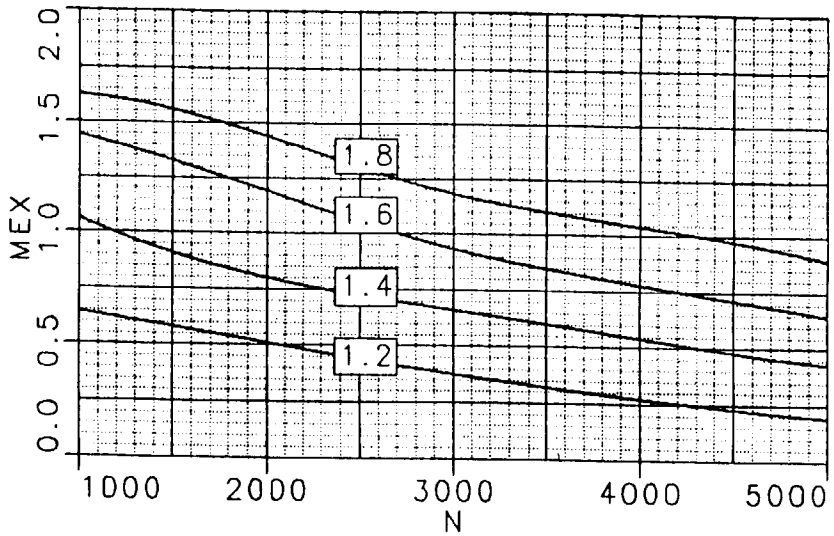

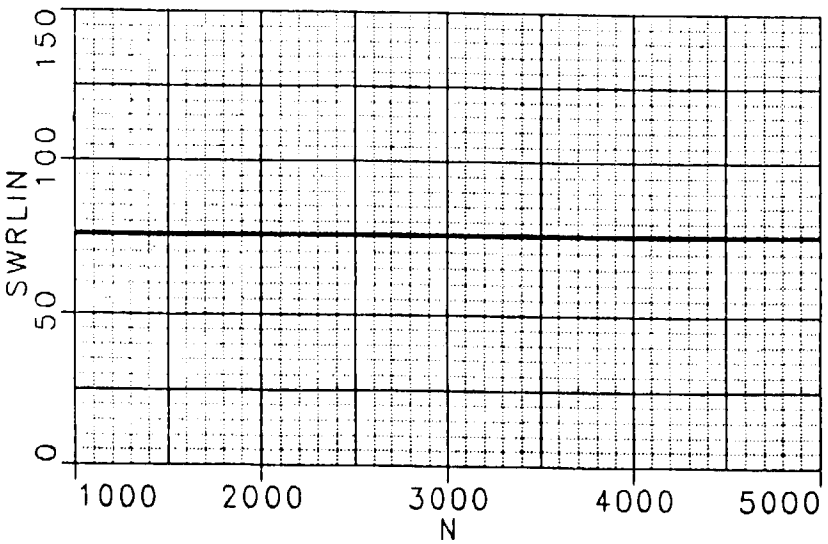

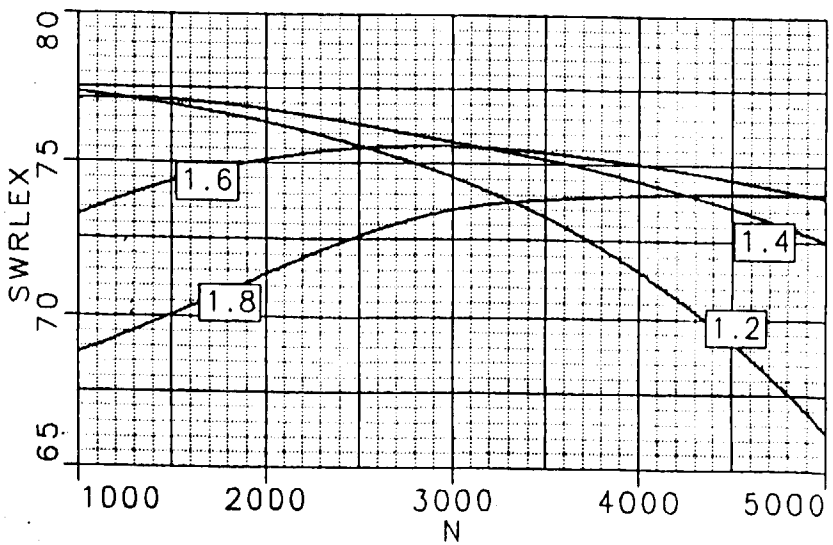

Lines of Constant

FIGURE 25D
OXIDIZER TURBINE BASELINE DESIGN

OTTR - Predicted Performance at Ptin=100 psia and Ttin=560 °R

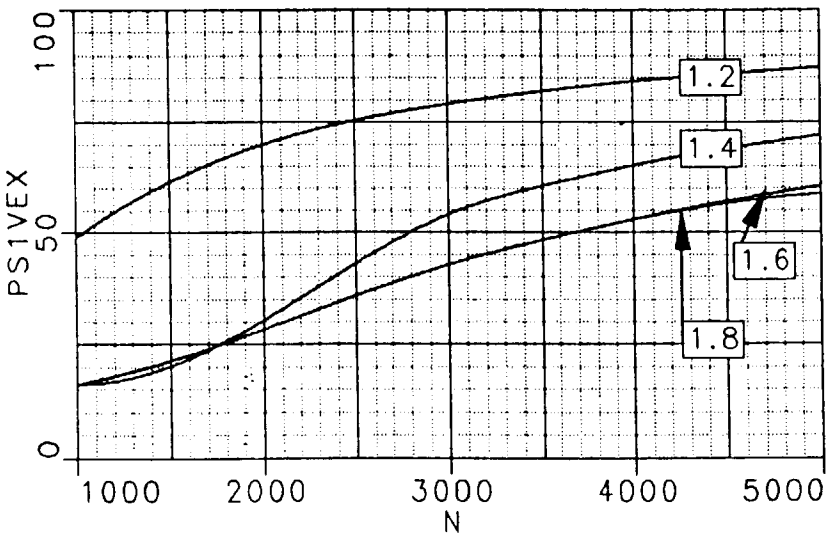

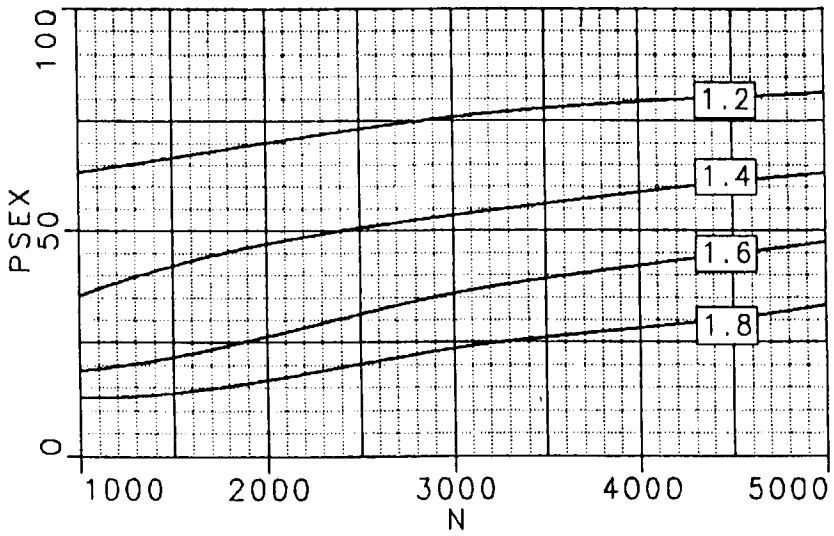

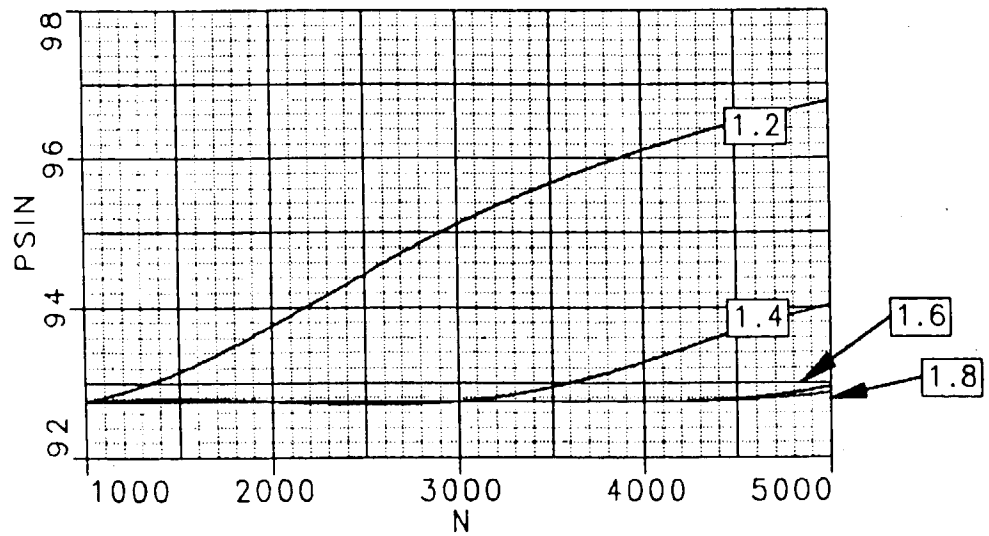

Lines of Constant Pressure Ratio

FIGURE 25E
OXIDIZER TURBINE BASELINE DESIGN

OTTR - Predicted Performance at Ptin=100 psia and Ttin=560 °R

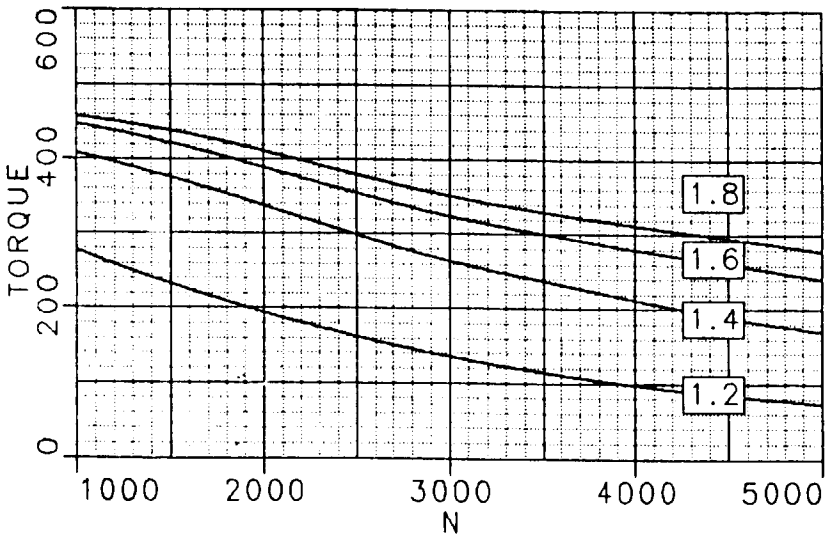

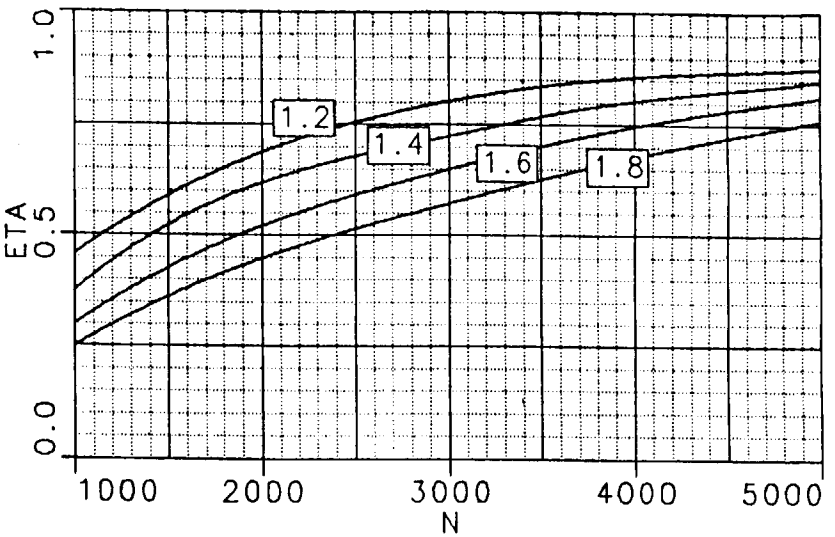

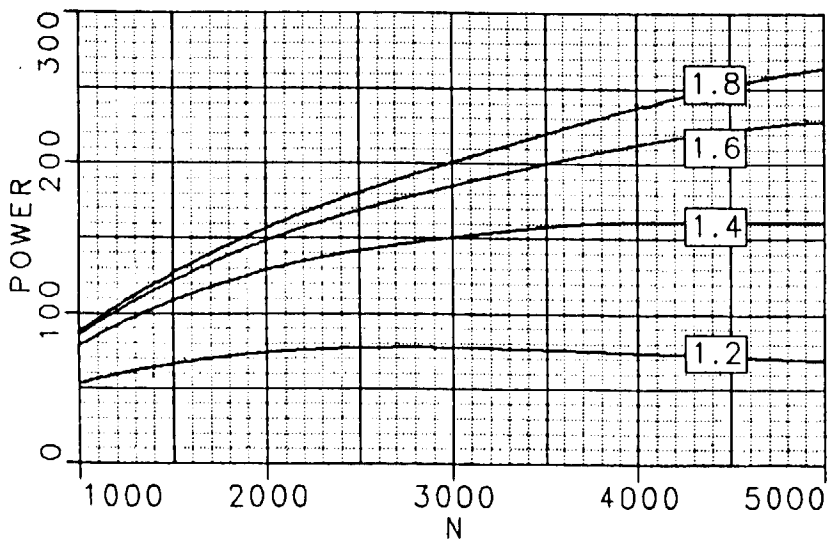

Lines of Constant Pressure Ratio

FIGURE 26A
OXIDIZER TURBINE BASELINE DESIGN

OTTR - Component Performance with Square Exit Volute

CALSOX Baseline Design

(115)

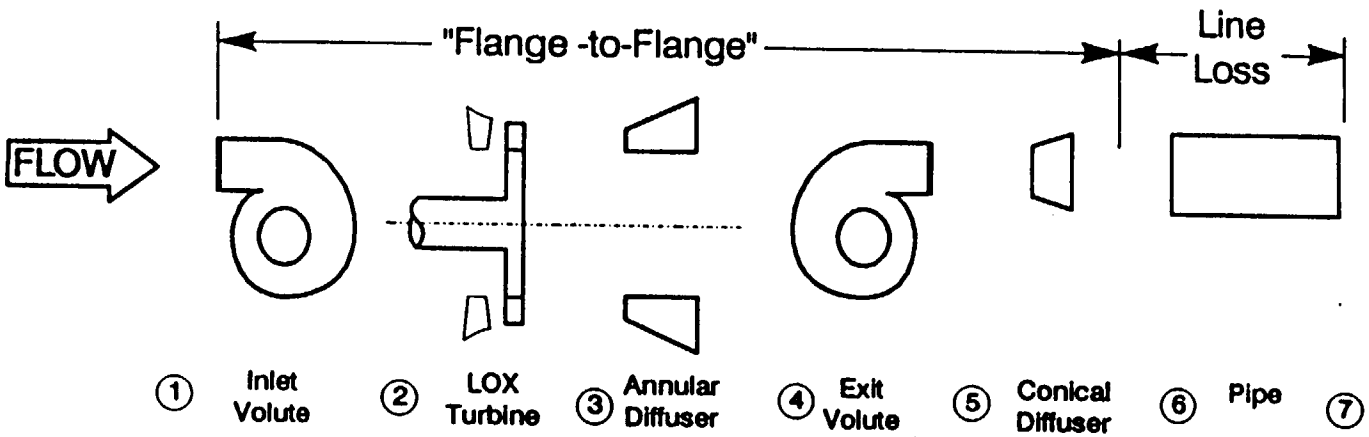

Mach Number Inlet Exit	.30 .33	.33 .84	.84 .80	.80 .49	.49 .25	
Pressure Loss $\Delta P_T / P_T$	.018		.026	.182	.010	
Velocity Head Loss $\Delta P_T / Q$	.310		.084	.625	.069	
Pressure Ratio $P_{T①} / P_{Texit}$ $P_{T①} / P_{Sexit}$	1.018 1.096	1.634 2.578	1.677 2.546	2.050 2.408	2.070 2.162	
Efficiency η_{T-T} η_{T-S}		.727 .392		.495 .413	.489 .464	

FIGURE 26B
OXIDIZER TURBINE BASELINE DESIGN

OTTR - Component Performance with Round Exit Volute

CALSOX Baseline Design

(115)

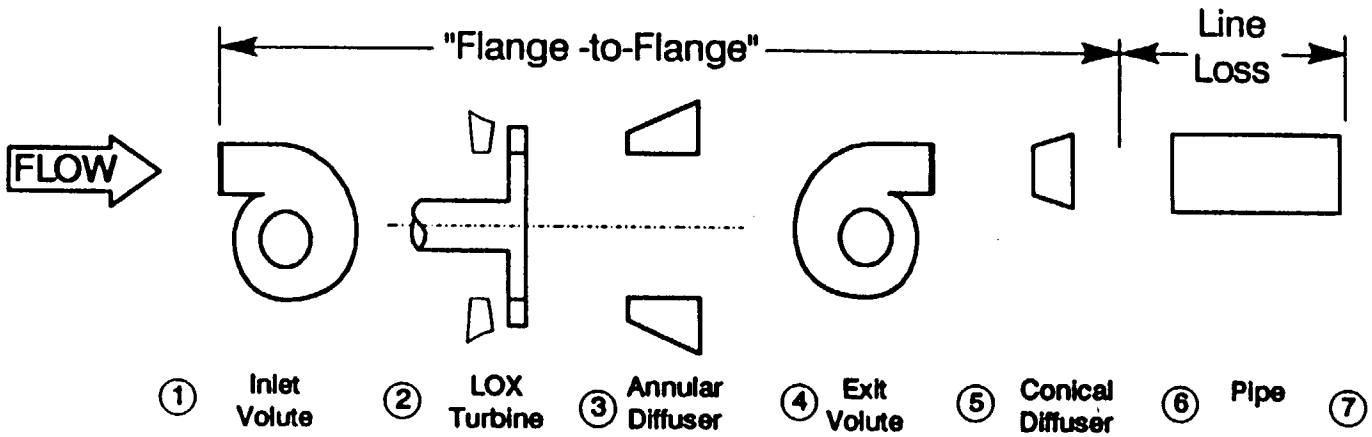

Mach Number Inlet Exit	.30 .33	.33 .84	.84 .80	.80 .61	.61 .25	
Pressure Loss $\Delta P_T / P_T$	.018		.026	.155	.018	
Velocity Head Loss $\Delta P_T / Q$	.310		.084	.532	.092	
Pressure Ratio $P_{T①} / P_{Texit}$ $P_{T①} / P_{Sexit}$	1.018 1.096	1.634 2.578	1.677 2.546	1.985 2.546	2.022 2.107	
Efficiency η_{T-T} η_{T-S}		.727 .392		.516 .391	.504 .478	

NASA
National Aeronautics and Space Administration

Report Documentation Page

1. Report No.	2. Government Accession No.	3. Recipient's Catalog No.

4. Title and Subtitle

Design of ETO Propulsion Turbine Using CFD Analyses

5. Report Date

April 1995

6. Performing Organization Code

7. Author(s)

F.J. de Jong, Y-T. Chan, and H.J. Gibeling

8. Performing Organization Report No.

R95-9084-F

10. Work Unit No.

9. Performing Organization Name and Address

Scientific Research Associates, Inc.
P.O. Box 1058
Glastonbury, CT 06033

11. Contract or Grant No.

NAS8-38865

13. Type of Report and Period Covered

12. Sponsoring Agency Name and Address

National Aeronautics and Space Administration
Washington, DC 20546-0001

NASA Marshall Space Flight Center

14. Sponsoring Agency Code

15. Supplementary Notes

16. Abstract

As one of the activities of the NASA/MSFC Turbine Technology Team, the present effort focused on using CFD in the design and analysis of high performance rocket engine pumps. A three-dimensional Navier-Stokes code was used for various turbine flow field calculations, with emphasis on the tip clearance flow and the associated losses. Both a baseline geometry and an advanced-concept geometry (with a mini-shroud at the blade tip) were studied at several tip clearances. The calculations performed under the present effort demonstrate that a state-of-the-art CFD code can be applied successfully to turbine design and the development of advanced hardware concepts.

17. Key Words (Suggested by Author(s))	18. Distribution Statement
Rocket Engine, Pump, Turbine, Tip Clearance, Viscous Flow, Navier-Stokes Code, Computational Fluid Dynamics	Unclassified-Unlimited

19. Security Classif. (of this report)	20. Security Classif. (of this page)	21. No. of pages	22. Price
Unclassified	Unclassified	88	

NASA FORM 1626 OCT 86